Investigating Inherited Renal Disorders and Identification of a Novel Cause of Joubert Syndrome

A thesis submitted for the degree of Doctor of Medicine

Sumaya Alkanderi

Institute of Genetic Medicine

Newcastle University

December 2018

Abstract

Joubert syndrome (JBTS) is a genetically heterogeneous neurodevelopmental ciliopathy that can have severe renal manifestations requiring renal replacement therapy. JBTS can be caused by mutation in 34 genes, however more than 50% of JBTS cases have unknown genetic causes. Through a multidisciplinary renal-genetics family clinic we studied a cohort of patients with inherited renal disorders and identified two families with JBTS phenotype and unknown molecular genetic diagnosis. We further investigated the underlying genetic aetiology of Joubert syndrome using combined homozygosity mapping of both families highlighted a candidate locus on chromosome 10, and whole exome sequencing revealed two missense variants in ARL3 within the candidate locus. The encoded protein, ADP ribosylation factor-like GTPase 3 (ARL3), is a small GTP-binding protein that is involved in trafficking lipid-modified proteins into the cilium in a GTP-dependent manner. Both missense variants replace the highly conserved Arg149 residue, which we show to be necessary for the interaction with its guanine nucleotide exchange factor ARL13B. Using patients derived fibroblasts, we identified that the mutant ARL3 protein is associated with reduced ciliary cargo protein INPP5E and NPHP3 localization in cilia.

Acknowledgment

First, I would like to express my sincere gratitude to my enthusiastic supervisors Prof. John Sayer and Dr. Colin Miles for their continuous support and guidance throughout my MD. Prof. Sayer, the physician, the scientist, the human being sets a high standard and an excellent example of the successful researcher. His knowledge, devotion, work ethics, always positive critical comments, compassion and sense of humour make him a respectful and admired team leader any research student would love to have. I was honoured to be his MD student.

I am profoundly grateful to Dr. Elisa Molinari who stood by my side since the first day she joined the renal team. She is a great scientist and I appreciate all her contributions of time, ideas, and problem solving. Much appreciation goes to Dr. Shalabh Srivastava who introduced me to cell culture and was of a constant support.

Special thanks to Dr. Shehab Ismail from the Beatson Institute for Cancer Research, Glasgow, for performing the guanine nucleotide exchange assay experiment, Dr. David steel kindly preformed retinal examination for our candidate patients and their unaffected relatives as well as obtaining skin biopsies, and Dr. Kathryn White from the Electron Microscopy Services. Heartful thanks go to the patients and their families.

Finally, I would like to thank my friends and family, despite the distance, they kept showering me with their love and encouragement. I am grateful for the comforting presence of my friends Hadeel and Olla and for my parents who supported me in all my pursuits, their prayers sustained me thus far. I owe a lot to my great mother, without her my research journey would have been impossible and to my husband and my boys for their continuous support.

And above all, I am grateful to Allah Almighty for granting me the knowledge, strength and health throughout my research.

Related Publications

1) <u>Lessons learned from a multidisciplinary renal genetics clinic</u>

   Sumaya Alkanderi, Laura M Yates, Sally A Johnson and John A Sayer

   QJM: An International Journal of Medicine, Vol. 110, No. 7, 8 February 2017, 453–457

2) <u>A human patient-derived cellular model of Joubert syndrome reveals ciliary defects which can be rescued with targeted therapies</u>

   Shalabh Srivastava, Simon A Ramsbottom, Elisa Molinari, Sumaya Alkanderi, Andrew Filby, Kathryn White, Charline Henry, Sophie Saunier, Colin G Miles and John A Sayer

   Human Molecular Genetics, Vol. 26, Issue 23, 1 December 2017, Pages 4657–4667,

3) <u>ARL3 Mutations Cause Joubert Syndrome by Disrupting Ciliary Protein Composition</u>

   Sumaya Alkanderi, Elisa Molinari, Ranad Shaheen, Yasmin Elmaghloob, Louise A Stephen, Veronica Sammut, Simon A Ramsbottom, Shalabh Srivastava, George Cairns, Noel Edwards, Sarah J Rice, Nour Ewida, Amal Alhashem, Kathryn White, Colin G Miles, David H Steel, Fowzan S Alkuraya, Shehab Ismail and John A Sayer.

   The American Journal of Human Genetics, Vol. 103, Issue 4, 4 October 2018, Pages 612-620

4) <u>Acidosis and Deafness in Patients with Recessive Mutations in FOXI1</u>

   Sven Enerbäck, Daniel Nilsson, Noel Edwards, Mikael Heglind, Sumaya Alkanderi, Emma Ashton, Asma Deeb, Feras E B Kokash, Abdul R A Bakhsh, William van't Hoff, Stephen B Walsh, Felice D'Arco, Arezoo Daryadel, Soline Bourgeois, Carsten A Wagner, Robert Kleta, Detlef Bockenhauer and John A Sayer

   Journal of the American Society of Nephrology, March 2018, 29 (3) 1041-1048

Table of Contents

List of tables

List of figures

List of Abbreviations

ADPKD   Autosomal dominant polycystic disease

ALSM   Alstrom syndrome

ARF   ADP ribosylation factor

ARL   ARF-like

ARPKD   Autosomal recessive polycystic disease

BBS   Bardet – Beidle syndrome

CAKUT   Congenital anomalies of kidney and urinary track

CHF   Congenital hepatic fibrosis

CTS   Ciliary targeting signal

ESRD   End stage renal disease

EVC   Ellis van Creveld syndrome

GAP   GTPase-activating protein

GDI   Guanosine nucleotide Dissociation Inhibitor

GEF   Guanine exchange factor

GFR   Glomerular filtration rate

GSF   GDI-like solubilizing factor

HUREC   Human Urine derived Renal Epithelial Cell

JBTS   Joubert syndrome

JS   Jeune syndrome

IFT   Intraflagellar transport

LCA	Leber congenital amaurosis
MKS	Meckel–Grüber syndrome
MRI	Magnantic resonance imaging
NGS	Next generation sequencing
NPHP	Nephronophthisis
OFD	oral-fascial-defect
PCR	Polymerase chain reaction
PKD	Polycystic kidney disease
SAG	Sonic Hedgehog pathway agonist
SEM	Scanning Electron Microscopy
SHH	Sonic Hedgehog
SLSN	Senior-Løken syndrome
SNV	Single nucleotide variants
SRP	Short rip polydactyly
SS	Sensenbrenner syndrome
VUS	Variant of unknown significance
UTI	Urinary tract infection
WES	Whole exome sequencing

Chapter 1 **Introduction**

1.1. **Inherited kidney disorders**

Inherited kidney disorders are classified as rare disorders, which affect a limited number of individuals, defined as affecting <1 in 2000 people in Europe or < 1 in 200 000 people in the USA (Schieppati et al., 2008). Rare kidney disorders include at least 150 different diseases with an overall prevalence of about 60-80 cases per 100 000 in Europe and the USA (Soliman, 2012). Inherited disorders have a well-recognised medical, psychosocial and economic burden on the affected families, as well as providing challenges for health care providers. Inherited kidney disorders, especially cystic kidney disease, are often known to cause chronic kidney disease progressing to end stage renal disease (ESRD) requiring dialysis or renal transplantation in both children and adult populations. Due to the recent advances in renal replacement therapy, individuals with inherited kidney disorders rarely die due to ESRD, however they experience a very poor quality of life.

Kidneys are vital organs, complex, highly specialised and target organs for diseases. The kidneys central role is in controlling body homeostasis, its excretory, metabolic and endocrine functions directly arbitrates essential interactions with other organs (Eckardt et al., 2013). The nephron is the functional unit of the kidney; each kidney is made of about one million nephrons. This highly specialised unit contains a filtration segment, the glomerulus, and renal tubules whose distal segments form collecting ducts that open in the renal pelvis. Kidney disease can originate from any segment of the nephron, and abnormal kidney function can manifest in several extra renal phenotypes (Devuyst et al., 2014).

1.2. **The role of next generation sequencing (NGS) in identifying the genetic cause of inherited kidney disorders**

Genetic research into inherited kidney disorders goes back to 1980s when the causative gene of autosomal dominant polycystic kidney disease (ADPKD) was first mapped to chromosome 16 in 1985 (Reeders et al., 1985). This was followed by the detection of 3 different point mutations at specific locus in *COL4A5* gene causing the kidney disorder Alport's syndrome (Barker et al., 1990). The year 2010 marked the

first success of exome sequencing in inherited kidney disorders, when Otto et al. (2010) used an approach of combining homozygosity mapping with whole exome sequencing (WES), identifying mutations of SDCCAG8 as the cause of retinal-renal ciliopathy (Senior-Løken syndrome). Next-generation sequencing (NGS) techniques became the preferable approach in inherited kidney disorders research and have improved the diagnostic efficiency. Examples of effective applications of NGS were reported for nephronophthisis genes analysis using DNA pooling and NGS (Otto et al., 2011). Multigene panels were successfully used in the diagnostic screening of Alport syndrome (Artuso et al., 2012). The application of NGS in the current clinical and genetic practice has increased the number of new genes identified to cause inherited kidney diseases. However, this technology requires accurate and reliable pool of databases that allow an assessment of the pathogenicity and population frequency of variants and the use of different disease models to determine the identified gene causality.

NGS technology gives more breadth to the number of genetic tests that can be efficiently performed, which by itself is meaningless if not combined with detailed and accurate phenotypic data attained by the clinicians. An informative diagnostic approach in inherited kidney disease starts with detailed family history and investigation, a proper characterisation of the renal phenotype, thorough systematic investigation to identify extrarenal features, and confirmatory tests (Joly et al., 2015).

There is no standard classification of inherited kidney disorders. Diseases may be grouped according to their main diagnostic features, grouped according to renal growth, structural or functional disorders, monogenic or polygenic disorders, or according to the presence or absence of systemic disease as primary or secondary kidney disorders (Hildebrandt, 2010, Eckardt et al., 2013, Devuyst et al., 2014). This study will focus on the investigation of inherited renal ciliopathies including the cerebello-retinal-renal syndrome called Joubert syndrome (JBTS).

1.3. Ciliopathies

Cilia are ancient organelles projecting from the cell surface. Cilia are classified into two classes: motile and immotile cilia. Motile cilia are found in the cell lining of brain ventricles, respiratory tract, and the oviduct. The beating nature of motile cilia function as a driving force to circulate and direct fluid flow in ventricles and tracts. On the other hand, immotile cilia are (also known as primary cilia) were thought to be evolutionary remnants; lacking obvious function. Not until the past decade when it was discovered that primary cilia have vital role in many key signalling pathways essential for development and homoeostasis (Hildebrandt et al., 2011a).

Ciliopathies are an emerging class of disorders that were recognised in the past decade by their unified underlying pathophysiology: dysfunction of the primary cilia (Badano et al., 2006). Dysfunction of any of protein complexes involved in the trafficking in and out or within the primary cilium interfere with its function and structure, giving rise to disorders that exhibit genetic and phenotypic heterogeneity (Waters and Beales, 2011). Ciliopathies are caused by mutations in more than 50 genes with protein products located in or around the primary cilium leading to multi-organ disorders affecting almost every major body system, starting with the brain, eyes, kidneys, liver, skeleton and ending with the limbs. Ciliopathies clinically and genetically overlap (Hildebrandt et al., 2011b). **Table 1.1** lists the known ciliopathies to date, their phenotypes and genetic mutations, ordered alphabetically.

Ciliopathy	Common Features	Gene(s)
Alstrom syndrome **(ALSM)**	Dilated cardiomyopathy, obesity, sensory neural hearing loss, retinitis pigmentosa, endocrine abnormalities, renal and hepatic manifestations	*ALMS1*
Bardet-Biedl syndrome (BBS)	Obesity, polydactyly, retinitis pigmentosa, anosmia, congenital heart defects	*BBS1, BBS2, BBS4, BBS5, BBS7, BBS9, BBS10, BBS12, ARL6, MKKS, TTC8, TRIM32, MKS1, CEP290, SDCCAG8, WDPCP, LZTFL1, PTHB1, C8orf37, IFT74, BBIP1, IFT27*
Ellis van Creveld syndrome (EVC)	Skeletal dysplasia, congenital heart defect, polydactyly; ectodermal dysplasia	*EVC1, EVC2*
Jeune Syndrome (JS)	Skeletal dysplasia, thoracic deformities, polydactyly, renal cysts, retinitis pigmentosa	*IFT80, DYNC2H1, CEP120, CSPP1, IFT140, IFT172, TTC21B, WDR19, WDR34, WDR35, WDR60*
Joubert syndrome **(JBTS)**	Hypoplasia of the cerebellar vermis (molar tooth sign), dysregulated breathing pattern, retinal dystrophy, renal anomalies	*INPP5E, TMEM216, AHI1, NPHP1, CEP290, TMEM67, RPGRIP1L, ARL13B, CC2D2A, OFD1, KIF7, TCTN1-3, TMEM237, CEP41, TMEM138, ZNF423, TMEM231, CSPP1, PDE6D, CEP104, B9D1, MKS1, KIAA0586, ARMC9, CPLANE1, CEP120, SUFU, KATNIP, PIBF1, TMEM107, B9D2*
Leber congenital amaurosis **(LCA)**	Early onset visual impairment (first year); pigmentary retinopathy	*GUCY2D, RPE65, SPATA7, AIPL1, LCA5, RPGRIP1, CRX, CRB1, NMNAT, CEP290, IMPDH1, RD3, RDH12, LRAT, TULP1, KCNJ13, GDF6, PRPH2*
Meckel–Gruber syndrome	Renal cysts, CNS anomalies (encephalocele),	*MKS1, TMEM216, TMEM67, CEP290, RPGRIP1L, CC2D2A, B9D1, B9D2,*

Ciliopathy	Common Features	Gene(s)
(MKS)	polydactyly, congenital heart deformity,	*TMEM107, TCTN2, NPHP3, KIF14*
Nephronophthisis (NPHP)	Renal fibrosis and renal cysts with or without extra-renal manifestations	*NPHP1, INVS, NPHP3, NPHP4, IQCB1, CEP290, GLIS2, RPGRIP1L, NEK8, SDCCAG8, TMEM67, TTC21B, ANKS6, CEP83, CEP164, DCDC2, IFT72, WDR19, ZNF423, MAPKBP1, AHI1, CC2D2A, XPNPEP3, ATXN10, SLC41A1*
Oral-facial-digital syndrome type 1 (OFD)	Oral cavity, face and digit anomalies; CNS abnormalities; cystic kidney disease; linked with male lethality	*OFD1*
Polycystic Kidney disease (PKD)	Renal cysts and extra-renal features	*PKHD1, PKD1, PKD2, SEC61A1, GANAB*
Senior-Løken syndrome (SLSN)	Retinal dystrophy and nephronophthisis	*NPHP1, NPHP4, IQCB1, SLSN3, SDCCAG8, WDR19, TRAS3IP1*
Sensenbrenner syndrome (SS)	Cranioectodermal dysplasia, narrow thorax, dental anomalies, hepatic and renal manifestations	*IFT122, WDR35, WDR19, IFT43*
Short rib polydactyly (SRP)	Lethal skeletal dysplasia, polydactyly, congenital renal dysplasia, multiple congenital anomalies	*NEK1, DYNC2H1, TTC21B, KIAA0586*

Table 1.1 Summary of Ciliopathies, their common features and causative genes.

	ALSM	BBS	EVC	JEUNE	JBTS	LCA	MKS	NPHP	OFD	PKD	SLSN	SS	SRP
Kidney disease	✓	✓		✓	✓	✓	✓	✓	✓	✓	✓	✓	✓
Hepatobiliary disease	✓	✓		✓	✓	✓	✓	✓	✓	✓		✓	✓
Retinal degeneration	✓	✓		✓	✓	✓	✓	✓	✓		✓	✓	
Intellectual disability	✓	✓	✓		✓	✓	✓		✓				
Cerebellar vermis Hypoplasia				✓	✓		✓		✓			✓	✓
Encephalocele					✓		✓						
Polydactyly		✓	✓	✓	✓		✓	✓	✓			✓	✓
Laterality defects		✓		✓			✓	✓			✓	✓	✓
Ectodermal dysplasia			✓	✓			✓		✓			✓	✓
Short bones			✓	✓			✓					✓	✓
Obesity	✓	✓											

Table 1.2 Ciliopathies phenotypic overlap

6

1.4. Renal manifestation of ciliopathies

In the perspective of primary ciliary dysfunction, the disease can manifest in any organ predominantly in the kidneys, liver, eye, and brain. It can have developmental phenotype presenting at birth or later during childhood depending on the severity of the underlying mutation as well as number of disrupted ciliary proteins. Pazour et al. (2000) were the first to link ciliary disruption to the development of cystic kidney disease in mammals.

The common and leading genetic cause of renal failure in paediatric and adult population are renal ciliopathies. The spectrum of renal phenotype in ciliopathies can be classified as polycystic, renal medullary cystic disease / nephronophthisis and cystic renal dysplasia.
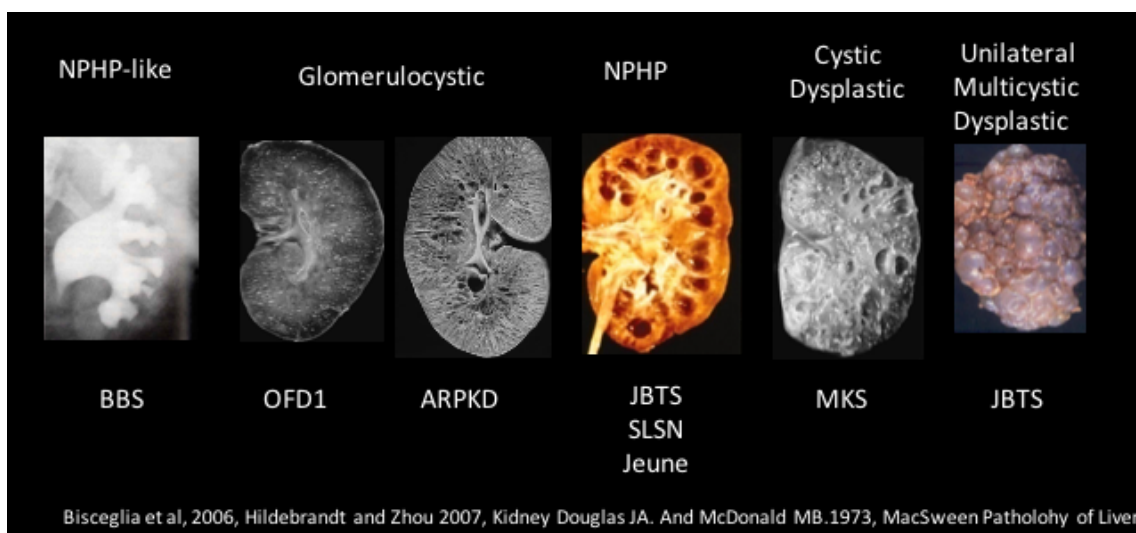
Figure 1.1 Kidney disease phenotypes seen in ciliopathies

1.4.1. Cystic kidney disease

Polycystic kidney disease characterised by the presence of multiple cysts in the kidneys, liver or both and can be recognised in neonatal period or during childhood. PKD is a group of monogenic disorders can be inherited in an autosomal dominant manner or recessive manner (Harris, 2009). Autosomal polycystic kidney disease (ADPKD) is found to be caused by a mutation in genes including *PKD1* encoding polycystin-1 (PC-1) and *PKD2* encoding polycystin-2 (PC-2) (Hughes et al., 1995, Mochizuki et al., 1996). Two additional genes have recently been implicated in ADPKD and include *GANAB* and *SEC61A1* (Porath et al., 2016, Bolar et al., 2016). Autosomal recessive polycystic kidney disease (ARPKD) is caused by homozygous or compound heterozygous mutations in *PKHD1* encoding fibrocystin protein. PC-1, PC-2 and fibrocystin proteins are found to form a complex and localised at the primary cilia and the basal body in addition to various cellular sites (Yoder et al., 2002, Ward et al., 2003). **Table 1.3** summarises the clinical presentation and expected outcome of the polycystic kidney disease.

	ADPKD	ARPKD
onset	Sometimes in utero or in Neonatal period, mostly 2nd and 3rd decade of life	Utero or neonatal period, sometimes childhood or adulthood
Incidence	1:400 – 1:1,000	1:20,000
cysts	Focal cysts along the nephron, mostly collecting duct	Fusiform dilatation of the collecting ducts
Signs and symptoms	Bilaterally enlarged kidneys, loin pain, renal colic, haematuria, UTI and hypertension	Bilaterally enlarged kidneys, loin pain, renal colic, haematuria, UTI and (severe) hypertension
Morbidity and mortality	Ruptured intracranial artery aneurysm Adulthood onset ESRD	Childhood onset ESRD Renal transplant in 30%
Other organs involved	Cysts in liver, pancreas and seminal vesicles	Congenital fibrocystic liver, portal hypertension, oesophageal varices and cholangitis

Table 1.3 Clinical summary of polycystic kidney diseases

1.4.2. Nephronophthisis

Nephronophthisis (NPHP) is an autosomal recessive inherited monogenic kidney disorder, which literally means "damage to the nephrons" (Arts and Knoers, 2013). NPHP manifests in progressive loss of renal function causing ESRD before the age of 30 years old (Simms et al., 2009). NPHP can be caused by more than 20 genes all were found to encode proteins localised to the centrosome and the primary cilia, and up to date list of genes are summarised in **Table 1.4** (Srivastava et al., 2018). NPHP is characterised by fibrotic tubule interstitial and a subsequent formation of renal cysts at the corticomedullary junction, such pathology cause depletion in glomerular filtration rate (GFR) and loss of distal tubules function. Clinical symptoms include polyuria, polydipsia, secondary enuresis, growth retardation and ESRD eventually (Hildebrandt et al., 2009).

Extrarenal manifestation can be associated with NPHP in 20% of cases, giving rise to different additional phenotypes of ciliopathies including Senior–Løken syndrome, Alstrom syndrome, Arima syndrome, Cogan syndrome, Joubert syndrome, Bardet-Biedl syndrome, Jeune syndrome, Sensenbrenner syndrome, Ellis-van Creveld syndrome and Saldino-Mainzer syndrome. NPHP extra renal involvements are retinopathy, cerebral vermis hypoplasia, intellectual disability, oculomotor apraxia, hepatobiliary disease, laterality defects and skeletal dysplasia (Salomon et al., 2009).

HGCN symbol	NPHP Type	Disorders	Key insights
NPHP1	NPHP1	NPHP/SLSN/JBTS	Cell-cell junction and ciliary transition zone protein
INVS	NPHP2	NPHP/SLSN	Role in wnt signaling
NPHP3	NPHP3	NPHP/SLSN/MKS	Murine model *pcy* has a hypomorphic Nphp3 allele
NPHP4	NPHP4	NPHP/SLSN	Role in both cilia and cell-junctions
IQCB1	NPHP5	SLSN/LCA	Localises to connecting cilium of photoreceptor cells
CEP290	NPHP6	JBTS/BBS/MKS/LCA/SLSN	Centrosomal protein
GLIS2	NPHP7	NPHP	Increase in apoptosis and fibrosis in murine model Glis2
RPGRIP1L	NPHP8	JBTS/MKS	Ciliary transition zone protein and facilitates vesicular docking of ciliary proteins
NEK8	NPHP9	NPHP	Links cilia and cell cycle defects in NPHP
SDCCAG8	NPHP10	SLSN/BBS	Implicates DNA damage and NPHP
TMEM67	NPHP11	NPHP/MKS/JBTS	Required for ciliogenesis
TTC21B	NPHP12	NPHP/JS	IFT protein
WDR19	NPHP13	NPHP/CED/JS	IFT protein
ZNF423	NPHP14	JBTS	Centrosomal protein and role in DNA repair signaling
CEP164	NPHP15	NPHP/SLSN/JBTS	Centrosomal protein and role in DNA repair signaling
ANKS6	NPHP16	NPHP	Functional module with INVS and NPHP3
AHI1	JBTS3	NPHP/JBTS	Important for cerebellar development
XPNPEP3	NPHPL1	NPHP	Mitochondrial defect linking ciliopathies with mitochondria and potential novel pathways of disease.
ATXN10	N/A	NPHP/SCA	Interacts with NPHP5
SLC41A1	N/A	NPHP-Like	Renal Magnesium transporter defect
CEP83	N/A	NPHP	Component of distal appendages of centriole
MAPKBP1	NPHP20	NPHP	Non-ciliary protein, involved in JNK signaling

Table 1.4 Genetic classification of Nephronophthisis, its related disorders and key insights. Obtained from *(Srivastava et al., 2018).*

1.4.3. Renal dysplasia

Ciliary dysfunction can be associated with other severe forms of kidney diseases. Meckel-Gruber syndrome is perinatally lethal and characterised by neural tube defect, polydactyly, bile duct proliferation and cystic renal dysplasia (Alexiev et al., 2006). This condition is caused by mutation in many genes encoding centrosomal and ciliary proteins. Another severe condition is the short-rib-polydactyly syndrome, a lethal skeletal ciliopathy, which exhibits congenital renal dysplasia (Thiel et al., 2011, Merrill et al., 2009). Gross kidney abnormalities have been reported in ciliopathies like horseshoe kidneys, lobulated kidneys as well as to urinary tract anomalies (Bergmann, 2012). in ciliopathies, the presence of asymmetrical renal disease is unexpected, however, unilateral multicystic dysplastic kidney were reported in few cases of JBTS (Fleming et al., 2017, Malaki et al., 2012).

1.5. Joubert Syndrome

Joubert syndrome (JBTS) is a neurodevelopmental ciliopathy with recessive inheritance causing cerebellar vermis hypoplasia (Joubert et al., 1969). The core of JBTS is the neurological phenotype appearing soon after birth, characterised by hypotonia, abnormal eye movement (oculomotor apraxia), intellectual disability, truncal ataxia, and respiratory control dysfunction (sleep apnoea) (Boltshauser and Isler, 1977). The neurological symptoms are still nonspecific and the hallmark of JBTS is the presence of "The Molar Tooth sign" on the axial brain MRI imaging (Poretti et al., 2014b). This pathognomonic feature was first described by Maria et al. (1997) arises from the hypoplasia and the dysplasia of the cerebellar vermis and of pontine and medullary structure, as well as the absence of decussation of the superior cerebellar peduncles and the pyramidal tracts. JBTS presentation can be purely neurological, patients present early in life with hypotonia, abnormal eye movement (includes: oculomotor apraxia, nystagmus, and strabismus), respiratory control dysfunction that alternate between sleep apnoea and tachypnoea or episodes of tachypnoea alone (Saraiva and Baraitser, 1992). Later in life, children acquire developmental delay, they might experience delayed speech (expressive and comprehensive) delayed walking, broad-based ataxia and difficulty in running and climbing. Intellectual disability and cognitive impairment seen nearly in all cases of JBTS with variable severity (Doherty, 2009). However, the cases can be complicated by the extra neurological manifestations, which range in severity. Therefore, patients diagnosed with JBTS undergo diagnostic examination and regular follow-up to assess and manage their multi-organ manifestations.
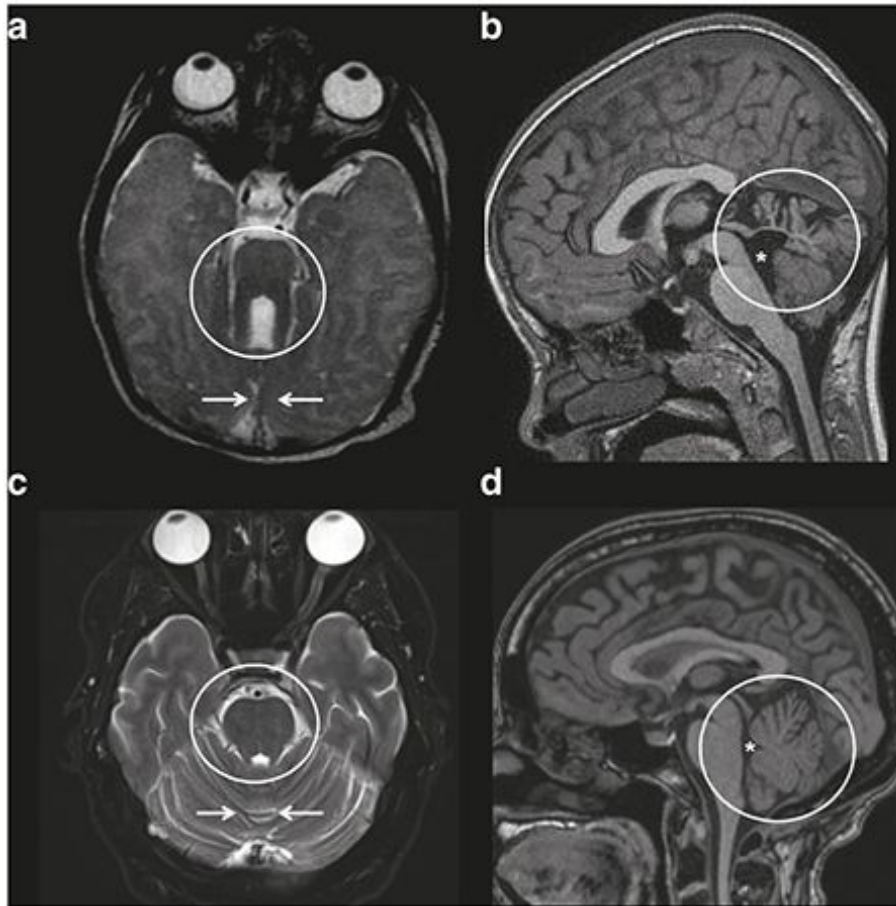
Figure 1.2 Brain magnetic resonance images (MRI) showing diagnostic findings of Joubert syndrome (JBTS) in comparison to normal findings.

(a) Axial brain MRI obtained at the level of the junction of the midbrain and pons showing the "molar tooth sign" (circle) and hypoplastic cerebellar vermis (arrows) in comparison to normal (c). (b) Sagittal brain MRI demonstrating hypoplasia of the cerebellar vermis (circle) and enlarged fourth ventricle (asterisk) in comparison to normal (d). Image taken from (Vilboux et al., 2017)

1.6. The extra neurological manifestations of Joubert syndrome

About 20-40% of JBTS patients develop renal involvement at any age in the form of nephronophthisis or cystic dysplastic kidneys, ocular involvement including chorioretinal coloboma, retinal dystrophy and blindness, hepatic involvement such as ductal plate malformation and fibrosis, dysmorphic facial features and/or skeletal involvement like dystrophy or polydactyly (Romani et al., 2013). Parisi et al. (2007) proposed a JBTS subtypes based on the presence or the absence of multiorgan involvement features to: Pure JBTS, JBTS with retinal involvement, JBTS with renal involvement, JBTS with liver involvement and JBTS with oral-facial –digital features.

1.6.1. Ocular features

The most common extra neurological involvements are ocular and oculomotor abnormalities. Eye movements abnormalities are seen in between 70-100% of JBTS patients including oculomotor apraxia, nystagmus, strabismus, and vertical gaze palsy (Pellegrino et al., 1997). The retinal defects were found to affect 30% of JBTS patients (Bachmann-Gagescu et al., 2015). Progressive photoreceptors degeneration found to be the leading cause of retinal dystrophy. The clinical presentation varies in severity and spectrum can range from congenital blindness to slowly progressing retinal dystrophy with persevered partial vision (Lambert et al., 1989).

1.6.2. Renal features

 The renal defects are present in almost one quarter of JBTS cases (Valente et al., 2013b). Two major forms of kidney diseases were reported in JBTS: juvenile nephronophthisis and cystic dysplastic kidneys. Juvenile NPHP characterised by microscopic cysts formation at the cortico-medullary junction of the kidneys, affecting the ability of kidney to concentre urine and conserve sodium. Presenting with polydipsia and polyuria in early life with normal glomerular filtration rate (GFR) (Salomon et al., 2009). As the disease progress, renal insufficiency occurs manifesting in anaemia and growth retardation and subsequently developing end stage renal disease (ESRD) at early teens. In a recent cohort of JBTS patient, 30% of cases were found to be associated with NPHP (Fleming et al., 2017). On the other hand, JBTS with cystic kidney dysplasia characterised by the presence of multiple cysts with variable sizes in foetal kidney or at birth known as Dekaban–Arima

syndrome (Dekaban, 1969). Comorbidity of retinal and renal involvement have been noted, with all JBTS patients with renal disease had retinopathy (Saraiva and Baraitser, 1992, Boltshauser et al., 1995, Brancati et al., 2007, Bachmann-Gagescu et al., 2015).

1.6.3. Hepatic features

The association of JBTS with liver disease known by the acronym COACH standing for Cerebellar vermis hypoplasia, Oligophrenia, Ataxia, Coloboma and Hepatic fibrosis (Satran et al., 1999). This congenital hepatic fibrosis (CHF) results from ductal plate embryonic malformation associated with cystic dilatation of primitive biliary structures and fibrous enlargement of the portal tracts. JBTS individuals may present with elevated liver enzymes and hepatomegaly. In some cases, patient can develop portal hypertension, oesophageal varices or liver cirrhosis (Gleeson et al., 2004). A very strong association has been established between the presence of coloboma and hepatic fibrosis in JBTS patients (Brancati et al., 2009, Doherty et al., 2010, Bachmann-Gagescu et al., 2015).

1.6.4. Skeletal features

Polydactyly has been reported in around 15% of JBTS cases (Brancati et al., 2010) as well as in the first case of reported JBTS (Joubert et al., 1969). Oral defect can present alongside polydactyly in a condition known as oral-facial-digital type VI syndrome (Poretti et al., 2008). A late manifestation of early infancy hypotonia is the development of mild to severe scoliosis, which requires a close monitoring especially during puberty.

1.7. The molecular genetic causes of Joubert syndrome

Like other ciliopathies, JBTS exhibits noticeable genetic heterogeneity. It is caused by recessive mutations in more than 30 genes (OMIM phenotypic series PS213300) which are known to encode proteins localised to the primary cilium and its basal body. Yet those identified genes explain the causative mutation in only 40-50% of JBTS cases (Valente et al., 2013b). Finding the correct molecular diagnosis provides accurate genetic counselling in families with JBTS child, predicting prognosis, family planning and prenatal diagnosis. Next generation sequencing (NGS), particularly whole exome sequencing (WES) studies, was a useful tool based on the complexity and heterogeneity of the disease to determine the genotype-phenotype correlation of JBTS, and equally identifying novel causative gene mutations.

1.7.1. JBTS#1: INPP5E

JBTS#1 is caused by homozygous or compound heterozygous mutations in *INPP5E* on chromosome 9q34 (Bielas et al., 2009). *INPP5E* encodes inositol polyphosphate-5-phosphatase (INPP5E) known to be exclusively localised in primary cilia, specifically the axoneme, of different cell types. Mutation in *INPP5E* often disrupt the catalytic domain of the protein decreasing its phosphatase activity leading to impaired phosphotidylinositol (ptdIns) signalling thus affecting the primary cilia role in mediating cell signals and neuronal function. JBTS1 patients reported retinopathy and colobomas as common extra neural manifestation, while 10% of JBTS1 patient may develop renal disease (Kroes et al., 2016). Mutation in INPP5E can also cause MORM an acronym for mental retardation, truncal obesity, retinal dystrophy, and micropenis syndrome (Bielas et al., 2009).

1.7.2. JBTS#2: TMEM216

JBTS#2 is caused by homozygous or compound heterozygous mutations in the *TMEM216* gene on chromosome 11q12 (Keeler et al., 2003). It encodes tetraspan transmembrane protein (TMEM216) that is localised to the base of the cilia and regulates signalling and trafficking of its partner proteins. *TMEM216* mutation affects ciliogenesis and docking of centrosomes. In addition to the neurological features JBTS2 patients had retinopathy, colobomas, polydactyly, and nephronophthisis. Some cases reported other miscellaneous features such as patent foramen oval and Dandy-Walker malformation. TMEM216 mutation causing JBTS2 in Ashkenazi

Jewish population (Edvardson et al., 2010, Valente et al., 2010). Mutation in the TMEM216 gene can also cause Meckel syndrome-2 (MKS2).

1.7.3. JBTS#3: AHI1

JBTS#3 is caused by homozygous or compound heterozygous mutations in *AHI1* on chromosome 6q23.3 (Dixon-Salazar et al., 2004). Ahi1 is found at the mother centriole and the basal body of the primary cilia in mice (Hsiao et al., 2009). AHI1 is required for ciliogenesis and proper vesicular membrane trafficking. JBTS3 patients often presents with the core neurological manifestation as well as retinal dystrophy with no renal or hepatic involvement (Valente et al., 2006a). However, in a report by Utsch et al. (2006), findings indicate that AHI1 mutation can cause JBTS with renal manifestation.

1.7.4. JBTS#4: NPHP1

JBTS#4 is caused by homozygous or compound heterozygous mutations in *NPHP1* on chromosome 2q13, NPHP1 encodes nephrocytsin-1 (Parisi et al., 2004). Nphp1 localized to the ciliary transition zone and functioned at an early stage of ciliogenesis in *C. elegans* (Williams et al., 2011). Mutation in NPHP1 can give rise to JBTS with retinal and renal involvement, as well as Senior-Loken syndrome-1 and juvenile nephronophthisis-1 (Sang et al., 2011).

1.7.5. JBTS#5: CEP290

JBTS#5 is caused by homozygous or compound heterozygous mutations in *CEP290* encoding the centrosomal protein CEP290 on chromosome 12q21(Valente et al., 2006b). CEP290 found to be involved in cilia assembly and ciliary protein trafficking. Mutation of *CEP290* account for 50% of genetically diagnosed JBTS case*s. CEP290* mutations can give rise to JBTS5 where patients develop neurological manifestation accompanied with retinal disease and renal involvement or Senior-Loken syndrome (SLNS6) (Sayer et al., 2006). Later reports showed evidence of CEP290 mutation causing Leber congenital amaurosis LCA (den Hollander et al., 2006), MKS4 (Baala et al., 2007a) and Bardet-Biedl syndrome (BBS14) (Leitch et al., 2008).

1.7.6. JBTS#6: TMEM67

JBTS#6 is caused by homozygous or compound heterozygous mutations in *TMEM67* on chromosome 8q22 (Baala et al., 2007b). It encodes the transmembrane

protein-67 (TMEM67) or Meckelin. TMEM67 is localised to the primary cilia and take roles in ciliogenesis, centriole migration and renal tubulogenesis (Dawe et al., 2006). JBTS6 patients often present with renal disease and have a high tendency to develop liver fibrosis. *TMEM67* truncating mutation was first found to cause MKS3 (Smith et al., 2006). When the brain imaging lacks the presence of MTS in cases of *TMEM67* mutation, NPHP11 is considered the diagnosis (Otto et al., 2009).

1.7.7. JBTS#7: RPGRIP1L

BTS#7 is caused by homozygous or compound heterozygous mutation in *RPGRIP1L* on chromosome 16q12. Found to be localised to the basal body and the centrosome of the primary cilia in different tissue, facilitating the vesicular docking of ciliary proteins at the transition zone (Delous et al., 2007). JBTS7 patients presents with the core neurological features, polydactyly, scoliosis and renal disease (Arts et al., 2007, Brancati et al., 2008). Mutation in *RPGRIP1L* may cause COACH (Doherty et al., 2010).

1.7.8. JBTS#8: ARL13B

JBTS#8 is caused by homozygous or compound heterozygous mutation in *ARL13B* on chromosome 3q11 (Cantagrel et al., 2008). It encodes member of the ADP-ribosylation factor-like (ARL) family of small GTPases of the RAS superfamily (ARL13B). ARL13B exclusively localised to ciliary axoneme and takes a role in Sonic Hedgehog (SHH) signalling (Larkins et al., 2011) and cilia formation by targeting INPP5E to the cilia (Humbert et al., 2012). JBTS8 patients exhibit the classic features with or without retinopathy.

1.7.9. JBTS#9: CC2D2A

JBTS#9 is caused by homozygous or compound heterozygous mutation in *CC2D2A* on chromosome 4p15. It encodes coiled-coil and C2 domains-containing protein 2A (CC2D2A). CC2D2A is localised in basal body of primary cilia, regulating cilia directed cargo vesicle docking at the transition zone. JBTS9 patients can develop retinopathy (Noor et al., 2008) , renal disease and hepatic fibrosis (Gorden et al., 2008, Doherty et al., 2010).

1.7.10. JBTS#10: OFD1

JBTS#10 is caused by mutation in the OFD1 gene on Xp22.2, giving rise to X-linked recessive inheritance JBTS (Coene et al., 2009). Mutation in OFD1 causing ciliary dysfunction and JBTS10 phenotype is associated with retinopathy and polydactyly or without (Field et al., 2012).

1.7.11. JBTS#11: TTC21B

JBTS#11 is caused by homozygous or compound heterozygous mutation in *TTC21B* on chromosome 2q24 (Davis et al., 2011). *TTC21B* encodes the retrograde intraflagellar transport (IFT) protein IFT139 which has been shown to localise to the cilia and regulate SHH signalling in primary cilia (Tran et al., 2014). Mutation in TTC21B can cause nephronophthisis-12 (NPHP12).

1.7.12. JBTS12: KIF7

JBTS#12 is caused by homozygous mutation in *KIF7* on chromosome 15q26.1 (Dafinger et al., 2011). Mutation in KIF7 associated with defective ciliogenesis and centrosome duplication resulting in SHH pathway disruption. Patients with JBTS12 exhibit classic JBTS with dysmorphism and polydactyly. Mutation in KIF7 were first reported to cause acrocallosal syndrome (ACLS), an autosomal recessive mental retardation with absence of corpus callosum, dysmorphism, hallux duplication and polydactyly (Putoux et al., 2011).

1.7.13. JBTS#13: TCTN1

JBTS#13 is caused by homozygous or compound heterozygous mutation in *TCTN1* on chromosome 12q24 (Garcia-Gonzalo et al., 2011). Tctn1 localized to the transition zone between the ciliary axoneme and the basal body and plays major role in SHH signalling activation (Reiter and Skarnes, 2006) and ciliogenesis. Patients with TCTN1 mutation acquired no renal or hepatic disease (Alazami et al., 2012).

1.7.14. JBTS#14: TMEM237

JBTS#14 is caused by homozygous or compound heterozygous mutation in *TMEM237* on chromosome 2q33. It encodes tetraspan transmembrane protein TMEM237 that interacts with other JBTS causing proteins at transition zone (Huang et al., 2011). The neuro-development features of JBTS14 was accompanied with polydactyly and renal cysts.

1.7.15. JBTS#15: CEP41

JBTS#15 is caused by homozygous or compound heterozygous mutations in *CEP41* on chromosome 7q32 (Lee et al., 2012a). CEP41 encodes the centrosomal protein-41 (CEP41) required for ciliary glutamylation regulating ciliary axonemal structure. In a small cohort of 8 patients with different *CEP41* mutation gave rise to JBTS15 with core neurological symptoms, polydactyly and colobomas. 2 out of 8 patients had retinopathy, 1 patient with unilateral renal disease and another with hepatic manifestations. Digenic inheritance has been reported with other JBTS causing genes: *KIF7* and *CC2D2A*.

1.7.16. JBTS#16: TMEM138

JBTS#16 can be caused by homozygous or compound heterozygous mutations in *TMEM138* on chromosome 11q12 (Lee et al., 2012b). It encodes transmembrane protein TMEM138 that is localised to the base of the cilia and regulates vesicular trafficking. TMEM138 mutations affect ciliogenesis and manifest in JBTS with retinal and renal involvement.

1.7.17. JBTS#17: C5orf42

JBTS#17 is caused by compound heterozygous mutation in *C5orf42* on chromosome 5p13 (Srour et al., 2012b). The neurological manifestations of JBTS#17 were associated with polydactyly with no evidence of with retinal, renal or hepatic disease (Bachmann-Gagescu et al., 2015). Mutation in *C5orf42* were first identified to cause OFD VI.

1.7.18. JBTS#18: TCTN3

JBTS#18 can be caused by homozygous or compound heterozygous mutations in *TCTN3* on chromosome 10q24, causing disruption of SHH signalling pathway (Thomas et al., 2012). In addition to core neurological manifestation of JBTS, patient with *TCTN3* mutation had severe scoliosis. Mutation in *TCTN3* were also found to cause OFD IV.

1.7.19. JBTS#19: ZNF423

JBTS#19 can be caused by homozygous and single heterozygous mutations in *ZNF423* on chromosome 16q12.1. The single heterozygous alleles suggesting a dominant negative effect (Chaki et al., 2012). Mutations resulted in phenotypic

21

variability of JBTS. ZNF423 is a nuclear and centrosomal protein found to directly interact with another JBTS causing gene *CEP290*.

1.7.20. JBTS#20: TMEM231

JBTS#20 is caused by homozygous and compound heterozygous mutations in *TMEM231* on chromosome 16q23.1 (Srour et al., 2012a). Mutations resulted in phenotypic variability of JBTS associated organ involvement, polydactyly, retinopathy and renal cysts were reported in different patients.

1.7.21. JBTS#21: CSPP1

JBTS#21 is caused by homozygous or compound heterozygous mutation in *CSPP1* on chromosome 8q13.1-q13.2 (Akizu et al., 2014). Mutation in *CSPP1* affect ciliogenesis and may alter SHH signalling pathway, resulting in a wide spectrum of severity of JBTS (Shaheen et al., 2014, Tuz et al., 2014).

1.7.22. JBTS#22: PDE6D

JBTS#22 is caused by homozygous mutation in *PDE6D* on chromosome 2q37.1 (Thomas et al., 2014). It encodes a basal body protein PDE6D which is essential for INPP5E ciliary trafficking through a functional network of many ciliary proteins (Humbert et al., 2012). Patients with JBTS22 commonly have polydactyly and develop retinal and renal manifestations.

1.7.23. JBTS#23: KIAA0586

JBTS#23 is caused by homozygous or compound heterozygous mutations in *KIAA0586* on chromosome 14q23.1(Bachmann-Gagescu et al., 2015). Mutation of *Talpid3*, *KIAA0586* orthologue in mice and chicken, is known to affect ciliogenesis and SHH signalling (Roosing et al., 2015). Mutation of *KIAA0586* give rise to classical JBTS without retinal, renal or hepatic involvement.

1.7.24. JBTS#24: TCTN2

JBTS#24 is caused by homozygous mutation in *TCTN2* on chromosome 12q24.31 (Huppke et al., 2015, Sang et al., 2011). It encodes TCTN2 that affects ciliogenesis in a tissue specific manner by interacting with other ciliary proteins at the transition zone (Garcia-Gonzalo et al., 2011). Patients with JBTS24 presented with

polydactyly and encephalocele, no evidence of retinal, renal or hepatic involvement. Mutation in TCTN2 can cause MKS8.

1.7.25.   JBTS#25: CEP104

JBTS#25 is caused by homozygous or compound heterozygous mutation in *CEP104* on chromosome 1p36.32 (Srour et al., 2015). Loss of function mutation of CEP104 can disrupt ciliogenesis by inhibiting cilia assembly (Tammana et al., 2013). No retinal, renal or hepatic disease were reported in JBTS#25 patients.

1.7.26.   JBTS#26: KIAA0556

JBTS#26 is caused by homozygous mutation in *KIAA0556* on chromosome 16p12.1. It encodes KIAA0556 protein localised at the basal body (Sanders et al., 2015). JBTS#26 patients exhibit milder form of JBTS with midline facial defect and rare association of growth hormone deficiency (Roosing et al., 2016b).

1.7.27.   JBTS#27: B9D1

JBTS#27 is caused by homozygous or compound heterozygous mutation in *B9D1* on chromosome 17p11.2 (Romani et al., 2014). It encodes the B9 domain-containing protein 1 B9D1 localised at the basal body and function within the transition zone proteins complex (Dowdle et al., 2011). Mutations in B9D1 can cause mild form of JBTS with no extra neural manifestation or lethal form of MKS (MKS8).

1.7.28.   JBTS#28: MKS1

JBTS#28 is caused by homozygous or compound heterozygous mutation in *MKS1* on chromosome 17q22 (Romani et al., 2014). *MKS1* mutation gave rise to pure JBTS in two unrelated patients. Mks1 is required for ciliogenesis and renal tubule formation (Dawe et al., 2006). Mutations in *MKS1* were first found to cause the lethal Meckel syndrome 1 (Kyttälä et al., 2006) as well as Bardet-Biedl syndrome 13 (Leitch et al., 2008).

1.7.29.   JBTS#29: TMEM107

JBTS#29 is caused by compound heterozygous mutations in *TMEM107* on chromosome 17p13.1 (Lambacher et al., 2016). Mutation in *TMEM107* can impair ciliogenesis and cause Meckel syndrome 13 (Shaheen et al., 2015).

1.7.30.   JBTS#30: ARMC9

JBTS#30 is caused by homozygous or compound heterozygous mutation in *ARMC9* on chromosome 2q37.1 (Van De Weghe et al., 2017). Patients with JBTS#30 develop typical neurological features of JBTS with polydactyly and retinopathy and lack the renal or the hepatic involvement.

1.7.31.   JBTS#31: CEP120

JBTS#31 is caused by homozygous or compound heterozygous mutation in *CEP120* on chromosome 5q23.2 (Roosing et al., 2016a). Mutations in *CEP120* can present with pure neurological JBTS symptoms without extra organ involvement as well as complex ciliopathy phenotype.

1.7.32.   JBTS#32: SUFU

JBTS#32 is caused by homozygous mutation in *SUFU* on chromosome 10q24.32(De Mori et al., 2017). It encodes Suppressor of Fused (SUFU) a main negative regulator SHH signalling pathway. Patients with JBTS#32 exhibit polydactyly and cranio-facial dysmorphism.

1.7.33.   JBTS#33: PIBF1

JBTS#33 is caused by homozygous or compound heterozygous mutation in *PIBF1* on chromosome 13q21 (Wheway et al., 2015). It encodes progesterone-induced blocking factor-1 (PIBF1). Patients can present with JBTS classical symptoms with polydactyly, retinal, renal or hepatic involvement.

1.7.34.   JBTS#34: B9D2

JBTS#34 is caused by homozygous or compound heterozygous mutation in *B9D2* on chromosome 19q13.2 (Bachmann-Gagescu et al., 2015). Skeletal abnormalities and facial deformities were reported with no renal or hepatic involvement. B9D2 also known to cause MKS10 (Dowdle et al., 2011).

1.8. Phenotypic / genotypic overlap in Joubert syndrome

As mentioned previously, JBTS have a noticeable genetic heterogeneity as well as phenotypic heterogeneity, that is biallelic or single allele mutations in many different genes cause the same disorder but with wide spectrum of severity and rang of other organs involvement. Some of the phenotypic association in JBTS are well developed and recognized and led to further classification of JBTS into clinical subgroups, which can guide in disease management in the absence of molecular genetic diagnosis. However, Molecular genetic diagnosis is important for family planning counselling, prognostic counselling and management of extra neural manifestations. Due to the broad heterogeneity in the clinical presentation and the genetic cause of JBTS, the preferred molecular genetic testing approach starts with multiple gene panel then followed by whole exome sequencing if the diagnosis not established (Vilboux et al., 2017).
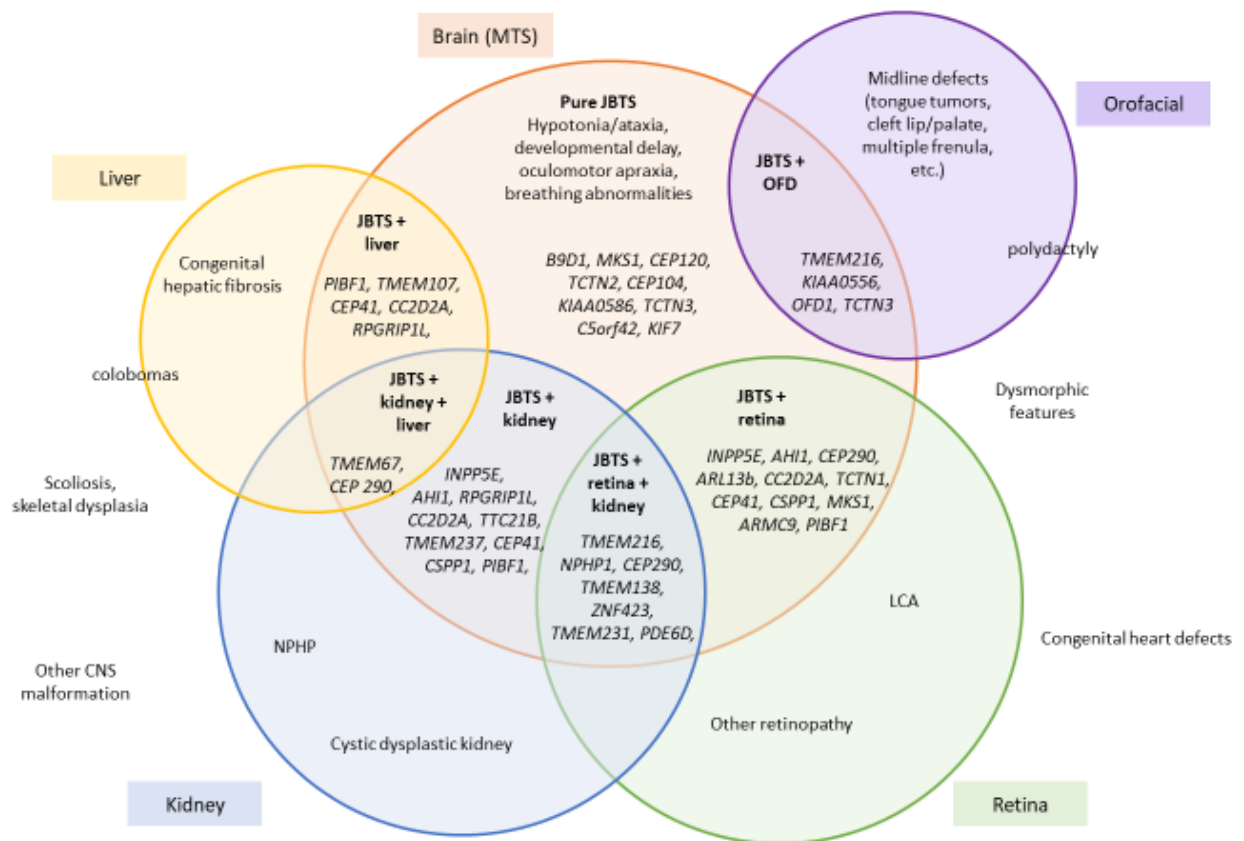
Figure 1.3 Genotype-phenotype correlation in Joubert Syndrome

1.9. The primary cilia

The primary cilium is a hair-like structure protruding from the cell surface in almost every cell type and is a highly conserved specialised organelle of the eukaryotic cell. The primary cilium consists of axoneme, the core of the cilium formed by a circular array of 9 microtubules doublets extending from the mother centriole named the basal body and a transition zone. Cilia assembly is thought to be linked to the cell cycle and happens to occur in consecutive steps. Ciliogenesis starts with the differentiation of mother centriole to the basal body, then the generation of the transition zone, finally the apical migration of axoneme to cell surface (Ishikawa and Marshall, 2011). Even though the ciliary membrane represents a continuation of the plasma membrane, the ciliary composition differs from the rest of the cell composition. Moreover, primary cilia lack the presence of ribosomes which restricts the protein synthesis within the cilium, which explains the presence of a highly specialised protein diffusion barrier at the transition zone that controls the trafficking of proteins in and out of the cilium. (Satir et al., 2010). An intraflagellar transport (IFT) machinery carries the proteins along the axoneme in two separate systems. A kinesin II-based system up toward the cilium tip and a dynein- based sysetem down toward the cilium base termed anterograde and retrograde IFT, respectively (Madhivanan and Aguilar, 2014). The IFT is essentially required for the assembly, elongation and the maintenance of the primary cilia.

The highly-specialised structure of the primary cilia allows it to function as cell antenna, sensing, transducing and responding to various stimuli from and to the surrounding environment. Those various stimuli are received via specific ciliary receptors found along the ciliary membrane, including mechanoreceptors, thermoreceptors, photoreceptors, osmoreceptors, olfactory receptors and hormones receptors. The cells response to these extracellular stimuli regulates proliferation, differentiation, polarity, growth and morphology. The primary cilia play vital role in regulating signalling pathways crucial for normal embryonic development like sonic hedgehog (SHH), Wnt and Notch pathways (Hildebrandt et al., 2011a, Goetz and Anderson, 2010).
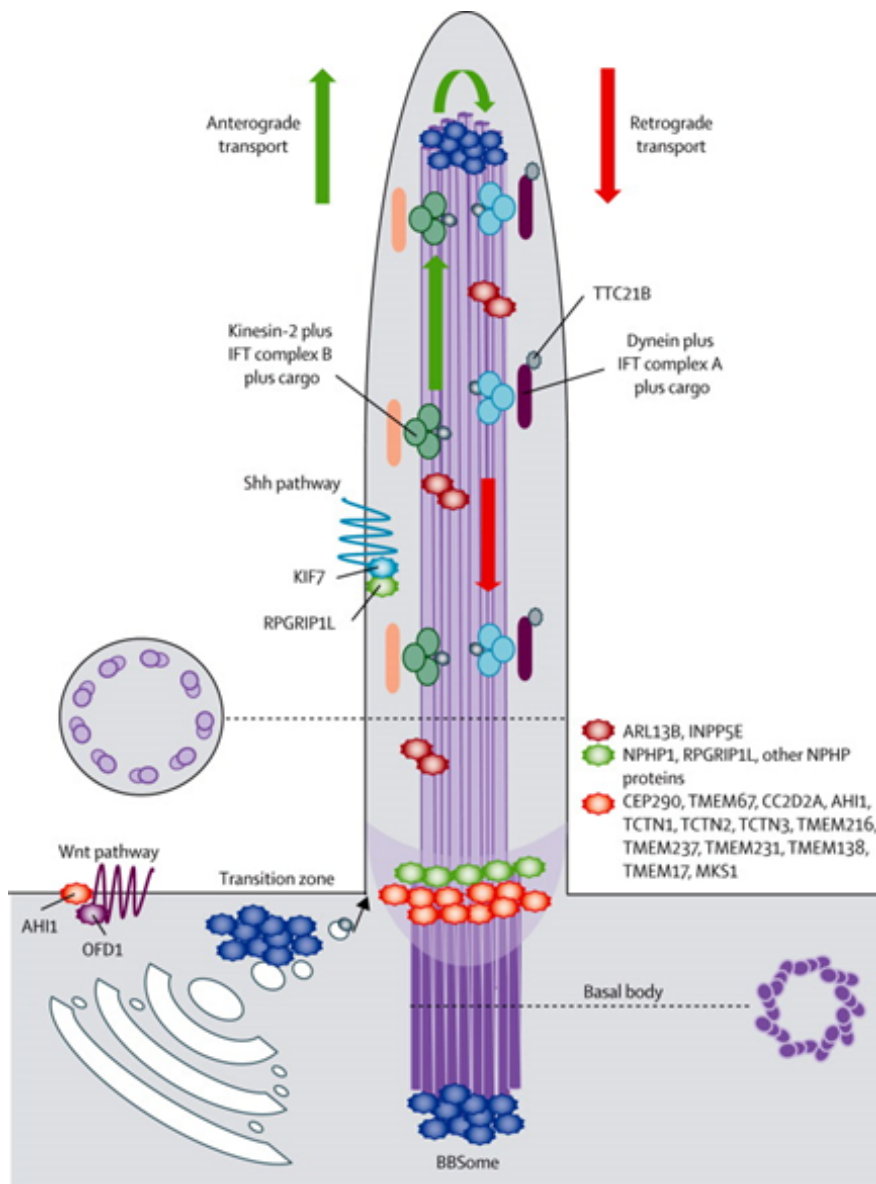
Figure 1.4 Schematic representation of the structure of the primary cilium and its protein complexes

Figure taken from (Romani et al., 2013)

1.10.   Maintaining the ciliary protein composition

It's the cilia distinct protein composition that promotes its signalling function. The primary cilia maintain its unique protein compositing through controlling protein access to and from the cilium as well as protein to protein interaction within the cilium. Proteins enter the cilia are either integral membrane proteins, small soluble proteins, large soluble proteins or membrane associated protein. Ciliary proteins gain their entry to the cilium by lateral transport from the plasma membrane and vesicular trafficking of ciliary proteins from Golgi at the base of the cilia (Nachury et al., 2010).

As mentioned above, primary cilium is an isolated domain, while the ciliary membrane separates the cilia projection into the extracellular compartment, it's the presence of the barrier at the base of the cilia that's draw its cellular boundaries. The barrier components are the periciliary membrane, transition fibres, ciliary necklace and ciliary pockets (Madhivanan and Aguilar, 2014). The periciliary membrane arises where the basal body distal appendages are attached. The transition fibres (arising from distal appendages) form a propeller like structure with nine sheets connecting the centriole directly to plasma membrane, allowing only too small vesicles to pass through. Distal to the transition fibres lies a septin ring believed to separate the periciliary compartment from the ciliary compartment and function as diffusion barrier at the base of the cilium (Hu et al., 2010). More distal is the transition zone where the ciliary necklace connects the axonem to the ciliary membrane, consisting of protein complexes forming 'Y-links' structures (Garcia-Gonzalo and Reiter, 2017). Ciliary proteins complex at the transition zone function as smart gate officers validating the access of ciliary cargo proteins preloaded at the transition fibres allowing their trafficking to the ciliary axonem.

Specialised short signal sequence were found to play essential role in directing and trafficking ciliary proteins to the cilia, known as Ciliary targeting signals (CTSs) (Malicki and Avidor-Reiss, 2014). CTSs were often found to localise at the protein C-terminus, less likely at the N-terminus or rarely at the intracellular loop. Many CTSs have been reported with different localisation and different role in ciliary targeting from one protein to another. A good example is the QVSAPA sequence, first being reported to mediate the interaction of Rhodopsin with its carrier Arf4 to be transported from Golgi in cases of retinitis pigmentosa caused by mutation in *RHO*

the gene encoding Rhodopsin (Deretic, 2006). In contrast, disruption of the same QVSAPA sequence in INPP5E has no effect on its ciliary localisation (Humbert et al., 2012). Small size soluble protein ciliary trafficking is mediated by diffusion and retention rather than active transport machinery, on the other hand, large soluble proteins require CTSs as well as GTP/GDP gradient to facilitate their entry at the base of the cilia (Kee et al., 2012).
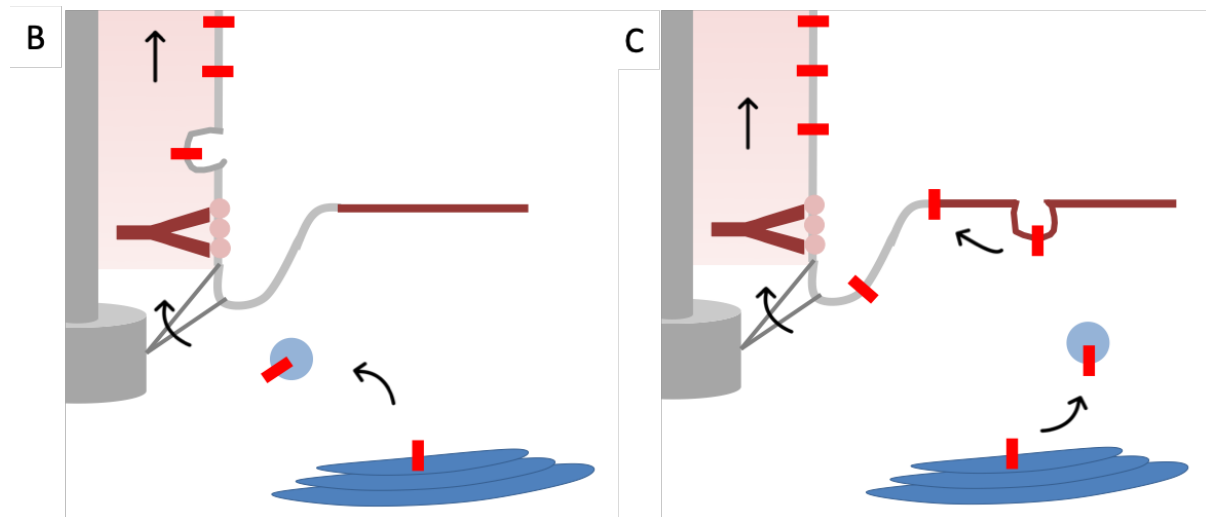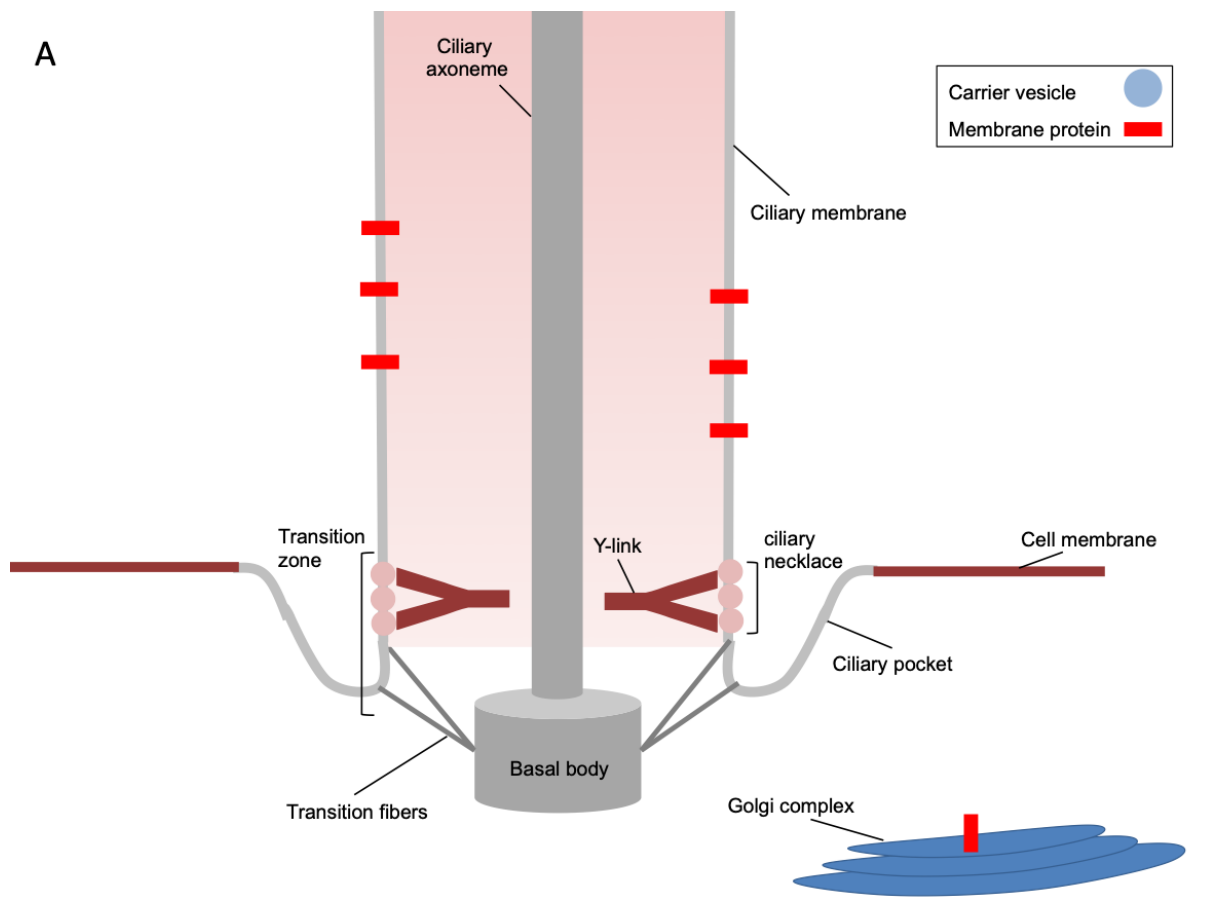
Figure 1.5 Ciliary membrane protein trafficking

(A) Structure of cilia base diffusion barrier "the transition zone" consisting of ciliary necklace, Y-links and transition fibres.

(B) Post Golgi vesicles delivering membrane protein to the cilia by fusing with ciliary membrane.

(C) Post Golgi vesicles are delivered to plasma membrane then cross the diffusion barrier to reach ciliary membrane

1.11. Ciliary trafficking of post-translational lipid-modified proteins

Myristolation and prenylation are post-translational lipid-modification of some of the membrane associated proteins to increase their membrane hydrophopicity. Myristolation is the addition of hydrophobic myristoyl group to protein N-terminus, while prenylation is the addition of hydrophobic prenyl group to protein C-terminus. Some of ciliary proteins are lipid-modified like INPP5E and PDE6. Lipid-modified ciliary proteins require solubilising factors to promote their ciliary trafficking known as Guanosine nucleotide Dissociation Inhibitor (GDI) like solubilising factors (GSFs) including PDE6D, UNC119a and UNC119b proteins (Wright et al., 2011). Upon their entrance to the cilia, GSFs bind to their releasing factors releasing the ciliary cargo to the ciliary membrane. ARL2 and ARL3 are known releasing factors, small G-proteins belong to the ADP ribosylation factor-like (Arf-like) subfamily (Ismail et al., 2011). ARL3 localises to the cilia whereas ARL2 function at the periciliary compartment. Releasing factors activity is GTP dependent, regulated by guanine exchange factor (GEF) promoting the binding of the release factor to the GSF and inducing a conformational shift releasing the ciliary cargo. Also, regulated by GTPase-activating proteins (GAP) that inactivate the release factor by switching it to the GDP-bound state. ARL3 has major role in cytokinesis and cilia signalling (Zhou et al., 2006). A heterozygous *ARL3* human mutation has been previously reported in a patient with retinal dystrophy and biallelic *ARL3* loss of function in mice leads to typical ciliopathy phenotype with severe manifestations (Schrick et al., 2006). ARL3 is regulated by its GEF ARL13B, cilia-specific protein when mutated in human gives rise to JBTS with retinopathy (Gotthardt et al., 2015). ARL3 also regulated by its GAP RP2, a pre-ciliary protein when mutated in human leads to X-linked non syndromic retinitis pigmentosa (Veltel et al., 2008).

1.12.   Patient-derived cells to model ciliopathies

The presence of primary cilia is a characteristic of various tissues and cell types as well as cultured cell lines. The early identification of primary cilia structure and frequency was done by electron microscopy, which is labour extensive and time-consuming process for research and experiments (Smith et al., 1969, Rieder et al., 1985). Later came the implication of immunostaining techniques experiments with antibody against microtubules (Ho and Tucker, 1989, Kilmartin et al., 1982). Alieva et al. (1999) proposed an experimental model using intensive immunofluorescence antibodies against primary cilia in different tissue cultures, to study cilia frequency and correlation to cell cycle using light microscopy.

Many investigators used patients derived cells to study the disease pathogenesis, especially for diseases like ciliopathies. Fibroblasts make the skin basal layer (dermis) contain primary cilia, which can be derived and cultured from skin biopsies (Wilson and McWhorter, 1963). In vitro, the monolayer fibroblast cell culture can reach confluency with percentage of ciliation up to 90% (Wheatley, 1995). The use of electron microscopy (**Figure 1.6**) and immunofluorescent staining microscopy (**Figure 1.7**) of patients derived fibroblasts cell culture had been widely reported using specific immunofluorescent antibodies against basal body, axoneme, cilia membrane and ciliary cargo proteins (Novarino et al., 2011). Such techniques allow good cilia visualisation and assessment of its structure and function.

A good example of human derived-cells to study primary cilia are the renal tubular epithelial cells. However, obtaining human renal tissue is a difficult process requiring invasive procedure such as renal biopsy. Renal biopsies can be traumatic and carry significant morbidity and a small, but real, risk of mortality (Corapi et al., 2012). Human urine derived renal epithelial cell (HUREC) culture is a non-invasive way of isolating human renal tubular epithelial cells from both adults and children and serving as an excellent model to study ciliopathies (Srivastava et al., 2017, Ajzenberg et al., 2015) **Figure *1.8*.**
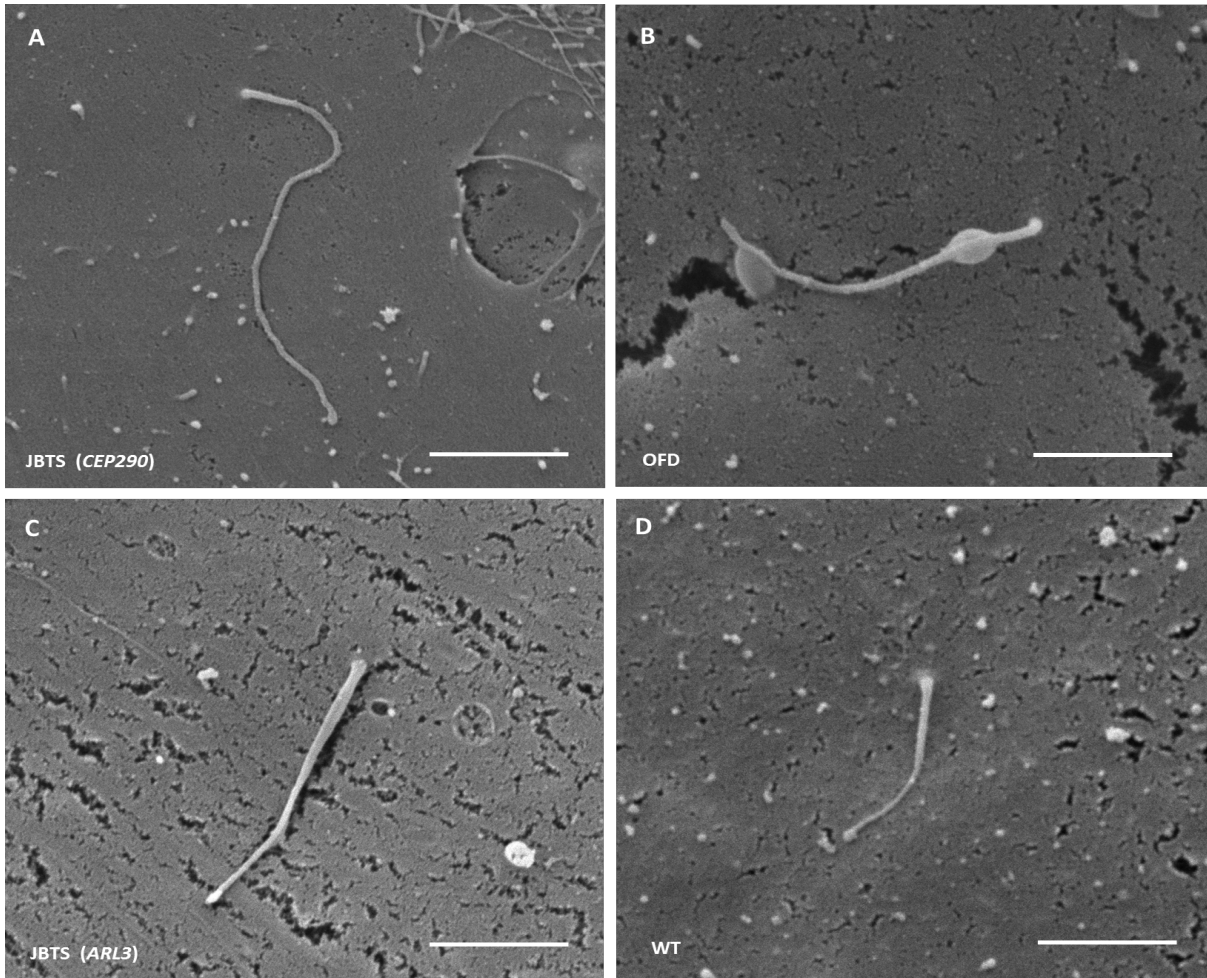
Figure 1.6 Scanning electron microscopy (SEM) images of patients-derived fibroblasts with ciliopathies.

Fibroblasts from affected individuals with ciliopathies seen under SEM showing:

   A. Long cilia in *CEP290* patient fibroblasts causing JBTS phenotype

   B. Dilatation of ciliary membrane phenotype in OFD patient fibroblasts

   C. Normal appearances of primary cilia in *ARL3* patient fibroblasts causing JBTS phenotype

   D. Wild type (WT) (Scale bar 2 μm).
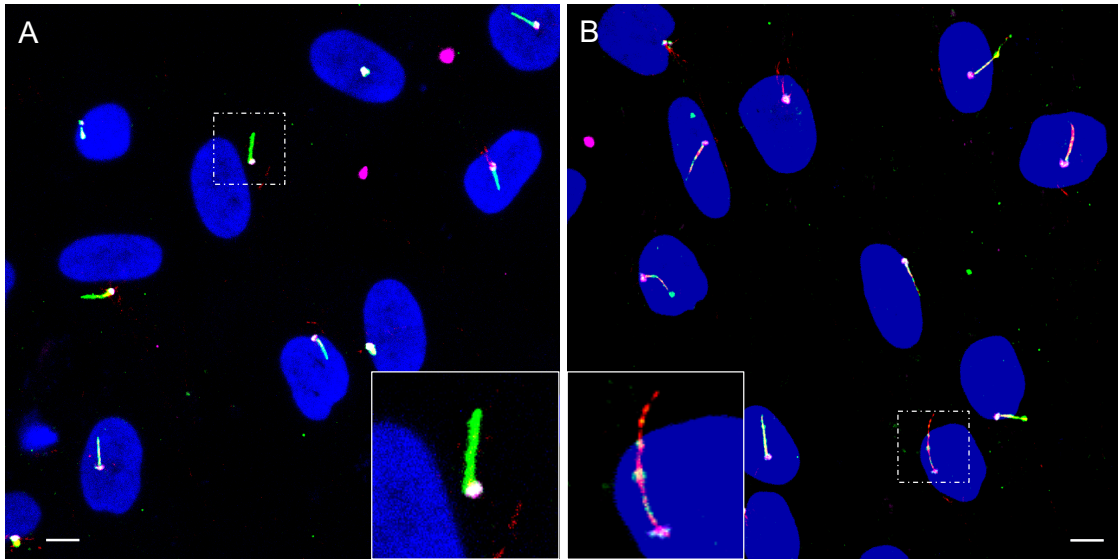
Figure 1.7 Fibroblast cilia derived from patient with *CEP290* mutation causing Joubert syndrome

Immunofluorescence staining using anti-alpha-acetylated tubulin (red) to identify axoneme and anti-ARL13B (green) to identify ciliary membrane in healthy carrier (A) and JBTS (B) cells in low power and zoomed. Scale bar 5 μm.
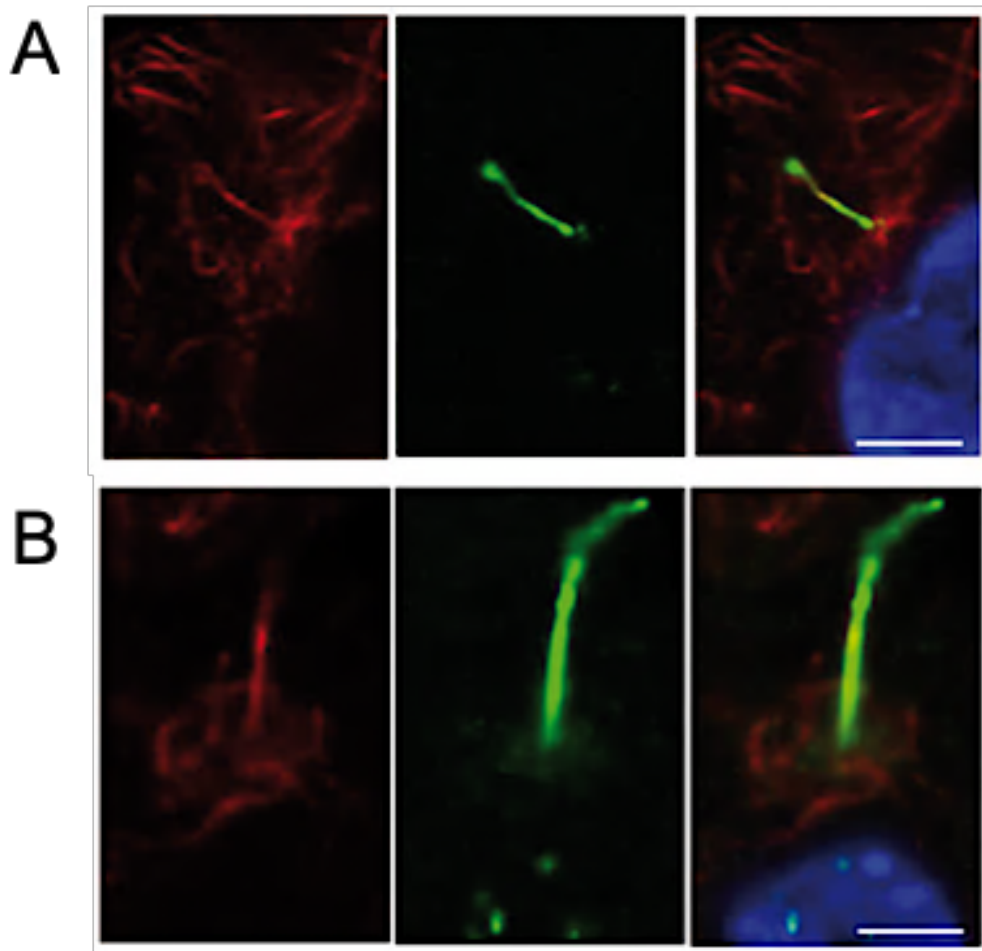
Figure 1.8 Human urine renal epithelial cell (HUREC) cilia derived from a patient with *CEP290* mutations causing JBTS phenotype

Immunofluorescence staining using anti-alpha-acetylated tubulin (red) to identify axoneme and anti-ARL13B (green) to identify ciliary membrane in wild type (A) and JBTS (B) cells (Scale bar 5 μm). Image taken from (Srivastava et al., 2017)

1.13. Aims of project

According to the literature ciliopathies are caused by mutations in more than 50 genes and up to date genetic causes of JBTS are unknown in >50% of the clinically diagnosed cases. Via the renal family genetics clinic, we aim to:

1. Define clinical phenotypes of cohorts of patients with renal ciliopathies.
2. Explore molecular genetic diagnosis in "unsolved" ciliopathy patients with Joubert syndrome in order to identify novel genetic causes; undertake whole exome sequencing and examine candidate gene variants with *in silico* tools and explore gene expression profiles.
3. Undertake cell biological studies to explore mechanism of action of novel JBTS causing gene.

Chapter 2 **Materials and Methods**

2.1. **Consent and ethical approvals**

All patients and their relatives consented to this study. Ethical approval was obtained from the National Research Ethics Service (NRES) Committee Northern and Yorkshire (09/H0903/36) for urine cell studies and NRES Committee North East – Newcastle and North Tyneside 1 (08/H0906/28+5) for DNA and biobanked fibroblasts. Following informed and written consent, blood samples were obtained from affected patients and their relatives and healthy gender and age-matched controls. Skin fibroblasts were obtained from patients and their relatives following informed written consent and stored in Newcastle MRC Centre Biobank for Neuromuscular and Rare Diseases.

2.2. **Clinical review of patients**

Patients and family members were seen within the context of a regional family renal genetics clinic, run by Professor Sayer at Newcastle Hospitals NHS Foundation Trust. This clinic allows pedigrees to be drawn, clinical history and examination to be performed and molecular genetic testing to be discussed. Families were invited to join and consent to research studies following these discussions.

2.3. **DNA sampling and genetic studies**

Genomic DNA was extracted from venous blood from affected siblings, unaffected siblings and their unaffected parents and relatives using a DNA extraction robot based at the Northern Genetics Service, Newcastle.

Genomic DNA (2μg) from two affected siblings and their parents was subjected to whole exome paired-end sequencing analysis with 100× coverage by generating 51 Mb Sure Select V4 libraries (Agilent Technologies, USA). The sequence reads were run on a HiSeq2500 platform (Illumina, San Diego, CA, USA). Bioinformatic pipelines provided by GATC generated vcf files. Ingenuity Variant Analysis web-based application and HomozygosityMapper (http://www.homozygositymapper.org/) was used for data analysis of vcf files. The variants of interest were further tested for likely pathogenicity using in silico prediction tools.

In silico prediction tools were used are PolyPhen-2 (http://genetics.bwh.harvard.edu/pph/), Provean (http://provean.jcvi.org/index.php),

and MutationTaster (http://www.mutationtaster.org/). PolyPhen-2 scores range from 0 to 1, the higher the score the more damaging the amino-acid substitution. Provean scores range from 0 to 1. The amino-acid substitution is predicted damaging if the score is ≤ 0.05, and tolerated if the score is > 0.05. Allele frequency of novel sequence variants was determined using the Exome Aggregation Consortium (ExAC) database (http://exac.broadinstitute.org/) and the Genome Aggregation database (gnomAD) (http://gnomad.broadinstitute.org). Z score is used to quantify deviation from expectation; synonyms variants are centred at zero and significant shift to higher values constrain missense and nonsense mutations.

The variants were confirmed using Sanger sequencing in all available family members to confirm segregation with disease status.

Primers for ARL3 exon 5 were designed using online tool Primer 3 (http://primer3.ut.ee/)

| ARL3 forward primer | 5'-TCGGTTAGCTGTCATGTTGC-3' | Predicted DNA |
| ARL3 reverse primer | 5'-CTGGGAAGCGAAGGTTGC-3' | length 400 bp |

Primers were constructed by Integrated DNA Technologies, Inc.

2.3.1. PCR Protocol

PCR reactions used 50-100 ng of genomic DNA, 10 pmol of forward and reverse primers and Taq PCR Master Mix (Qiagen, cat No. 201445)

A typical 30 µl PCR reaction consisted of 1 µl of DNA, 1 µl of forward and reverse primers, 15 µl Master Mix and 12 µl water.

Using a touchdown PCR, cycling conditions were as follow; 95°C for 10 min, 94°C for 20 s, 72°C for 20 s, 72°C for 1 min, 94°C for 20 s, 54°C for 20 s, 72°C for 1 min for 20 cycles, 72°C for 10 min and a final hold of 4°C to stabilise and prevent degradation of PCR product.

2.3.2. Agarose Gel electrophoresis

PCR amplification products were analysed using Agarose gel electrophoreses. 3 ml of 6X loading dye (Promega, G190A) was added to 5 ml of PCR products to track the migration during electrophoresis, then loaded on 2% agarose gel (NBS biological

Agarose Low EEO cat # NBS-AG500) with 1X TAE buffer. GelRedTM (Biotium, cat # 41003) was added to the gel mixture prior casting to visualise the DNA fragments band. 5 ml 100bp DNA ladder (Promega, G2101) was loaded to determine the size of DNA product (400 bp). DNA bands were sufficiently separated after 30 minute at 100V.

2.3.3. DNA purification

DNA purified from PCR products by centrifugation using Wizard ® SV gel and PCR clean up system (Promega, REF A9281). An equal volume of Membrane binding solution was added to the PCR amplifications. Then the dissolved mixtures were transferred to collection tubes with SV Mini-columns and centrifuged at 16,000x g for 1 min after incubation period of 1 minute at room temperature. Followed by washing steps, 700 µl of Membrane wash Solution added then then centrifuge at same speed for 1 min to remove solution. Washing repeated but with 400 µl Membrane wash solution and 5 min centrifugation. Recentrifugation of the last wash for 3 minutes with microcentifuge lid open to allow evaporation of residual ethanol. Last step, DNA elution was prepared by transferring SV Mini-columns to 1.5 ml centrifuge tube, adding 50 µl of Nuclease-free water and incubation at room temperature for 1 min. centrifuge at same speed for 1 minute the discard the mini-column and store DNA at 4°C.

DNA purified from PCR products were sent with forward primer for Sanger sequencing to GATC Biotech (Cologne, Germany).

Sequenced data were downloaded as ab1, seq or fas file and analysed using software including MutationSurveyor and Chromas.

2.4. Fibroblasts 2D cell culture

Skin biopsies taken from patients and controls unaffected carrier parents and unaffected wild type sibling by Dr David Steel, Sunderland Eye Infirmary and stored in Newcastle Biobank. Specimens were transported in a sterile tube containing 6 ml of Ham's F-10-complete Medium at 4°C before processing.

Patients and control fibroblasts were isolated from skin biopsies, grown at 33°C in T25 cell culture flasks with Fibroblast growth medium. After reaching confluency of 80-90%, cells were detached using 3ml of trypsin and re-suspended with growth

media. After centrifugation for 5 min at 1200 rpm, cells were re-suspended in growth media and splitting in 1:4.

2.4.1. Fibroblast growth medium

DMED 1X (Thermo Fisher, 41966-29), 10% foetal bovine serum (Thermo Fisher, cat # 10500056) and 1% Penicillin /Streptomycin (Thermo Fisher, 15070-063).

For ciliogenesis and ciliary protein signal intensity experiments, cells were seeded on coverslips and grown to 70-90% confluency then starved for 48 h (in minus FBS medium) to induce ciliogenesis.

For the SAG experiment, cells were seeded on coverslips and grown to 70-90% confluency then cells were treated with 100 nM SAG (Tocris cat# 4366) after 24 h of starvation. Next, cells were incubated for another 24 h in starvation medium.

Cells on coverslips were fixed with 100% ice cold methanol for 15 min, washed three times with Phosphate-buffered saline (PBS).

2.5. Immunofluorescence staining

Coverslips were blocked for 30 min to 1 h in PBS with 10% bovine serum albumin. For indirect immunostaining of primary cilia, primary antibodies diluted in blocking solution rabbit anti-INPP5E 1:100 (Proteintech 177197-1-AP), rabbit anti-GLI3 1:200 (Abcam ab69838) and mouse anti-PERICENTRIN 1:1000 (Abcam ab28144) and incubated in room temperature for 1 hr or in 4 °C overnight NPHP3 1:100 (Proteintech 22026-1-AP). Followed by three washes with PBS 15 min each. Cells were incubated at room temperature for 1 h with Alexa Fluor conjugated secondary antibodies diluted in blocking solution 1:400 donkey anti-rabbit Alexa Fluor 488 (Thermo Fisher Scientific); goat anti-mouse Alexa Fluor 647 (Thermo Fisher Scientific) followed by three washes 15 min each.

For direct immunostaining of primary cilia, Zenon Tricolor Rabbit IgG Labelling Kit (Thermo Fisher, Z-25360) was used. Primary antibody ARL13B 1:400 (Proteintech, 17711-1AP) diluted in PBS was mixed with 5 µl of labelling mix, incubated at room temperature for 5 min. 5 µl of blocking mix was added, followed by a further incubation for 5 min. Cells were incubated overnight in 4°C in labelled antibody solution followed by three washes in PBS-Tween 20% 15 min each. Cells were re-fixed in 4% PFA for 15 min at room temperature then washed 3 times with PBS.

Coverslips were mounted on slides using mounting medium with DAPI Vectashield (Vector Laboratories Ltd, H-1200).

2.6. Confocal microscopy

Images were obtained with confocal microscopy (Nikon A1), with an optical magnification of 60X and additional digital zooming of desired filed to gain better image quality. Z-stacks were created using the same laser intensity as well as camera settings. Images were captured and exported as ND2 file.

Image analysis obtained using Fiji (ImageJ) software.

2.6.1. Cilia length and ciliation rate

For experiment quantifying the percentage of ciliogenesis, 4-5 60X fields were analysed then the average was calculated. For each field the percentage of ciliated cells labelled with ARL13B was scored as a proportion of total nuclei labelled with DAPI. The segmented line tool was used to measure cilia length from base of axoneme (PERICENTRIN) to cilia tip on a maximum intensity projection of a z-stack.

2.6.2. Ciliary antibody signal intensity

For antibody signal intensity quantification experiments, 4-5 60x fields were analysed. On a sum slices intensity projection of a z-stack, freehand tool was used to mark cilia borders using ARL13B signal, the region of interest (ROI) constructed to measure the mean signal intensity of ciliary antibody staining (e.g. INPP5E, NPHP3 or GLI3). Then ROI was duplicated and dragged to nearby area to correct for local background intensity by simple subtraction.

2.7. Electron microscopy methods

Processing and imaging technique for scanning electron microscopy (SEM) were provided by Dr. Kathryn White, EM Research Serveries, Newcastle University.

Patients and control fibroblasts cells were seeded on transwell filters and incubated for 24 h in fibroblast growth media at 37°C. Then were starved for 48 h to induce ciliogenesis.

Samples were fixed in 2% glutaraldehyde Sorenson's phosphate buffer solution (provided by EM services, Newcastle University) and kept in 4°C overnight. Prior sending to EM services, samples were dehydrated in ethanol solutions (25%, 50%,

75% - 30 minutes each). Followed by 2X wash with 100% ethanol 1 h each. A final dehydration with carbon dioxide in a Baltec Critical Point Dryer was used. Samples were then mounted on sticky carbon discs and coated with gold, 5-10 nm, using a Polaron SEM Coating Unit. Samples were examined using TESCAN VEGA LMU Scanning Electron Microscope and the images were collected with TESCAN supplied software.

2.8. Human urine-derived renal epithelial cells culture (HURECs)

Urine sample were collected from patients / controls (50-100 ml) in sterile containers, kept in 4°C while and processed within 4 h of collection. Samples were transferred to falcon tubes and centrifuged for 10 min at 400 rcf then the pallet was re-suspended in 10 ml of washing buffer. Further centrifugation of the suspension for 10 min at 200 rcf. Later the pallet was re-suspended in 2 ml of primary media and plated in a single well of 12-well plate and incubated at 37°C and 5% CO2. For the next 96 h, 1 ml of primary media was added each day. On day 4, 4 ml of primary media were decanted and replaced with 1 ml of proliferation media. Every day, 1 ml of media was removed and 1 ml of fresh media was added.

The epithelial cells begin to appear on day 5-14 and can be used for passaging or experiments after reaching 80- 90% confluence.

2.8.1. Primary medium for HUREC culture

Primary medium for HUREC has the following components – 5% Fetal Calf Serum, Penicillin/Streptomycin (140 U/ml+140 U/ml), Amphotericin B, Supplements of REGM Single quot kit, DMEM/High Glucose, Ham's F12 Nutrient Mix.

2.8.2. Proliferation Medium for HUREC culture

Proliferation medium for Human Urine derived Epithelial Cell culture has the following components - Penicillin/Streptomycin (140 U/ml+140 U/ml), Amphotericin B, Supplements of REGM Single kit (Lonza, CC-3190), REBM medium from the REGM Bullet kit (Lonza, CC-4127).

2.8.3. Washing Buffer for HUREC culture

Washing Buffer is DPBS (Thermo-Fisher) supplemented with Penicillin/Streptomycin (140 U/ml+140 U/ml), Amphotericin B (1 µg/ml).

2.9. **siRNA *ARL3* knockdown experiment**

HURECs (0.05×10^6) were transfected with 5 pmol Negative Control siRNA (AM4611, ThermoFisher) and siGENOME Human *ARL3* siRNA- SMARTpool (DharmaconTM, M-011813-00-0005), using Lipofectamine RNAiMAX (ThermoFisher, 13778150) under manufacturer's instructions.

2.9.1. Whole cell RNA extraction

HURECs were grown to confluency on 6-well plates and treated as described above. 48 h after transfection, cells were rinsed with PBS to remove floating dead cells, media and transfection reagents. 200 µl of protein extraction buffer (4 M urea, 125 mM Tris pH 6.8, 4% SDS, 10% glycerol, 5% β-mercaptoethanol and 0.02% bromophenol blue solution) was added and the cells were removed from the well using cell scrapper. Samples were aliquoted and stored at 20°C until required.

RNA was extracted by spin technology using RNeasy® mini kit (QIAGEN) according to the manufacturer's instructions, and quantified using a NanoDrop 2000 Spectrophotometer (Thermo Fisher Scientific).

2.9.2. Reverse Transcription

Reverse transcription was required to produce cDNA from RNA using SuperScript III® Reverse Transcriptase (Invitrogen). 1 µg of RNA was reverse-transcribed using RT-PCR was required to confirm the knockdown of ARL3 gene at protein level.

2.9.3. RT-PCR methods

The resulting cDNA was diluted 10-fold in nuclease-free water. Real-time PCR was carried out in a 10 µl reaction volume containing the following: 0.5ul of each primer (10uM stock) with 0.5 µl water, 4 µl of cDNA and 5 µl of PrimeTime® Gene Expression Master Mix (IDT). The PCR was run using a QuantStudio™ 7 Flex Real-Time PCR System (Applied Biosystems) using the following settings: 95°C for 20 seconds, followed by 40 cycles of 95°C for 1 second 60°C for 20 seconds. The PrimeTime® assays used were as follows: GAPDH (Hs.PT.39a.22214836), HPRT1 (HsPT.58.20881146), and ARL3 (Hs.PT.56a.40668589) all structured by Integrated DNA Technologies, Inc.

2.10.   Homology modelling

Human ARL3 (UniProt accession code P36405) and ARL13B (UniProt accession code Q3SXY8) were modelled on the crystal structure of the Arl3-Arl13B complex from *Chlamydomonas reinhardtii* (PDB accession code 5DI3) using HHPred (REf1) and Modeller (REF2) software. Structures were visualised, and figures prepared using PyMOL (http://www.pymol.org/).

2.11.   Protein expression and purification

Chlamydomonas reinhardtii and murine full-length ARL3, *Chlamydomonas reinhardtii* ARL13B 18-278, and human full-length UNC119A were expressed and purified as previously described (Ismail et al., 2012). Human ARL13B 18-278 was cloned into pET20b with an N-terminal 12×His-tag and purified using the same protocol as ARL3 with the addition of 10% glycerol to the purification buffers and storing the protein in 5% glycerol. p.Arg149His mutation in *ARL3* and p.Glu86Arg mutation in *ARL13B* were introduced using the Q5 site directed mutagenesis kit (NEB).

2.12.   Guanine nucleotide exchange assay

Murine ARL3 used for GST pull-downs was exchanged with the non-hydrolysable analogue of GTP, GppNHp. 300 µM ARL3 was incubated with 2 mM GppNHp and 0.14 U/µL Alkaline Phosphatase (Roche) overnight at 15°C. Excess nucleotides were removed by size exclusion chromatography on a Superdex S200 Increase column (GE Healthcare). GppNHp-loaded ARL3 was quantified using HPLC analysis and C18 columns (UltiMate3000, Thermo Fisher Scientific). For the GEF assay, nucleotide exchange of murine and *Chlamydomonas reinhardtii* ARL3 proteins with mantGDP was carried out by incubating 100 µM ARL3 protein with 200 µM mantGDP for 2 h at room temperature in the presence of 50 mM EDTA. For nucleotide exchange to GppNHp on human and *Chlamydomonas reinhardtii* ARL13B, 100 µM ARL13B was incubated with 500 µM GppNHp and 50 mM EDTA, also for 2 h at room pressure. All reactions were carried out in 20 mM tris pH 7.5, 150 mM NaCl, 5 mM MgCl2 and 2 mM DTT and were stopped by adding 100 mM MgCl2. Unbound nucleotides were removed by using a PD10 desalting column (GE Healthcare), and the proteins were concentrated using Amicon Ultra 0.5 mL units (Merck Millipore) with a molecular weight cut-off of 3 kDa. All reactions were carried out in 20 mM Tris pH 7.5, 150 mM NaCl, 5 mM MgCl2 and 2 mM DTT at room

temperature. Fluorescence polarisation was measured at an excitation of 366 nm and emission of 450 nm. 0.5 μM of CrARL3•mantGDP was measured for 100 s, after which 10 μM GppNHp was added and measured for an additional 100 s. Finally, 5 μM of *Cr*ARL13B•GppNHp was added and changes in fluorescence polarisation were recorded for 300 s. The same was repeated for *Hs*ARL13B, but starting with 1 μM of murine ARL3•mantGDP to which 400 μM GppNHp was added followed by 5 μM *Hs*ARL13B.

2.13. **GST pull-downs**

30 μg of GST-tagged full-length UNC119A and 60 μg of GppNHp-loaded murine ARL3 WT and p.Arg149His were incubated in 20 mM Tris pH 7.5, 150 mM NaCl, 5 mM MgCl2 and 2 mM DTT for 15 minutes at room temperature before adding to Glutathione sepharose 4 FF beads (GE Healthcare) and incubating for a further 20 minutes. Beads were washed 5 times in reaction buffer before eluting with reaction buffer containing 20 mM Glutathione.

Chapter 3   **Overview of Renal-Genetic Family Clinic**

3.1. **Introduction and aim**

Inherited kidney disorders are classified under rare disorders, which affect a limited number of individuals defined as affecting <1 in 2000 people in Europe or < 200 000 people in the USA (Schieppati et al., 2008). Rare kidney disorders include at least 150 different diseases with an overall prevalence of about 60-80 cases per 100 000 in Europe and the USA (Soliman, 2012).

Inherited disorders have a well-recognised medical, psychosocial and economic burden on the affected families, as well as the health care provider. Inherited kidney disorders are known to cause chronic kidney disease progressing to end stage renal disease (ESRD) requiring dialysis or renal transplantation in both children and adult populations. The primary causes of chronic kidney disease in children differ from those in adults. In the UK, the causes of ESRD in children include congenital anomalies of the kidneys and urinary tract (CAKUT) in ~ 35% of cases, congenital nephrotic syndrome in 10% and cystic kidney disease in 5% of cases (Karger and Paris, 2013). A report from the USA agreed with the causes of childhood ESRD with an increased prevalence of CAKUT of 49.1% (Smith et al., 2007). CAKUT is also responsible for a significant proportion of adult or late onset ESRD, whereas, autosomal dominant polycystic kidney disease (ADPKD) accounts for ~10% of adult ESRD in the UK (Julie Gilg, 2015). Mutations in genes encoding transcription factors essential for renal development and maintenance including *WT1*, *PAX2* and *HNF1B* may lead to both renal tract malformation and renal syndromes with significant extra renal manifestations (Thomas et al., 2011). Mutations in the *COL4* genes give rise to inherited collangenopathies such as Alport syndrome (a recognised cause of adult onset kidney disease) and familial haematuria syndromes (Gast et al., 2016).

Early recognition and awareness of inherited kidney disorders are required by taking a detailed family history (McCloskey et al., 2016). Diagnosis and management of these forms of disease are extremely important. The diagnostic process of inherited disorders practiced by most clinical geneticists is long and exhausted, with clinical assessments followed by subsequent laboratory and genetic testing based on each previous test being negative. The combined practice of a multidisciplinary clinic and

the application of next-generation sequencing has facilitated a more streamlined identification of the genetic causes of inherited kidney diseases.

We aim to describe a cohort of patients attending a multidisciplinary renal genetics family clinic in the north of England and the insights gained from this clinic experience.

3.2. Materials and Methods

A multidisciplinary renal genetics family clinic was established in 2010 in the Renal Services Department of Freeman Hospital, Newcastle Upon Tyne Hospitals NHS Foundation Trust. The clinic aims to find precise molecular genetic diagnosis for patients with inherited renal disorders, guide management, provide genetic screening, and proper genetic counselling to the attending families. The clinic is hosted every three months where the patients and their families have the opportunity to meet with an adult nephrologist, paediatric nephrologist and a clinical geneticist simultaneously in the same clinic session and room. The clinic is a gateway to perform genetic testing, using targeted single gene screening and gene panels available by the UK Genetic Testing Network (UKGTN, https://ukgtn.nhs.uk/). A retrospective review of clinic cases and their molecular genetic diagnosis over a 5-years period was performed. Patients' data were reviewed from the hospital electronic records. Individual's age at referral, date of birth, sex, ethnicity, address and reasons for referral were extracted. The probands' medical history and a three-generation family pedigree/history were taken and the presence or the absence of a genetic diagnosis prior referral was noted. Outcomes includes genetic diagnosis following the clinic visit and specific management plans were reached when possible.

3.3. **Results**

3.3.1. Newcastle family renal genetics clinic demographics

Between 2010 and 2015 a total of 244 individuals were seen in the clinic, 80 probands and 164 family members; 50 affected relatives and 114 unaffected relatives. The number of relatives ranged from 1 to 7 family members in total and with a mean of ~3 members per referral. The age of probands at their first clinic review ranged between newborns to adults of 57 years of age. A fifth of probands were under 18 years old and the mean age at the time of referral was ~19-year-old. Probands were from white Europeans families with no know consanguinity, except six probands of Asian origin, two of whom were from consanguineous families.

Referrals were from different NHS services; the clear majority were from paediatric nephrology services accounting for 56 of the 80 probands. The rest were from adult nephrology (14 cases), primary care (4 cases), clinical genetics (3 cases), surgery (2) and oncology (1 case) **Figure *3.1***.
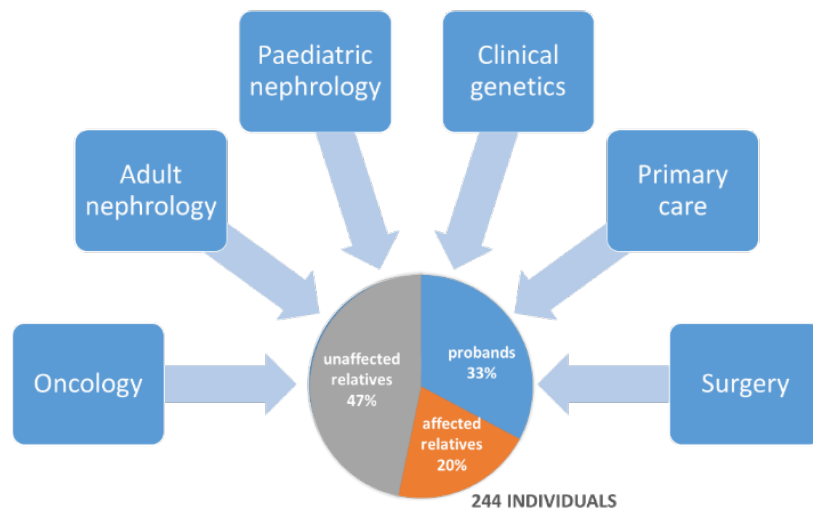
Figure 3.1 Origin of referral into Newcastle family renal genetics clinic

The renal family genetic clinic at Freeman Hospital in Newcastle upon Tyne was designed to be a tertiary referral centre serving not only local referrals but also attracting cases from the whole of the north of England. Individuals were referred from as far as Scarborough (99 miles) and Whitehaven (97 miles) **Figure *3.2***.
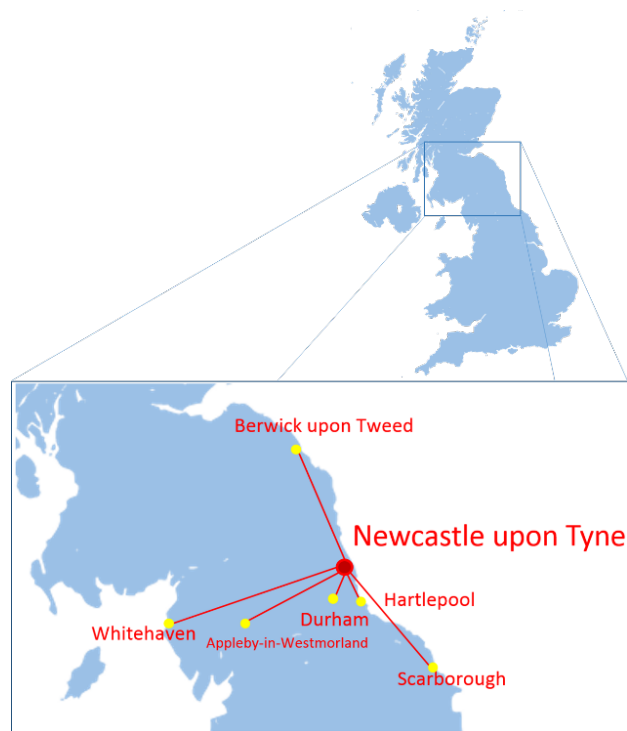
Figure 3.2 Reach of Newcastle family renal genetics clinic

3.3.2. The clinic setting

The probands and their relatives met the clinicians in a relaxed outpatient setting, initial investigations included blood pressure and urine sample to detect proteinuria and haematuria. Explaining the aim of clinic was crucial to reassure some of the individuals regarding their visit. Discussion, usually bidirectional, detailed medical history and extended family medical history were taken by physicians, on the other hand, family questions and concerns were answered. Following consent venous blood samples or mouth swabs were collected from probands and their relatives for DNA extraction and molecular genetic testing. Genetic testing was personalised for each case and varied between targeted gene test, panels, whole exome or whole genome sequencing as well as segregation studies in some cases. Renal imaging was requested when applicable and other specialist referrals were ordered when required to further investigate cases with extra renal manifestations.

Generally, the reviewed individuals had an unknown or imprecise clinical genetic diagnosis and were referred to find a molecular genetic diagnosis and further investigations to clarify the clinical picture. This was the common reason for referral in 62 probands, whereas eighteen probands had a known genetic diagnosis in hand prior to referrals and were referred for genetic counselling, genetic screening for other family members and disease management with regards to their genetic results **Table 3.1**. The probands clinical features and reasons for referrals varied, yet most common reasons were for investigating suspecting familial haematuria in patients presented with proteinuria or investigating a possible diagnosis of inherited cystic kidney disease **Figure 3.3**. The remainder of the referrals were a mix of syndromic and isolated kidney diseases. A precise molecular genetic diagnosis successfully achieved following the clinic in 26 cases (42%) out of 62 cases referred without genetic diagnosis **Table 3.2**. Despite targeted genetic testing of candidate genes, some cases remained unsolved. This include nine probands and their relatives who have been recruited into further genetic projects the Newcastle pilot study of the Genomics England 100000 Genomes Project **Figure 3.4**.
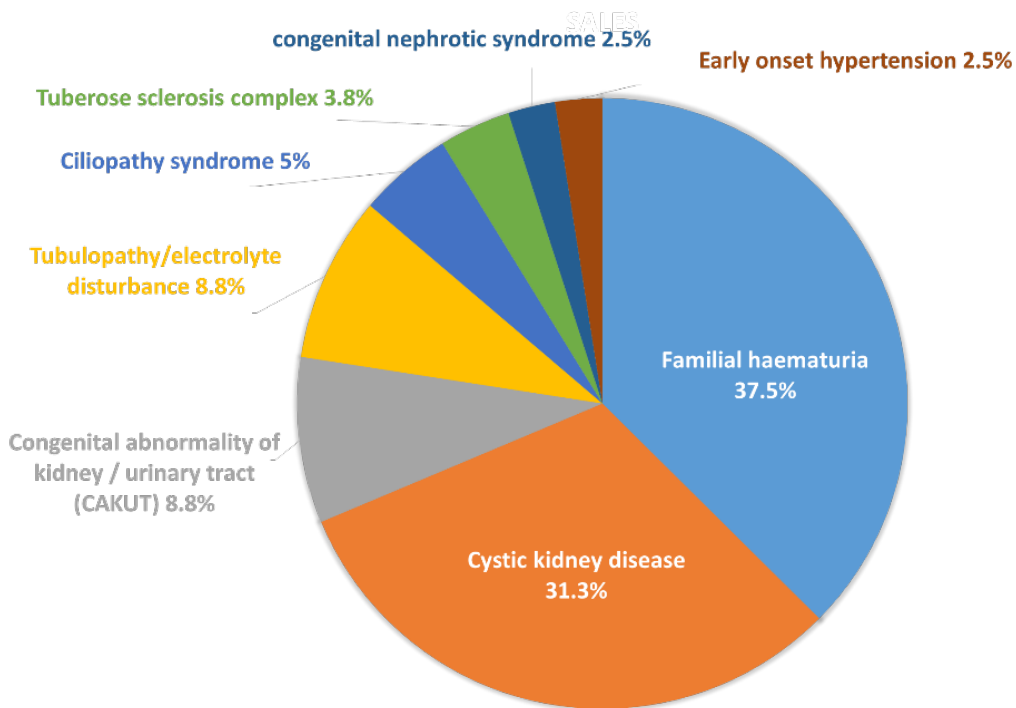
Figure 3.3 Clinical features of the proband and reason for referral to the family renal genetics clinic

Clinical Diagnosis	Gene	Number of probands
Diabetes insipidus	*AVPR2*	3
Joubert syndrome	*C5ORF42*	1
Joubert Syndrome	*CEP290*	1
Autosomal dominant Alport syndrome	*COL4A3*	1
X-linked Alport syndrome	*COL4A5*	1
Renal cysts and diabetes syndrome (RCAD)	*HNF1B*	1
Oro-facial-digital syndrome	*OFD1*	1
Donnai-Barrow syndrome	*LRP2*	1
Autosomal Recessive Polycystic Kidney Disease (ARPKD)	*PKHD1*	1
Autosomal Dominant Tubulointerstitial Kidney Disease (ADTKD)	*MUC1*	1
Autosomal Dominant Tubulointerstitial Kidney Disease (ADTKD)	*REN*	1
Autosomal Dominant Tubulointerstitial Kidney Disease (ADTKD)	*UMOD*	5

Table 3.1 Known molecular genetic diagnosis prior to clinic

Reason for Referral	Clinical Diagnosis	Gene	Number of probands
Suspected ciliopathy syndrome	Joubert syndrome	*CC2D2A*	1
Suspected ciliopathy syndrome	Joubert syndrome	*CEP290*	1
Tubulopathy	Bartter syndrome	*CLCNKB*	1
Familial haematuria	Autosomal dominant Alport syndrome	*COL4A3*	3
Familial haematuria	Autosomal dominant Alport syndrome	*COL4A4*	4
Familial haematuria	X-linked Alport syndrome	*COL4A5*	9*
Congenital nephrotic syndrome	Congenital nephrotic syndrome	*NPHS1*	1
CAKUT	Renal coloboma syndrome	*PAX2*	1
Cystic kidney disease	Autosomal dominant polycystic kidney disease	*PKD1*	4
Tubulopathy	Hypomagnesemia with secondary hypocalcemia	*TRPM6*	1

Table 3.2 Confirmed clinical and molecular diagnosis following clinic visit

*Includes one proband with a VUS (which segregated with phenotype) in *COL4A5*.

Congenital anomalies of the kidney and urinary tract (CAKUT)
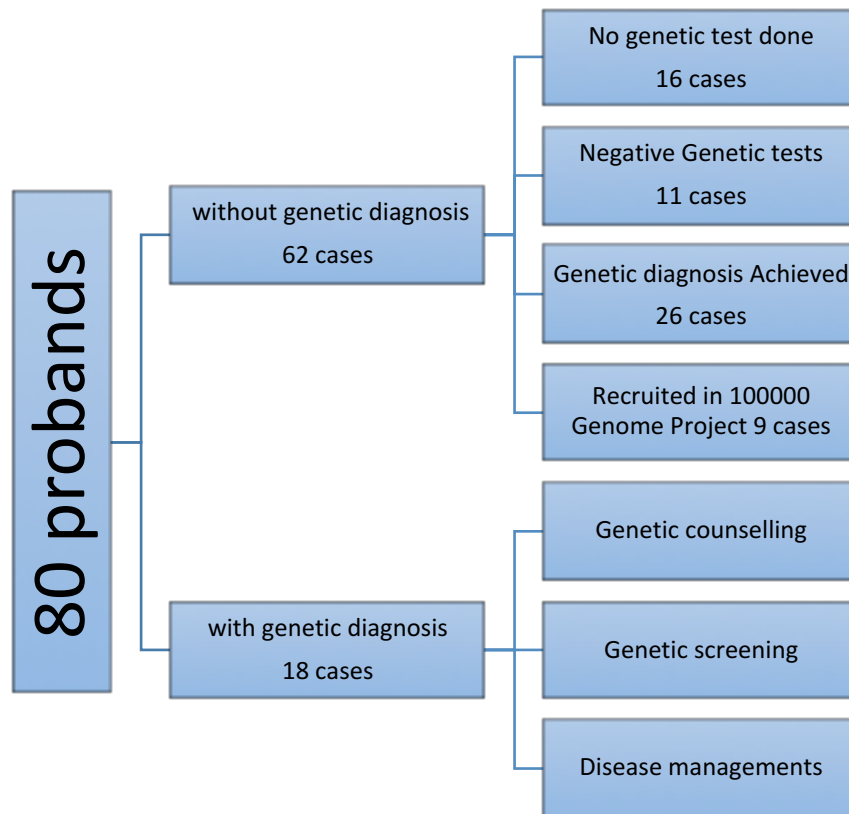
Figure 3.4 Family renal genetics clinic outcomes following clinic review

3.4. **Discussion**

3.4.1. Stories from the clinic

<u>*COL4A3, COL4A4* and *COL4A5* genes</u>

The most common reason for referral was suspected familial haematuria, with 16 probands being diagnosed with mutation in one of the *COL4A3/4/5* genes making it the most common molecular diagnosis made post clinic visits. Families were identified with X-linked, autosomal dominant and autosomal recessive *COL4A3/4/5* disease. Taking a thorough family history and extended pedigree helped to predict the likely pattern of inheritance before being confirmed by molecular results. No common or founder mutations were observed in this cohort. *COL4A3/4/5* variants identified were either previously reported as pathogenic mutations or were novel changes with predicted pathogenicity. However, in one proband, the molecular genetic tests result in *COL4A5* variant with uncertain significance which required further segregation studies to confirm the pathogenicity and correlate genotype with phenotype.

<u>*PKD1* and *PKD2* genes</u>

Autosomal dominant polycystic disease (ADPKD) is a common disorder and usually can be easily identified and diagnosed (Rossetti and Harris, 2007). Despite that, in ~1% of cases it can present early in life with renal cysts and missed diagnosed or confused with other congenital cystic kidney diseases. *PKD1* and *PKD2* genes were not routinely screened in probands with cystic kidney disease, however, individuals were tested when the clinical diagnosis was uncertain, there was an early onset presentation, or a precise molecular genetic diagnosis was needed for family planning decisions.

A new molecular genetic diagnosis of *PKD1* mutation was identified in four families. In two families, kidney cystic changes were recognized with early onset presentation of the disease. In both cases, the molecular genetic diagnosis helped other family members discover their options regard live-donor kidney transplantation and genetic screening.

Another family was referred to the clinic with an 8-week-old child who had presented with a febrile illness and a renal ultrasound diagnostic of ADPKD. The molecular

genetic tests identified a truncating uni-allelic PKD1 mutation. This mutation believed to be de novo. The early recognition and genetic diagnosis of ADPKD in childhood permit the early detection and treatment of hypertension and maybe in the future it will allow the early use of disease modifying drugs such as tolvaptan and other novel therapies.

CEP290 gene

The diagnosis of *CEP290* mutation was made in a family with retinal-renal-cerebellar syndrome (Joubert syndrome), a ciliopathy with broad phenotypic and genotypic spectrum. The proband had presented with visual loss, cystic kidney disease and rapid decrease in renal function. Providing the family with the precise molecular genetic diagnosis helped the family in decision making regarding family planning and renal transplantation. Moreover, it narrowed the planned investigations and allowed the patient to avoid invasive procedures such as renal biopsy. Percutaneous renal biopsy procedure complications are occasional yet serious and include haemorrhage requiring blood transfusion (0.9%), angiographic intervention (0.6%), and in very rare occasions nephrectomy (0.01%) and death (0.02%) (Corapi et al., 2012).

PAX2 gene

Many kidney diseases are syndromic with extra renal manifestations. The unique setting of the clinic facilitates thorough examination of probands and relatives giving enough time to explore renal and extra renal involvement. In 25 cases, excluding ADPKD, there were extra renal involvements include deafness, retinal defects, skeletal abnormalities, liver fibrosis and gout, all of which are pointing to rare syndromes. A previously reported family presented with autosomal dominant pattern of progressive renal failure, congenital renal dysplasia and a history of eye disease (Adam et al., 2013). A diagnosis of renal coloboma syndrome was proposed and the patient underwent ophthalmological examination which revealed optic nerve coloboma. The diagnosis was confirmed with *PAX2* mutations segregating with the renal and eye phenotype **Figure 3.5**. Once again, finding the precise molecular genetic diagnosis helped to identify at risk family members by mutation screening. In addition, mutation positive individuals were able to escape the invasive diagnostic renal biopsy and had targeted renal and ophthalmic investigation.
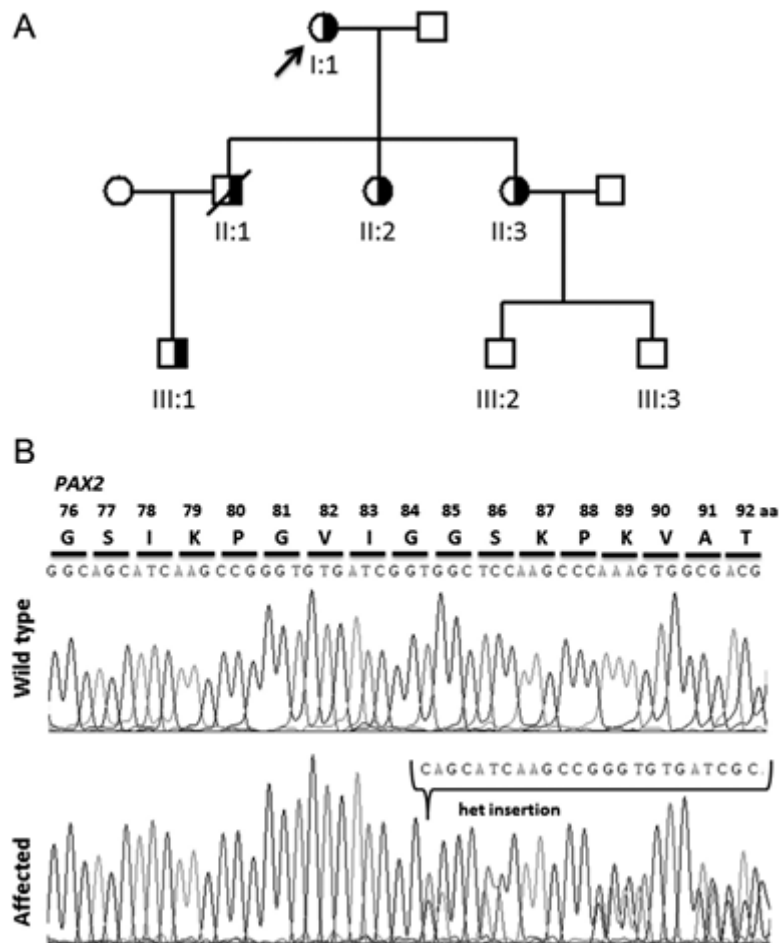
Figure 3.5 *PAX2* Family pedigree and mutational analysis.

(A) The family pedigree is shown. Males are represented by squares, females by circles. Half-shaded symbols indicated heterozygous mutation status. The proband is marked with an arrow. The genetic diagnosis in II:1 is presumed. (B) Sequence chromatograms of the wild-type and affected patient showing the heterozygous insertion mutation c.228_251dup, p.Ser77_Gly84dup within *PAX2*.

Clinical Diagnosis	Gene	Molecular Genetics
X-linked Alport syndrome	*COL4A5*	het c.2042G>T p.Gly681Val
X-linked Alport syndrome	*COL4A5*	het c.3454G>A pGly1152Ser
X-linked Alport syndrome	*COL4A5*	het c.4732A>T p.Ser1578Cys
X-linked Alport syndrome	*COL4A5*	het c.3410G>C p.Gly1137Ala and c.3427G>A p.Gly1143Ser
X-linked Alport syndrome	*COL4A5*	hemi c.2801delC p.Pro934fs COL4A5
X-linked Alport syndrome	*COL4A5*	hemi c.3410G>C p.Gly1137Ala and c.3427G>A p.Gly1143Ser in exon
X-linked Alport syndrome	*COL4A5*	het c.891+5G>A sequence changes
X-linked Alport syndrome	*COL4A5*	het c.4977-11_4977-5del
X-linked Alport syndrome	*COL4A5*	Hemi c.1396G>T p.Gly466Ter
AD Alport syndrome	*COL4A4*	het c.3679G>A p.Gly1227Arg
AD Alport syndrome	*COL4A4*	het c.667_667insA, p.Gly223fs
AD Alport syndrome	*COL4A4*	het c.3052G>C p.Gly1018Arg
AD Alport syndrome	*COL4A4*	het c.81_86delACTCAT p.Ile29_Leu30del
AD Alport syndrome	*COL4A4* *COL4A3*	compound het *COL4A3* c.1184G>A p.Gly295Glu and *COL4A4* c.4870_4873delGAAG p.Glu1624fs
AD Alport syndrome	*COL4A4* *COL4A3*	compound het *COL4A3* c.1184G>A p.Gly295Glu and *COL4A4* c.4870_4873delGAAG p.Glu1624fs

Clinical Diagnosis	Gene	Molecular Genetics
AD Alport syndrome	*COL4A3*	het c.1184G>A p.Gly395Glu
Joubert syndrome	*CEP290*	compound het c.2817G>T p.Lys939Asn and c.2848dupC p.Gln950Profs*6
Joubert syndrome	*CC2D2A*	compound het c.2999A>T p.Glu1000Val and c.248-4.248-3 ins AAGTTTT
Bartter syndrome	*CLCNKB*	compound het c.1481delA p.Gln494fs and c.512A>C p.His171Pro
Congenital nephrotic syndrome	*NPHS1*	homo c.3478C>T p.Arg1160X
Renal coloboma syndrome	*PAX2*	het c.228_251dup p.Ser77_Gly84dup
ADPKD	*PKD1*	het c.1967T>A p.Leu656Gln
ADPKD	*PKD1*	het c.8486T>A p.Val2829Glu
ADPKD	*PKD1*	het c.6487C>T p.Arg2163*
Hypomagnesemia with secondary hypocalcaemia	*TRPM6*	compound het c.2391+6T>G and c.2562_2569dupGCTGTTCA p.Thr857fs

Table 3.3 Molecular genetic diagnosis identified post clinic visit

Autosomal dominant (AD), autosomal dominant polycystic kidney disease (ADPKD)

3.4.2. Lessons from the clinic

The Newcastle family renal genetic clinic is not unique in the UK. Other clinics have been established in London (Adalat et al., 2010), Manchester and Cambridge with different renal genetic emphasis, for example the Cambridge clinic has an interest in kidney stones. These multidisciplinary clinics are increasingly required to facilitate the practise of personalised medicine. A report from Australia describes similar experience of multidisciplinary renal genetics clinic, where a confirmed molecular genetics tests provided a diagnosis in half of the referred cases (Mallett et al., 2016). The genetic testing also changed the diagnosis in around quarter referrals. In the age of genomics, such approaches facilitate the recognition, diagnosis and management of inherited disorders.

Seeing the family together has great benefits. The physicians have the chance to observe different affected family members at the same setting. In some cases, they were able to identify the variable phenotype and incomplete penetrance. It also demonstrates the complexities of monogenic disorders, the difficulties genetic counsellors face in predicting long term prognosis for probands and affected relatives. Most important is being able to identify the most appropriate and informative individual in whom to start the investigation and the genetic testing. Later, cascade genetic screening proceeds in an effective manner, enabling confirmation of variants to be tested for segregation with disease phenotype in other family members. One more advantage of seeing the family together, is that specialist's advice and disease management plans are given the whole family at the same time avoiding receiving mixed messages when different individuals are seeing different specialists in isolation. In this way, a balanced and consistent report letter can be sent back to the referring doctor and the primary care physician. Families referred to the clinic are introduced to the most recent advances regarding management of the disease, disease support groups (local and international) and an opportunity to be recruited and involved in an active research project a rare disease programmes such as The National Registry of Rare Renal Disease ((RaDaR) www.rarerenal.org).

Setting up multidisciplinary clinic is costly in nature and may become more so given the expensive costs of the genetic tests. With the increased affordability of NGS, the cost of individual gene test is high compared to large panel and whole exome sequencing. The positive application of NGS in diagnosing cases with rare inherited kidney disorders is now easily recognised (Jacob et al., 2013, Shashi et al., 2014). Clinicians should also bear in mind the cost effect of frequent specialist visits, multiple and invasive investigations and hospital admissions that may be carried out among multiple members of the fame family without co-ordination, when following the traditional way of diagnosis. Attending the renal genetic clinic maximised the use of time for clinicians and families. Identifying a molecular genetic diagnosis in large family of affected patients and at-risk relatives limits the need for invasive, costly and unnecessary investigations in multiple family members.

3.5. **Conclusion**

Inherited kidney diseases are rare disorders with lots of challenges including reduced quality of life, a prolonged diagnostic odyssey and their considerable effect on the health care system. Our renal genetic family clinic experience strongly emphasised the importance of attaining a precise molecular genetic diagnosis. Identifying a precise molecular genetic diagnosis has its beneficial value to both the patients and their physicians. It manifests in proper disease mechanism explanation, more accurate prediction of disease prognosis regarding renal function and extra renal manifestations. With a correct molecular diagnosis in hand, the investigation cascade to identify at risk relatives will be more focused, and non-relevant tests and invasive procedures can be avoided. It also allows for early management of the disease starting with life style modifications. When a clear diagnosis is developed in paediatric nephrology patient it will eventually ensure smoother and planned transition into adult nephrology services. To many families, having a firm diagnosis aids in family planning decisions through assisted reproductive medicine. In addition, when the prognosis of the disease required renal transplantation, healthy relative donors can be identified.

Having the opportunity to study cohort of patients with inherited kidney disorders over a long period of time and successfully identifying the molecular genetic diagnosis broadens our understanding of the disease mechanisms, prognosis and outcomes. This also helps affected families to understand more fully their inherited disease and its implications to them and their family.

The application of NGS technology gives more depth to the genetic tests, which by itself is meaningless if not combined with detailed and accurate phenotypic data attained by the clinicians. Genomic England's future vision is to allow the practice and the feasibility of genomic medicine throughout the NHS services to reach efficient and precise molecular genetic diagnosis for a better clinical care. Despite the obstacles accompanying such genomic medicine programmes, the expected benefits can be enormous (Manolio et al., 2013).

Chapter 4   Whole Exome Sequencing Identifies a Novel Cause of Joubert Syndrome

4.1. Introduction and aim

Joubert syndrome (JBTS) is a neurodevelopmental ciliopathy with autosomal recessive inheritance, first described in 1969 (Joubert et al., 1969). The hallmarks of JBTS are the neurological phenotypes, characterised by hypotonia, abnormal eye movement (oculomotor apraxia), intellectual disability, truncal ataxia, and respiratory control dysfunction (sleep apnoea and/ or tachypnoea) (Boltshauser and Isler, 1977). A key diagnostic feature of JBTS is the presence of "the molar tooth sign" on the brain axial magnetic resonance imaging (MRI) (Poretti et al., 2014a). This pathognomonic abnormality arises from series of cerebellum and midbrain abnormalities; the hypoplasia and the dysplasia of the cerebellar vermis and of pontine and medullary structure, as well as the absence of decussation of the superior cerebellar peduncles and the pyramidal tracts.

In a large cohort of JBTS patients, only 27% of the cases had purely neurological phenotype (Vilboux et al., 2017). Whereas, most of the cases were complicated by the extra neurological manifestations, which may present at different ages and ranges of severity (Kroes et al., 2016, Bachmann-Gagescu et al., 2015). Therefore, patients clinically diagnosed based on the presence of the molar tooth sign undergo serial thorough diagnostic examination and regular follow-up to assess and manage their multi-organ manifestations. The most common extra-neural manifestation are retinal defects, renal defects and hepatic defects. About 20-40% of JBTS patients develop renal involvement at any age in the form of nephronophthisis or cystic dysplastic kidneys, retinal dystrophy and blindness, hepatic involvement such as ductal plate malformation and fibrosis. More rare manifestation includes chorioretinal coloboma or optic nerve coloboma, dysmorphic facial features and/or skeletal involvement like dystrophy or polydactyly (Romani et al., 2013).

Like other ciliopathies, JBTS exhibits noticeable genetic heterogeneity making the molecular genetic diagnosis of the disorder challenging. JBTS is caused by recessive mutations in more than 30 genes (http://omim.org), which are known to encode proteins localised to the primary cilium and its basal body.

Yet those identified genes explain the causative mutation in only 40-50% of JBTS cases (Valente et al., 2013a). Next generation sequencing (NGS), particularly whole exome sequencing (WES) studies, is a useful tool based on the complexity and heterogeneity of the disease to determine the genotype-phenotype correlation of JBTS, and equally to identify novel causative gene mutations (Vilboux et al., 2017). However, many cases of JBTS remain genetically unsolved.

Here we used a combination of homozygosity mapping and whole exome sequencing, a valuable strategy for gene discovery to investigate an unsolved JBTS family.

Locus name	Gene symbol	Chromosome locus	JBTS phenotype
JBTS1	*INPP5E*	9q34.3	With or without colobomas, retinal or renal manifestations
JBTS2	*TMEM216*	11q12.2	With retinal and renal manifestation; with or without polydactyly
JBST3	*AHI1*	6q23.3	With retinal manifestation; with or without renal manifestation
JBTS4	*NPHP1*	2q13	With retinal and renal manifestation
JBTS5	*CEP290*	12q21.32	With retinal and renal manifestations
JBTS6	*TMEM67*	8q22.1	With renal and hepatic manifestation
JBTS7	*RPGRIP1L*	16q12.2	With renal manifestation; with hepatic manifestation
JBTS8	*ARL13B*	3q11.1-q11.2	With or without retinal manifestation
JBTS9	*CC2D2A*	4p15	With or without retinal manifestations; with hepatic manifestation; renal manifestations
JBTS10	*OFD1*	Xp22.2	With or without retinal manifestation
JBTS11	*TTC21B*	2q24.3	With renal manifestation
JBTS12	*KIF7*	15q26	Classic JBTS with dysmorphism and polydactyly
JBTS13	*TCTN1*	12q24.11	With or without retinal manifestation
JBTS14	*TMEM237*	2q33.1	With renal manifestation
JBTS15	*CEP41*	7q32.2	Classic JBTS with polydactyly and coloboma: with or without retina, renal or hepatic manifestation
JBTS16	*TMEM138*	11q12	With retinal and renal manifistations
JBTS17	*C5orf42*	10q24	Classic JBTS with or without polydactyly
JBTS18	*TCTN3*	10q24.1	Classic JBTS with or without OFD features
JBTS19	*ZNF423*	16q12.1	With retinal and renal manifestations

Locus name	Gene symbol	Chromosome locus	JBTS phenotype
JBTS20	*TMEM231*	16q23.1	With retinal and renal manifestations
JBTS21	*CSPP1*	8q13.1-q13.2	With or without retinal or renal manifestations
JBTS22	*PDE6D*	2q37.1	With retinal and renal manifestations
JBTS23	*KIAA0586*	14q23.1	Classic JBTS
JBTS24	*TCTN2*	12q24.31	Classic JBTS
JBTS25	*CEP104*	1p36.32	Classic JBTS
JBTS26	*KIAA0556*	16p12.1	With midline orofacial deformity
JBTS27	*B9D1*	17p11.2	Classic JBTS
JBTS28	*MKS1*	17q22	Classic JBTS; with retinal manifestation
JBTS29	*TMEM107*	17p13.1	With retinal and hepatic manifestations
JBTS30	*ARMC9*	2q37.1	With polydactyly and retinal manifestation
JBTS31	*CEP120*	5q23.2	Classic JBTS
JBTS32	*SUFU*	10q24.32	Classic JBTS with polydactyly and dysmorphism
JBTS33	*PIBF1*	13q21.3-q22.1	With retina, renal or hepatic manifestations
JBTS34	*B9D2*	19q13.2	With skeletal manifestation and dysmorphism

Table 4.1 Summary of genes causing Joubert syndrome, their locus and phenotype

4.2. Materials and methods

All patients and their relatives consented to this study. Ethical approval was obtained from the UK National Research Ethics Service (NRES) Committee Northern and Yorkshire (09/H0903/36) and NRES Committee North East – Newcastle and North Tyneside 1 (08/H0906/28+5). Following informed and written consent, blood samples or mouth swaps were obtained from affected patients and their relatives.

Genomic DNA (2 μg) from three affected siblings and their parents was subjected to whole exome paired-end sequencing analysis with 100× coverage by generating 51 Mb Sure Select V4 libraries (Agilent Technologies, USA). The sequence reads were run on a HiSeq2500 platform (Illumina, San Diego, CA, USA). Ingenuity Variant Analysis web-based application and Homozygosity Mapper (http://www.homozygositymapper.org/) was used for data analysis. The variant of interest was further tested for likely pathogenicity using in silico prediction tools (Mutation taster, SIFT, PolyPhen2, and CADD). Selected variant was further considered and validated by Sanger sequencing in all available family members to confirm segregation with disease status.

4.3. Results

4.3.1. Clinical features of JBTS family

A consanguineous family, who originated from Pakistan, consisted of healthy parents and six children, including three affected siblings who had clinically diagnosed with JBTS. The eldest sibling (II:1) a 21-year-old female, presented during early childhood (aged 4years) with night blindness progressed to bilateral visual loss. **Table 4.2**. Later, she developed ataxia, developmental delay and complained of frequent attacks of urinary tract infections. She also reported thermoregulation problems and an episode of transverse myelitis. Her clinical investigation showed evidence of renal scarring and her brain MRI revealed the molar tooth sign that is pathognomonic of JBTS **Figure 4.1**. The other two affected sisters (II:4 and II:5) had a very similar presentation with neurodevelopmental delay and retinal dystrophy. II:4 is a 12-year-old female with developmental delay, ataxia, sleep apnoea, progressive visual loss, night blindness and thermoregulation problems. Her past medical history did not reveal any renal complaint and her renal ultrasound was normal. II:5 is a 9-year-old female with developmental delay, ataxia, sleep apnoea, progressive visual loss, and night blindness; furthermore, she developed oculomotor apraxia. Just like her oldest sister, she experienced recurrent attacks of UTI and the renal ultrasound reported unequal sized kidneys. An axial image of the brain MRI showed the pathognomonic molar tooth sign in the three affected sisters. To further investigate the three siblings' eye phenotypes, retinal fundal examination was conducted **Figure 4.2**. Coloured fundal photographs of the eyes showed granular alterations of retinal pigment epithelium with subtle spicule formation particularly around major vascular arcades (particularly in oldest sibling II:1) and arteriolar attenuation. Additionally, autofluorescent retinal images displayed stippled hypo-autofluorescent areas concentrated around the arcades, particularly the inferior arcades seen clearly in youngest sibling II:5. By contrast, ring of hyper-autofluorescence was noted around fovea in II:4 and II:5. Horizontal optical coherence tomography scan was applied and demonstrated thinning of outer nuclear layer and loss of ellipsoid and external limiting membrane lines with preservation of inner retinal lamination in all three siblings.

	II:1	II:4	II:5
Age (years)	21	12	9
Central Nervous symptoms	Developmental delay, ataxia	Developmental delay, ataxia	Developmental delay, ataxia
Ocular symptoms	Rod cone dystrophy, night blindness, progressive visual loss	Rod cone dystrophy, night blindness, progressive visual loss	Rod cone dystrophy, night blindness, progressive visual loss, oculomotor apraxia
eGFR (mL/min/1.73m^2)	75	>90	>90
Renal symptoms	Recurrent UTI	None	Recurrent UTI
USS Renal	Renal scarring bilaterally	Normal USS	Unequal kidney size
Other	Thermoregulation problems; episode of transverse myelitis	Thermoregulation problems; sleep apnoea	

Table 4.2 Clinical features of JBTS in affected family members
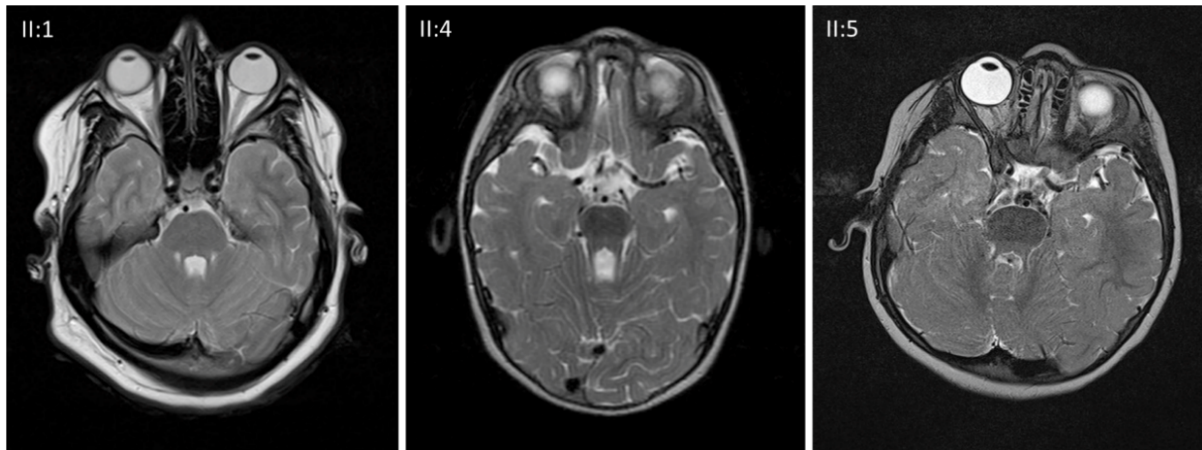
Figure 4.1 Axial brain MRI of the affected siblings.

Images showing the appearance of the cerebellar vermis the "molar tooth sign", presenting as a deepened interpeduncular fossa and thickened, elongated superior cerebellar peduncles.
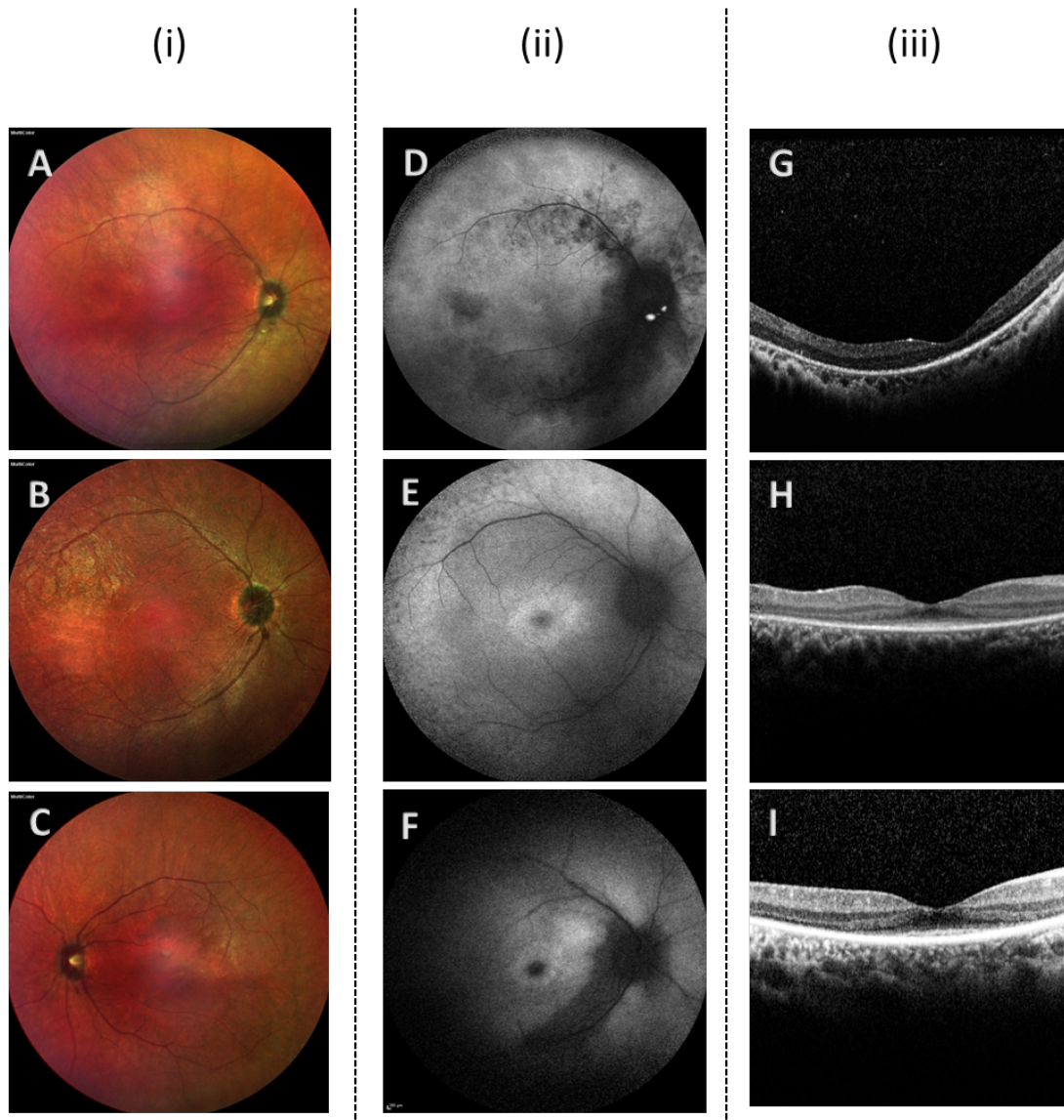
Figure 4.2 Retinal phenotypes in 3 JBTS affected siblings

(i): Colour fundal photographs of the eyes showing granular alterations of retinal pigment epithelium with subtle spicule formation particularly around major vascular arcades (particularly in oldest sibling, A&B) and arteriolar attenuation.

(ii): Blue autofluorescent images with stippled hypo-autofluorescent areas concentrated around the arcades, particularly the inferior arcades seen clearly in youngest sibling (F). Ring of hyper-autofluorescence around fovea in middle and youngest siblings (E and F respectively).

(iii): Horizontal optical coherence tomography scans (50 degree in H, and 30 degree in I &J) demonstrating thinning of outer nuclear layer and loss of ellipsoid and external limiting membrane lines with preservation of inner retinal lamination in all three siblings.

4.3.2. Molecular genetics investigation of JBTS family

Molecular genetic investigations were performed including whole exome sequencing and variant analysis combined with homozygosity mapping. This approach was taken rather than targeted ciliopathy gene panel as the gene panel was not representative of recently identified genes. The whole exome sequencing in the affected index case was analysed for variants in all known JBTS genes using Ingenuity Variant Analysis software. This did not reveal a likely deleterious biallelic variant in any of the known JBT-related genes (JBTS1-34). Homozygosity mapping in two affected cases (II:4 andII:5) identified four shared regions of homozygosity on chromosome 6, 10, 16 and 18. A thorough re-analysis was performed using combined WES data of two affected siblings and their unaffected parents (II:4, II:5, I:1 and I:2) considering exome variants spanning the shared homozygous region with a potential link to a ciliopathy phenotype **Table 4.3**. One single previously unreported homozygous variant was identified on chromosome 10 locus (chr10: 101569997-109106128 (hg19)) a homozygous nucleotide substitution lead to missense mutation in exon 5 of *ARL3,* encoding ARL3 a small GTPase, and causing a single nucleotide change c.446G>A, leading to alteration in the protein coding sequence, arginine to histidine p. Arg149His. *ARL3* gene is a small target for genetic variation, its protein product consisting of 182 amino acid only. (Ref sequence NM_004311.3: c.446G>A, p.(Arg149His))*.* No other pathogenic homozygous alleles were found in all the three affected individuals. The ARL3 R149 residue is highly conserved throughout evolution in all species except *D. melanogaster* and in silico prediction tools suggest that the missense change is likely to be pathogenic **Table 4.4**.
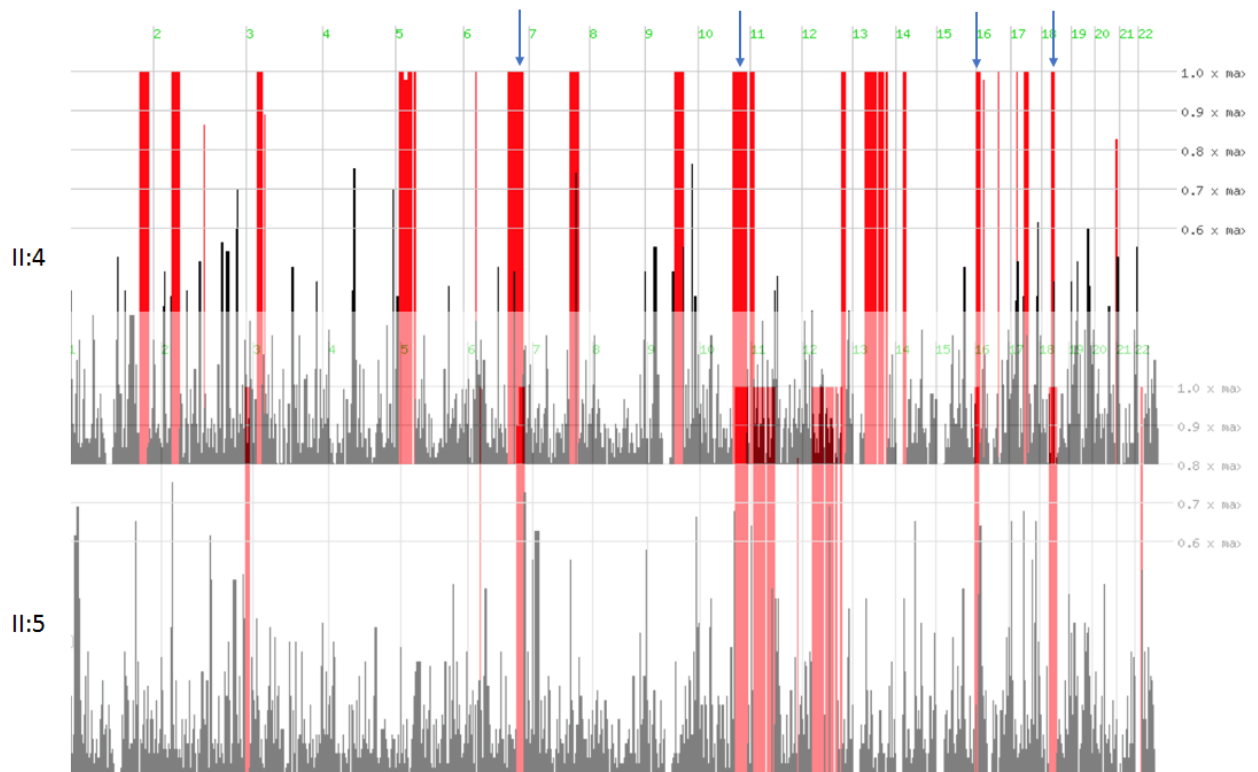
Figure 4.3 Genome wide homozygosity mapping in affected siblings II:4 and II:5.

The standard plot of homozygosity score (Y axis) and genomic region chromosomes 1-22 (X axis). The regions with excess homozygosity compared to control population are shown as red bars and the shared regions of homozygosity between the two siblings are marked with blue arrows.

Affected member*	II:4	II:5
Number of variants	145724	144048
Variants of high confidence	130033	128453
SNVs/Indel ≤ 1% in HapMap18 and 1000 Genome database	7213	7038
Predicted deleterious	1066	800
Biological Context (Known JBTS genes)	0	0
Biological Context (Primary cilia / ciliopathies)	22	3
Homozygous predicted pathogenic alleles	1	1

Table 4.3 Filtering criteria used for single nucleotide variants (SNVs) and insertion and deletion selection (Indels).

*Affected members after screening of kindred based on clinical features.

a.

Variant: chr10 | 104445628 | q24.32 | SNV | T (ARL3 p.R149H)

Details | Path to Phenotype | Variant Findings

Sample Details (2 of 2 cases, 2 of 2 controls)

Name	Subject	State	Genotype	Compound Heterozyg:	Call Quality	Upstream Filtering	Read Depth	Genotype Quality	Allele Fraction	Copy Number	Inferred Activity
J8_JBTS	II:4	case	Hom	No	2303.77	Pass	71	99	100	-	loss
J7_JBTS	II:5	case	Hom	No	2267.77	Pass	70	99	100	-	loss
J43	I:1	control	Het	No	3072	Pass	122	-	53.28	-	normal
J41	I:2	control	Het	No	3072	Pass	114	-	44.74	-	normal

Coding Effects

Gene Symbol	Region	Transcript ID	Transcript Variant	Protein Variant	Translation Impact	SIFT Function Prediction
ARL3	Exonic	NM_004311.3	c.446G>A	p.R149H	missense	Damaging

b.

c.

Human		E	I	A	E	G	L	N	L	H	T	I	R	D	R	V	W	Q	I	Q	S	C	S	A
mutated	not conserved	E	I	A	E	G	L	N	L	H	T	I	H	D	R	V	W	Q	I	Q	S	C	S	A
P. troglodytes	all identical	E	I	A	E	G	L	N	L	H	T	I	R	D	R	V	W	Q	I	Q	S	C	S	A
F. catus	all identical	E	I	A	E	G	L	N	L	H	T	I	R	D	R	V	W	Q	I	Q	S	C	S	A
M. musculus	all identical	E	I	A	E	G	L	N	L	H	T	I	R	D	R	V	W	Q	I	Q	S	C	S	A
G. gallus	all identical	E	I	A	E	G	L	N	L	H	T	I	R	D	R	V	W	Q	I	Q	S	C	S	A
T. rubripes	all identical	E	I	A	E	G	L	N	L	H	T	I	R	D	R	I	W	Q	I	Q	A	C	S	A
D. melanogaster	all conserved	E	V	A	E	K	M	S	L	V	Q	L	Q	G	R	T	W	E	I	K	A	C	T	A
C. elegans	all identical	E	I	T	R	K	L	N	L	D	L	L	R	D	R	T	W	H	I	Q	A	C	S	A
X. tropicalis	all identical	E	I	A	E	G	L	N	L	H	T	I	R	D	R	V	W	Q	I	Q	S	C	S	A

Figure 4.4 Molecular genetic investigation of JBTS family.

(A) A screenshot of Qiagen Integrated Variant Analysis software demonstrating *ARL3* homozygous allele in two affected siblings and a het allele in both parents.
(B) Genomic and exon structure of *ARL3* with the homozygous mutation R149H in exon 5 shown.
(C) Evolutionary conservation of R149 amino acid residue (highlighted in red).

Nucleotide change (Ref sequence NM_004311)	Amino acid change	Mutation Taster	PolyPhen2	SIFT	CADD[*] Score	ExAC[**] allele frequency	gnomAD[***] allele frequency
c.446G>A	p.R149H	Disease Causing	Probably damaging	Deleterious	34	1 het allele in 121,358 (0.00000824)	1 het allele in 246,132 (0.000004063)

Table 4.4 In silico analysis of the mutation.

in silico prediction tools used (Mutation taster, PolyPhen2, SIFT and CADD Score) suggest that the missense change is likely to be pathogenic with a very low allele frequency determined by ExAC and gnomAD database.

*CADD Score, Combined Annotation Dependent Depletion, score >20 indicates the 1% most deleterious amino acid substitution

**ExAC, Exome Aggregation Consortium database

***gnomAD, Genome Aggregation database.

To confirm segregation of *ARL3* variant, we Sanger sequenced all three affected individuals (I:1, II:4 and II:5), their healthy parents (I:1 and I:2) and their three unaffected siblings. Sanger sequencing confirmed that the mutation was present in all three affected children and segregated from both parents. The mutations were homozygous in the three affected siblings, heterozygous in the parents and one unaffected sister, and wild type in another two unaffected siblings **Figure 4.5**.
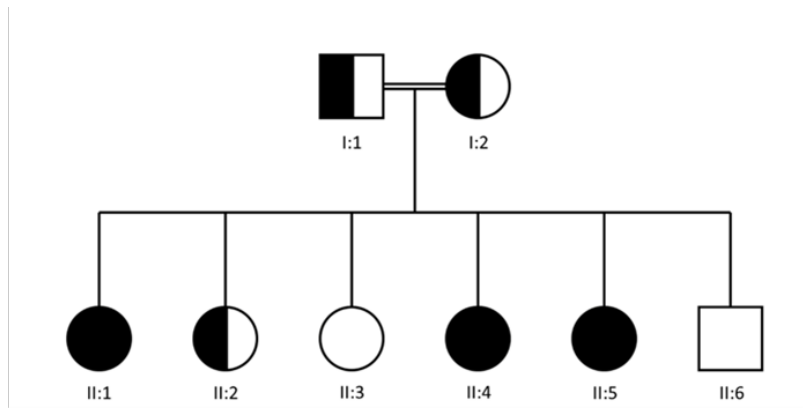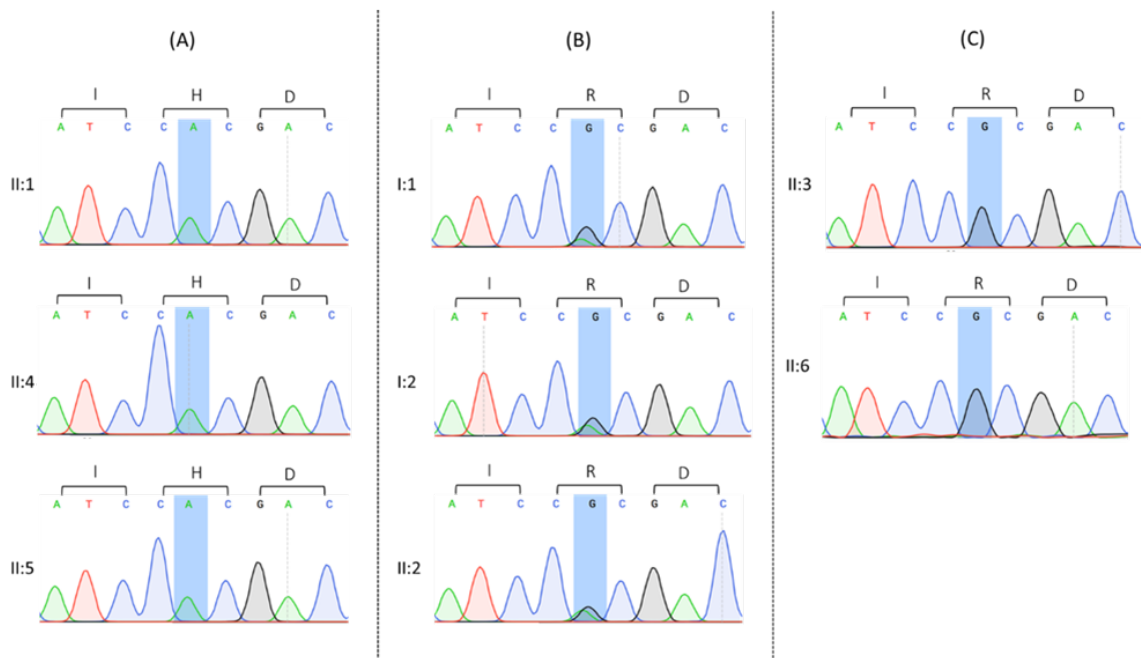
Figure 4.5 Sanger sequencing confirmation of segregation of *ARL3* mutation.

a. The pedigree of JBTS family showing the number of the affected siblings and the outcome of segregation analysis; affected (shaded), carriers (half shaded) and wild-type (unshaded).

b. Sequence chromatogram of all family members. (A) Showing homozygous variant in affected siblings, (B) showing heterozygous variants in carrier parents and one sibling and (C) showing wild type variant in unaffected siblings.

4.4. Discussion

Here we used a combination of homozygosity mapping and WES to investigate an unsolved family with JBTS phenotype with predominantly brain and retinal phenotype. Molecular genetic data analysis on our JBST family revealed a novel homozygous missense mutation in *ARL3* gene, a homozygous missense mutation Arg149His. In silico tools showed the variant pathogenicity ant the ExAC Browser and gnomAD do not have any homozygous pathogenic variants reported within ARL3 and that the gene is relatively intolerant to variation (positive Z score of 0.44). The mutation was confirmed using Sanger sequencing to be homozygous in the affected siblings, heterozygous in the parents and another sibling, and wild type in two other healthy siblings. *ARL3* gene belongs to the group of small GTPases, localises to the cilium and has main prole in ciliary protein trafficking. ARL3 functions as molecular switch by binding and hydrolyzing GTP during cellular processes, they bind to many lipid-modified protein complexes to control their localisation (Zhang et al., 2013). The small GTPase is switched on by guanine nucleotide exchange factor (GEF) namely the cilia specific protein ARL13B, then binds to its effectors which are lipid-modified proteins (Gotthardt et al., 2015). In the pre-ciliary compartment, it's then switched off by a GTPase-activating factor (GAP) namely Retinitis protein 2 (RP2) (Ismail et al., 2012).

GTPase role in ciliary protein trafficking has been recently recognised, two members of this family are known to be mutated in human ciliopathies, Bardet-Biedl syndrome (*ARL6*) (Fan et al., 2004) and Joubert syndrome (*ARL13B*) (Cantagrel et al., 2008). To date, no mutations in *ARL3* reported to cause a human ciliopathy disorder, however, heterozygous missense variant of ARL3 was reported by Strom et al. (2016) in a Caucasian family with non-syndromic retinitis pigmentosa. On the other hand, *Arl3* knockout mice show typical ciliopathy manifestation with renal, hepatic and pancreatic cysts formation, impaired photoreceptors development and failure to thrive beyond 3 weeks of age (Schrick et al., 2006). Studies in *C. elegance* and *Leishmania*, showed ciliary localisation of Arl3 and intraflagellar transport disruption when mutated (Cuvillier et al., 2000, Li et al., 2010). ARL3 has many known effectors (Wright et al., 2011). When activated, ARL3 binds to a specific effector that carries ciliary cargo. ARL3 binds to the cargo-carrier protein complex at the transitional zone causing conformational changes and unloading the ciliary cargo **Figure 4.6**.
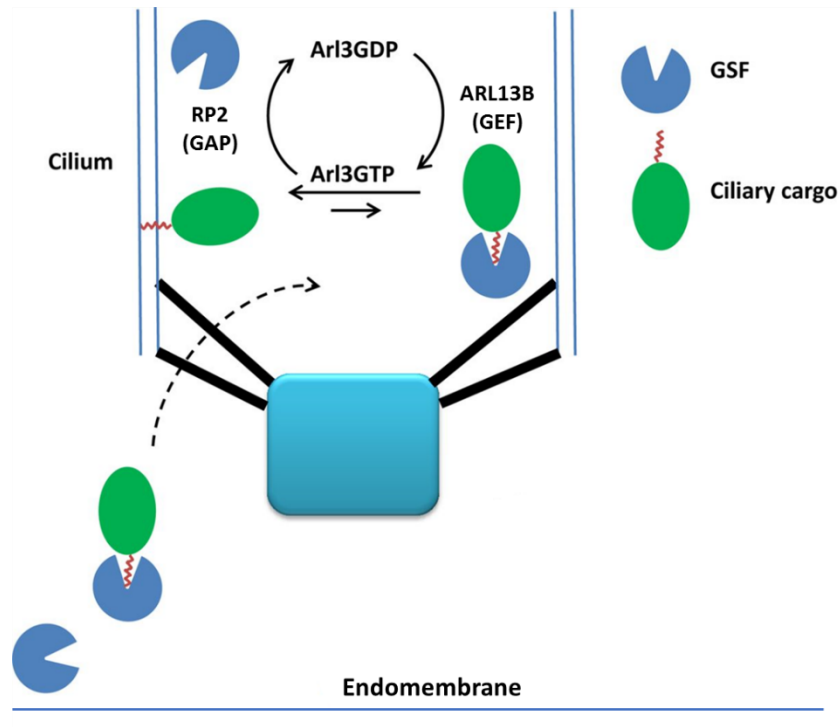
Figure 4.6 A model for sorting and shuttling of lipid modified ciliary cargo into the cilia.

The GDI-like solubilizing factor (GSF) (blue; e.g. Unc119b) binds to the lipid-modified tail of the ciliary cargo (green). This is transported to the cilium, whereby Arl3, maintained in a GTP-bound state by Arl13b, binds the GSF, forcing a conformational shift, which releases the ciliary cargo to the ciliary membrane. Binding of Arl3 to the GAP RP2 results in an inactive, GDP-bound state.

Several investigators from Europe and North America were asked to screen their cohorts of patients for similar gene findings. Researchers contacted were Friedhlem Hildebrant, Rachel Giles, Sophie Saunier and Dan Doherty. Gene data were posted on GeneMatcher (https://www.genematcher.org/) to find other families, but we didn't have a response.

We finally reached a group in Saudi Arabia at King Faisal Specialist Hospital and Research Centre led by senior specialist Fowzan AlKuraya, who had a cohort of 35 unsolved JBTS-affected individuals. After screening their WES databases for our proposed gene *ARL3*, they found a single previously unreported homozygous missense variant in *ARL3* in an index individual, causing a single nucleotide change c.446G>A, leading to alteration in the protein coding sequence, arginine to cystine p. Arg149Cys and fully co-segregated with the JBTS phenotype in the family **Figure 4.8**. No additional *ARL3* pathogenic variants were identified in their WES databases, which are relatively enriched with autozygosity **Figure 4.7**.

The Saudi Arabian family comprising first-cousin healthy parents and six children, including the 5-year-old male index individual (II:5). He presented with developmental delay, multicystic dysplastic left kidney **Figure 4.9**.D, night blindness, and mild dysmorphic features, including ptosis **Figure 4.9**.B. His MRI of the brain showed severe vermis hypoplasia with abnormal thick cerebellar peduncles configured in the shape of a typical molar tooth sign **Figure 4.9**.C, as well as abnormal configuration of the midbrain, thinning of the pontomesencephalic junction and midportion of the midbrain, and mild decreased brain volume with a paucity of white matter in the frontotemporal region and dilated ventricular system.
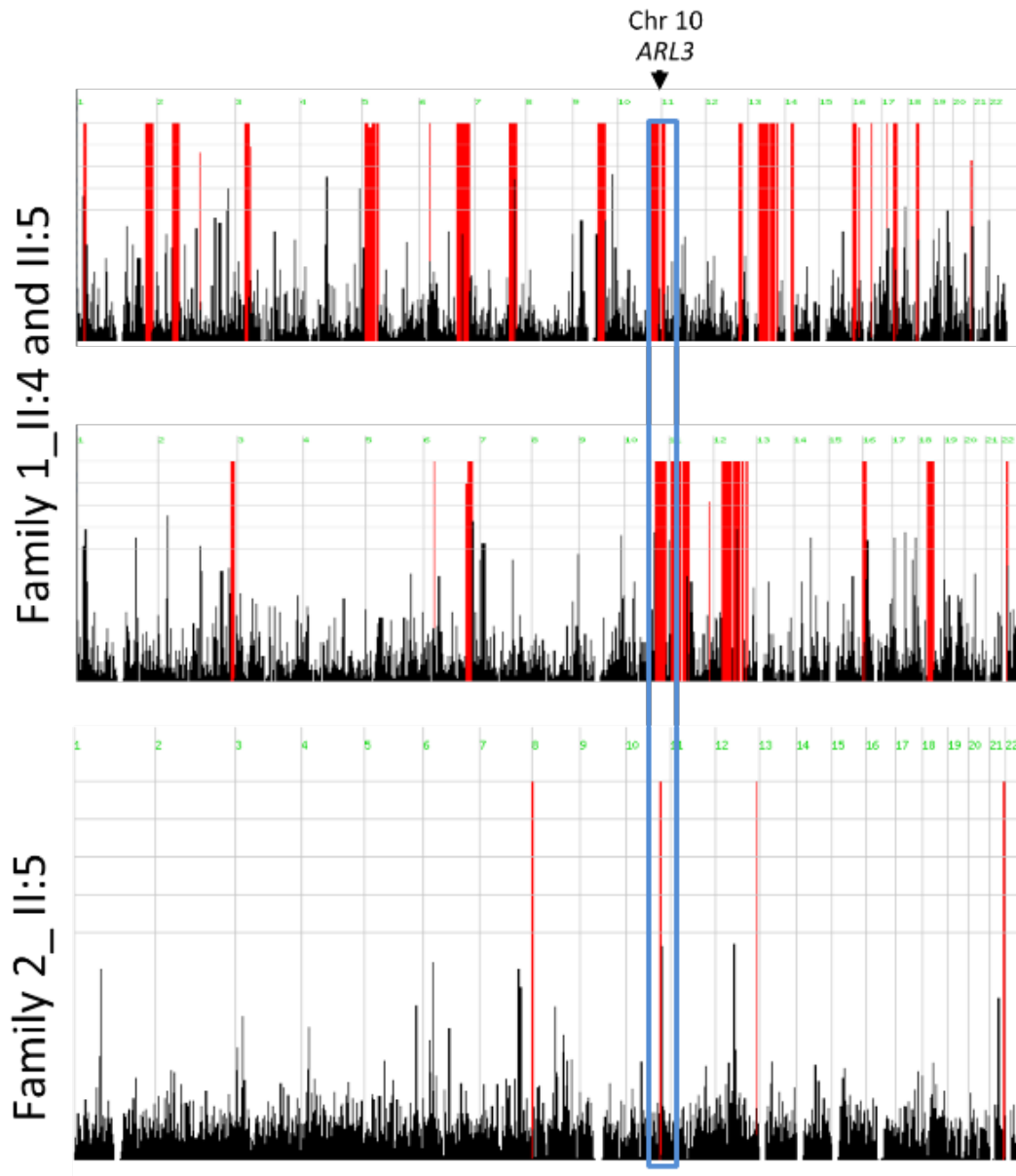
Figure 4.7 . Genome wide homozygosity mapping of patient in the two JBTS families

The plot showing the shared homozygous region between the affected members of the two families on chromosome 10 (blue rectangle). Regions of homozygosity are shown in red and the position of *ARL3* is marked with black arrow.
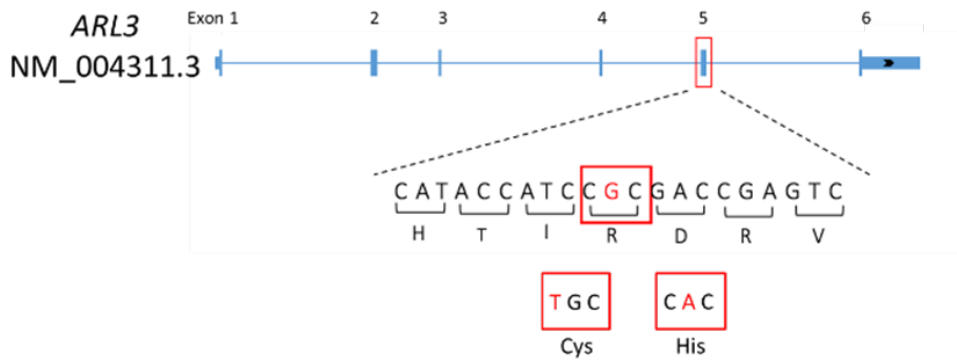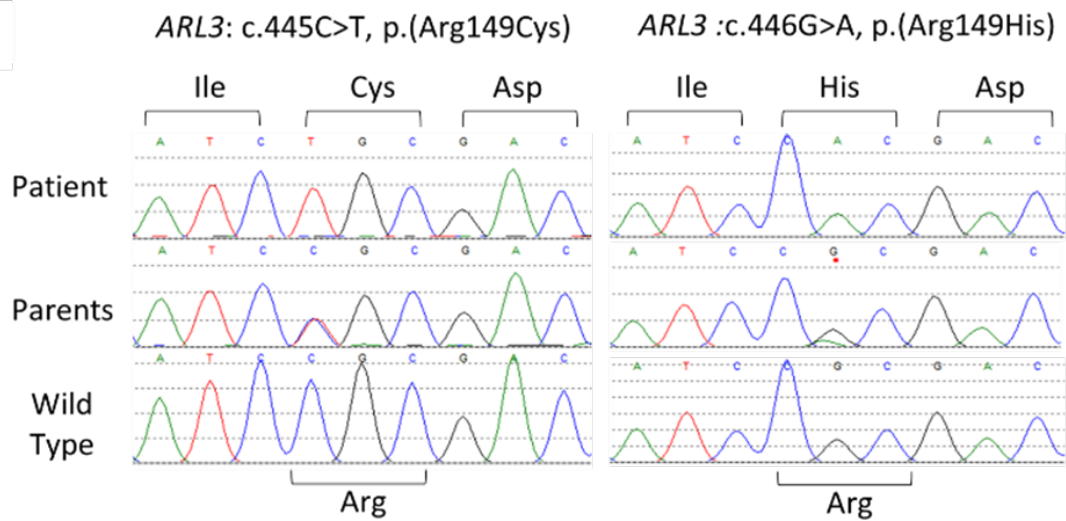
Figure 4.8 Molecular genetics investigations of the two JBTS families

(A) Schematic representation of nucleotide changes within *ARL3* both leading to the homozygous missense mutations affecting Arg149 residue (Arg149Cys and Arg149His) are located in exon 5.
(B) Sequence chromatogram of the two different mutations in *ARL3* identified.
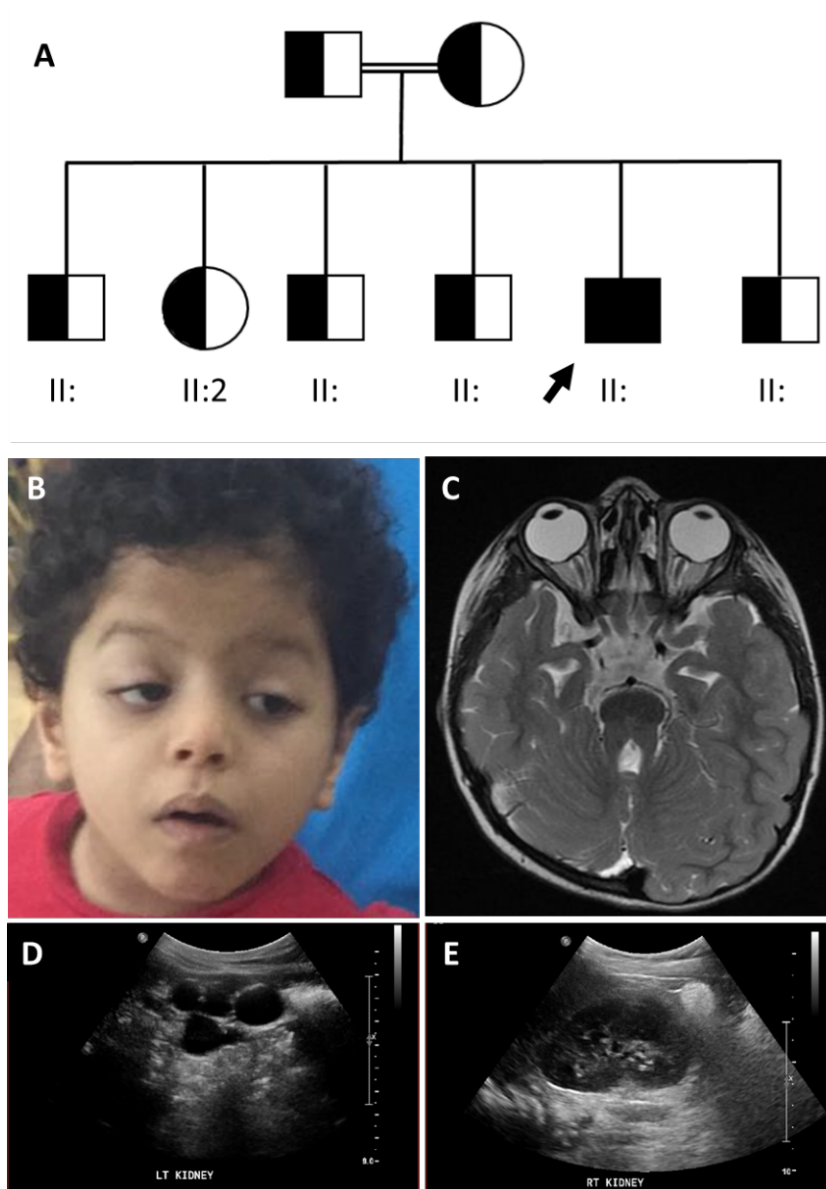
Figure 4.9 Clinical and radiological images to the affected member of 2nd family

(A) The Pedigree family 2 showing the affected index (arrow) and the outcome of segregation analysis (affected (shaded) and carriers (half shaded).
(B) Facial photo of the index family 2 (II:5) showing the mild dysmorphic feature and ptosis.
(C) Brain MRI images of the index family 2 (II:5) showing evidence of molar tooth sign - cerebellar vermis hypoplasia and elongation of superior cerebellar peduncles
(D) and (E) Ultrasound image of the kidney of the affected member family 2 (II:5) showing the echogenic multicystic dysplastic in the left kidney (D) and normal right kidney (E).

Chapter 5 Characterization of Novel *ARL3* Homozygous Mutation Causing Joubert Syndrome

5.1. Introduction and aim

ADP ribosylation factor (ARF)–like proteins (ARLs) are enzymatically active small GTP-binding proteins (G proteins) in the Ras superfamily. ARLs G-proteins family include 16 members, and the role of most ARLs is to regulate the assembly of multi-protein complexes by regulating protein membrane trafficking and phospholipids composition (Kahn et al., 2005). Small G proteins are considered molecular switches cycling between a GTP-bound 'on' and a GDP-bound 'off' states which activate and inactivate, respectively, the G protein (Cherfils and Zeghouf, 2013) leading to conformational changes at the switch region where the effector binds. Small G proteins are switched on by a guanine nucleotide exchange factor (GEF) and cannot hydrolyse GTP in the absence of a GTPase-activating protein (GAP). GEF and GAP modulators are found to be distinct and exclusive against each ARL protein. Unlike other small G proteins, the ARLs have an N-terminal amphipathic helix instead of lipid modification at the C terminus (Burd et al., 2004, Gillingham and Munro, 2007). The GTP-bound active G protein functions through interaction with specific effectors involved in trafficking of lipid-modified proteins. When binding to GTP, a loop of beta sheets between the switch region is formed, called the interswitch, displacing the N-terminal amphipathic helix from hydrophobic pocket and promoting insertion of the helix into an adjacent bilayer, facilitating protein trafficking (Donaldson and Jackson, 2011).

ARL3 is a soluble, small G protein that has been identified in all ciliated organisms and localizes to the cilium and centrosome. ARL3 found to be colocalised with its effector RP2 and PDED at different parts of photoreceptors, cell body, inner segment and connecting cilium (Grayson et al., 2002) (Zhang et al., 2004). ARL3 has major role in cytokinesis and cilia signalling (Zhou et al., 2006). ARL3 is regulated by its GEF ARL13B, cilia-specific protein when mutated in human gives rise to JBTS with retinopathy. ARL3 also regulated by its GAP RP2, a pre-ciliary protein when mutated in human leads to X-linked non syndromic retinitis pigmentosa (Veltel et al., 2008). *ARL3* human heterozygous mutation has been previously reported in patient with retinal dystrophy. While a loss of biallelic *ARL3* loss of function in mice leads to

typical ciliopathy phenotype with severe manifestations (Schrick et al., 2006). Among ARL3 effectors are the Guanosine nucleotide Dissociation Inhibitor (GDI) GDI-like solubilizing factors (GSFs) PDE6D, UNC119A, and UNC119B, whose function to solubilise and transport post translational lipidated proteins. GSF release of lipidated cargo protein is ARL3- GTP dependent (Ismail et al., 2012, Ismail et al., 2011). The segregation of ARL3 regulators GEF (cilia specific ARL13B) and GAP (pre-ciliary RP2) are thought to generate an ARL3-GTP gradient inside the cilium ensuring the specific release of lipidated cargo protein, solubilised by GSFs, in the cilia (Gotthardt et al., 2015).

We aim to study the impact of *ARL3* variant Arg149 on the mechanism of ARL3-ARL13B interaction, to investigate the structural and the functional effect of the *ARL3* Arg149His variant on patient fibroblasts.

5.2. **Results**

5.2.1. Homology models of ARL3-ARL13B complex

To study the effect of *ARL3* variant detected on the interaction of ARL13B with ARL3, a homology modelling study was performed. Human ARL3 and ARL13B were modelled on the crystal structure of the Arl3-Arl13B complex from *Chlamydomonas reinhardtii.* ARL3 conserved variants were located at the in a loop between α4 and β6 domains and predicted to interrupt the ARL3-ARL13B interaction. ARL3 precise residue (Arg149) is essentially required for the interaction with its GEF ARL13B conserved residue (Glu88). Superimposition of the crystal structures of ARL3 in complex with its known interactors UNC119A and BARTL1, the GAP RP2, and GEF ARL13B, showed exclusive *Cr*ARL13B-*Cr*ARL3 complex interface interaction between the conserved residues ARL3 (Arg148) and ARL13B (Glu86). **Figure 5.1**.**b**
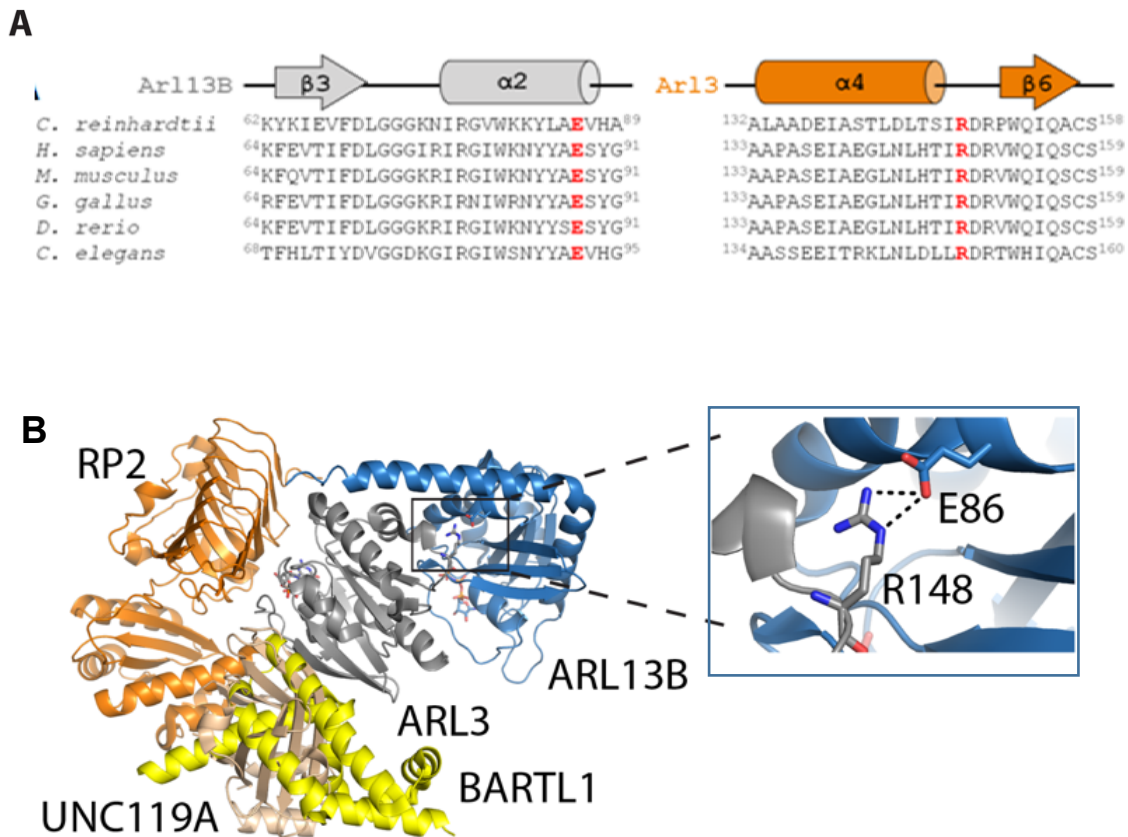
Figure 5.1 Homology models of ARL3-ARL13B complex

The Human ARL13B-ARL3 Complex Is Predicted to Involve an Interaction between Evolutionarily Conserved Glutamate and Arginine Residues

(A) Partial amino acid sequence alignments of the ciliary GEF, ARL13B, and ARL3. Highlighted in red are the evolutionarily conserved glutamate residue located in the switch II domain of ARL13B (E86 [Glu86] in *C. reinhardtii* ARL13B [*Cr*ARL13B]) and the arginine residue in the loop region between the α4 and β6 domains of ARL3 (R148 [Arg148] in *Cr*ARL3).

(B) Superimposition of the crystal structures of ARL3 (gray) in complex with its known interactors: the effectors UNC119A (salmon; PDB: 4GOJ) and BARTL1 (yellow; PDB: 4ZI2), the GAP RP2 (orange; PDB: 3BH6), and GEF ARL13B (blue; PDB: 5DI3). On the right side is a zoomed-in view of the salt bridge between Glu86 and Arg148 at the *Cr*ARL13B-*Cr*ARL3 complex interface.

90

5.2.2. Functional investigation of ARL3-ARL13B interaction mechanism

To functionally investigate the effect of ARL3 mutation on the interaction with ARL13B, a florescence-based polarisation experiments were carried by our collaborators at the Structural Biology of Cilia Lab, Beatson Institute for Cancer Research, Glasgow. Human ARL3 wild-type (WT) or mutant (R149H) were bound to fluorescently-labelled GDP, and an excess of unlabelled GTP was added in the presence or absence of ARL13B. The capability of nucleotide exchange was then tracked for both versions of the protein by recording the fluorescence polarisation over time. When adding ARL13B GEF, wild-type ARL3 showed clear acceleration of nucleotide exchange activity. Whereas, under similar conditions, mutant ARL3 R149H failed to show acceleration of the nucleotide exchange in the presence of ARL13B **Figure 5.2.A**. To confirm our results, the highly conserved *C. reinhardtii* ARL3 wild-type and mutant R148H proteins were used under similar conditions. Wild-type *Cr*ARL3 showed clear acceleration of nucleotide exchange activity, while, mutant *Cr*ARL3 R148H failed to show acceleration of the nucleotide exchange in the presence of *Cr*ARL13B **Figure 5.2.B**. The integrity of the mutant protein was confirmed using GST pull-down study, where both WT and R149H ARL3 proteins were pulled down equally by UNC119A **Figure 5.2.D**. To further study the ARL3-ARL13B interaction, we performed a reverse charge mutation E86R in ARL13B, using *C. reinhardtii* proteins. As we predicted, mutant *Cr*ARL13B E86R failed to accelerate the nucleotide exchange of wild type *Cr*ARL3 **Figure 5.2.C**.
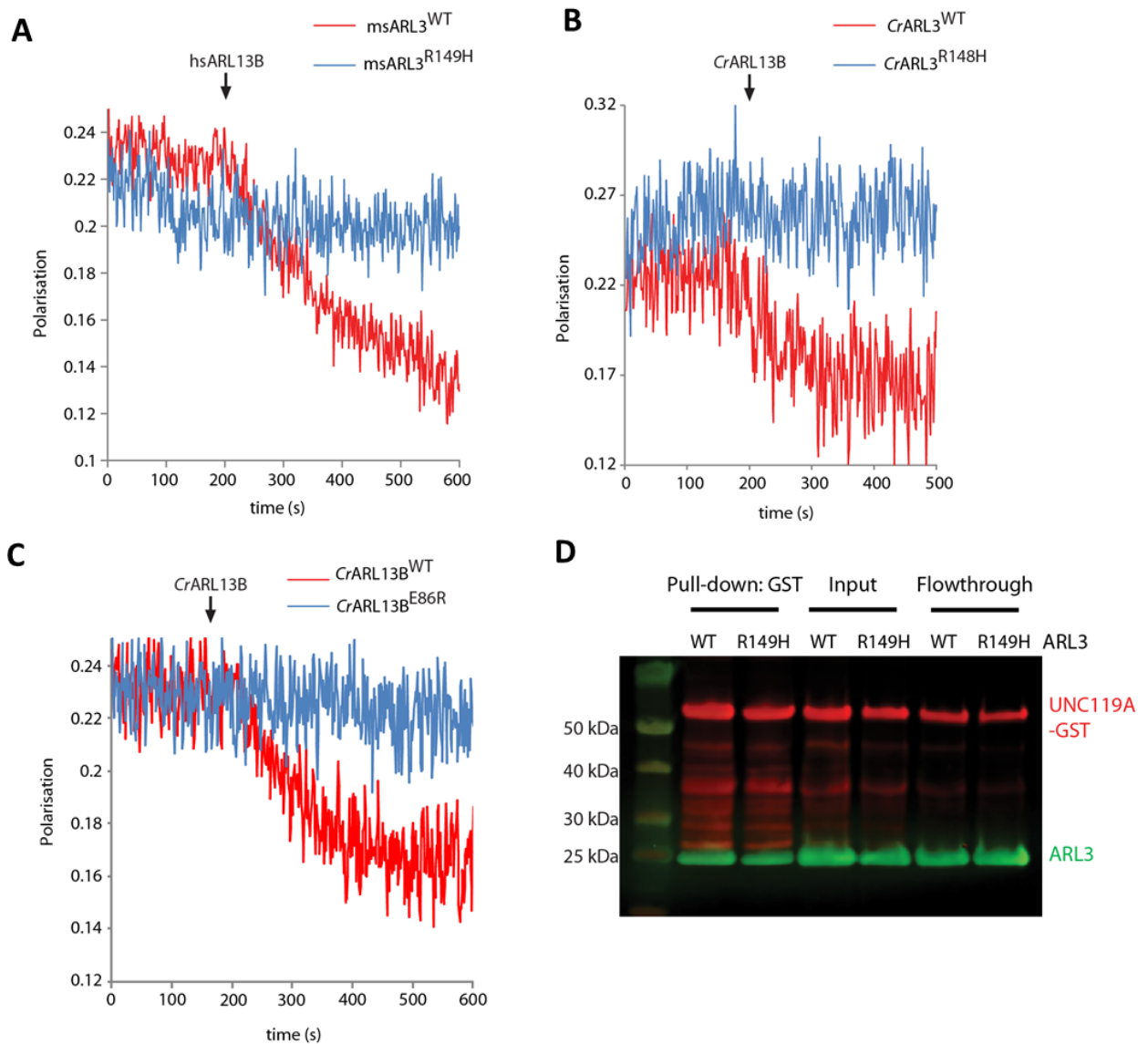
Figure 5.2 Functional investigation of ARL3-ARL13B interaction.

(A) Assay of GEF activity for murine WT ARL3 (ARL3WT) and R149H ARL3 (ARL3R149H). Fluorescence polarization was measured for 1 µM mantGDP-loaded ARL3, to which 400 µM GppNHp and 5 µM H. sapiens ARL13B (HsARL13B) were added. Nucleotide exchange was shown by only ARL3WT.

(B) Assay of GEF activity with fluorescence polarization measurements of 0.5 µM mantGDP-loaded CrARL3WT and CrARL3R148H, to which 10 µM GppNHp (GTP analog) and 5 µM CrARL13B·GppNHp were added at the indicated time points. Only CrARL3WT showed nucleotide exchange, as indicated by the drop in fluorescence polarization.

(C) Assay of GEF activity with fluorescence polarization measurements of 0.5 µM mantGDP-loaded CrARL3WT and 5 µM CrARL13B·GppNHpWT or CrArl13bE86R, to which 10 µM GppNHp (GTP analog) was added at the indicated time points. Only CrArl13bWT showed nucleotide exchange, as indicated by the drop in fluorescence polarization.

(D) 30 µg of full-length UNC119A-GST was used to pull down 60 µg of murine ARL3WT and ARL3R149H that were loaded with the GTP analog GppNHp. Proteins were detected on immunoblots with anti-GST (red) and anti-His (green) antibodies.

5.2.3. Structural analysis of the ARL3 mutation variant in patients

To determine the effect of the *ARL3* mutation variant detected at the cellular level, ciliary morphology was studied in human patients. Fibroblasts were isolated from skin biopsies obtained from all three affected individuals in JBTS family (II:1, II:4 and II:5) in addition to controls (both parents (I:1 and I:2) and an unaffected sibling (II:3)). Evaluation of percentage of ciliation, cilia length and morphology were performed after 48 h of serum starvation.

Figure 5.3.b

Cilia were identified based on ARL13B antibody staining. No significant difference in percentage of ciliation rate found between affected (mean = 75.7, 86.8 and 81% in II:1, II:4 and II:5, respectively) and controls (mean = 90.3, 84.25 and 83.6% in I:1, I:2 and II:3, respectively). Mutant fibroblasts showed variable ciliary lengths (mean length = 5.9, 7.8, and 6.8 µm in II:1, II:4, and II:5, respectively) compared to the steady ciliary length reported in the control (mean length = 5.7, 6.0 and 6.1 µm in I:1, I:2 and II:3, respectively) with no significant differences between the two groups.
Figure 5.3

Scanning electron microscopy (EM) on patients and control fibroblasts confirmed the previous findings of no significant changes in cilia length. **Figure 5.4**. EM images also showed no difference in the structural appearance of the primary cilia.
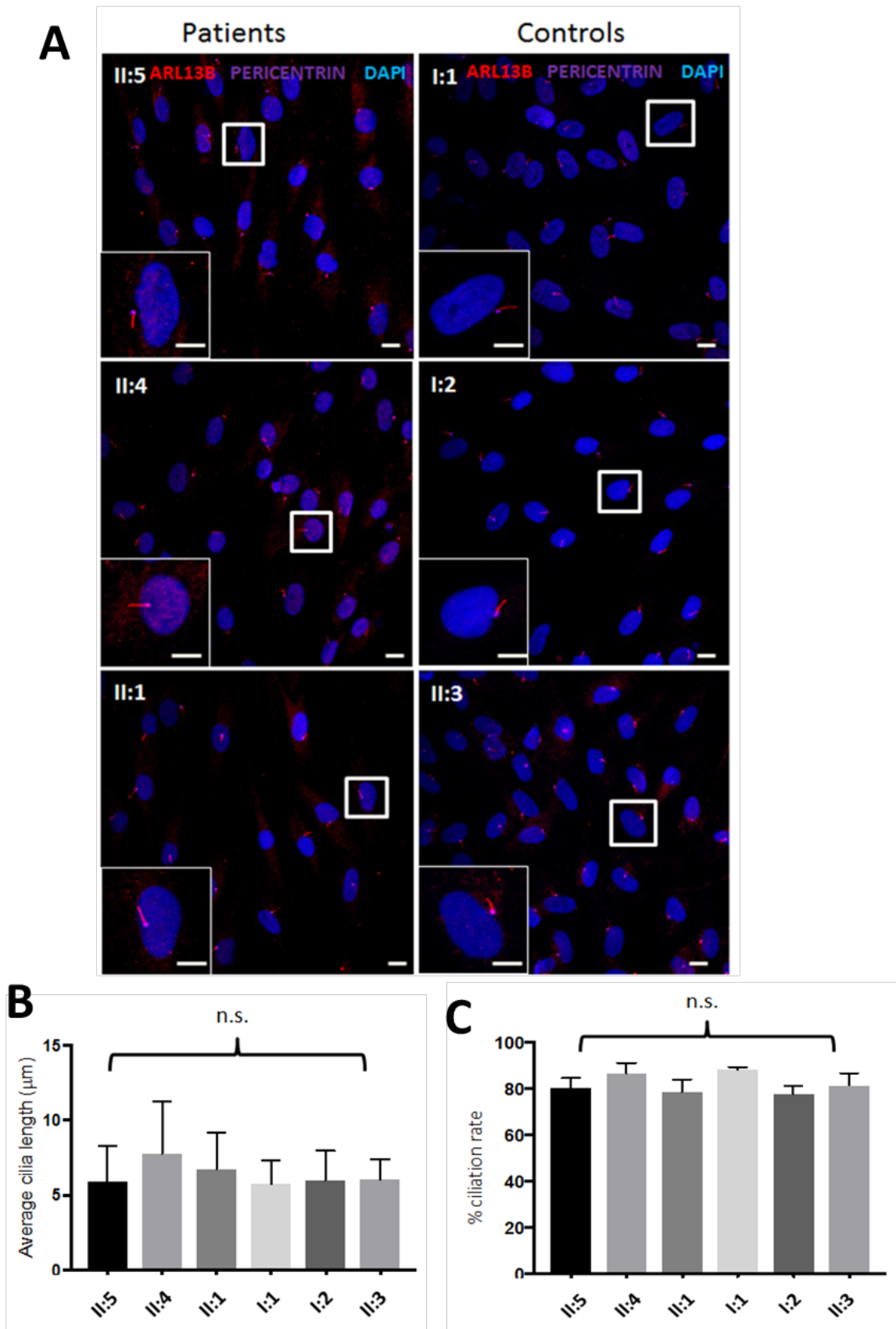
Figure 5.3 Immunofluorescence analysis of cilia length in ARL3 mutant and control fibroblasts.

(A) Fibroblasts from affected individuals (II:1, II:4 and II:5) and controls (I:1, I;2, II:3) were imaged using immunofluorescence microscopy following staining with anti-ARL13B (red) to identify ciliary membrane, anti-PERICENTRIN (magenta) to identify the ciliary base and DAPI (blue) to identify the cell nucleus. Scale bar = 10 μm.

(B) Quantification of cilia length from affected and control fibroblasts (n.s. not significant, ANOVA, n > 30 cilia in each group).

(C) Percentage ciliation rate in affected and control fibroblasts (n.s. not significant, ANOVA, n > 90 cells in each group).
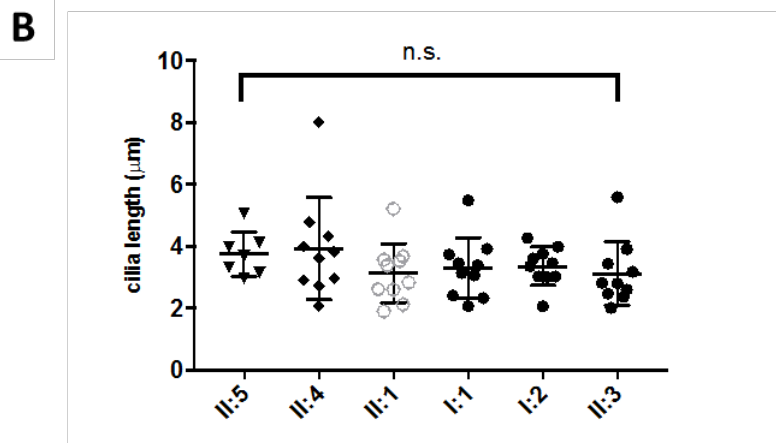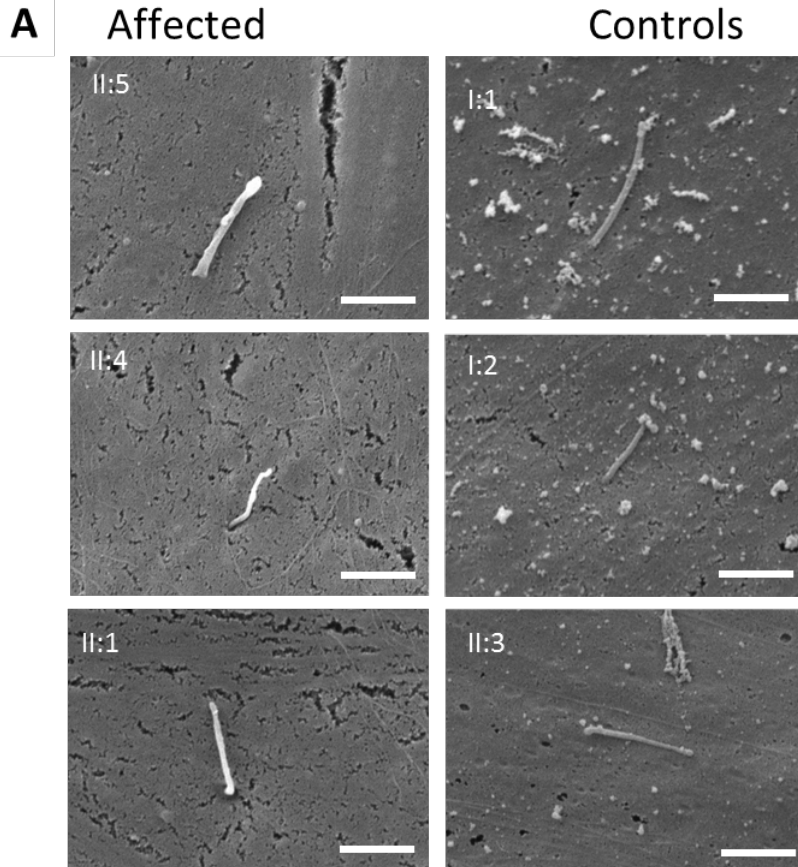
Figure 5.4 Scanning electron microscopy (SEM) and quantification of cilia length in ARL3 mutant and control fibroblasts

(A) Fibroblasts from affected individuals (II:5, II:4, II:1) and controls (I:1, I;2, II:3) seen under SEM reveal normal appearances of primary cilia (Scale bar 2 μm).

(B) Dot plot to show quantification of SEM cilia length, bars represent mean (n.s. not significant, ANOVA, n = 10 cilia in each group).

5.2.4. Functional analysis of the ARL3 mutation variant in patients

Protein trafficking to primary cilia is mediated by several small GTPases. Lipidated cargo proteins are post-translationally modified either carrying hydrophobic myristoyl group to N-terminal or internal glycine residues of protein or carrying prenyl group to C-terminal cysteine(s) of the target protein. While the myristoyl and prenyl motifs facilitates protein anchoring to cell membrane, GSF carrier proteins are required to facilitate their transport. The key role for ARL3-GTP, its GAP (RP2), and GEF (ARL13B) in trafficking of lipidated cargo proteins is the docking of cargo-carries complex at proper membrane destination. ARL3 functions as an allosteric release factor of all GSFs members: PDE6D, UNC119A/B. PDE6D is involved in trafficking of prenylated proteins, while UNC119A/B traffics myristoylated proteins (Gotthardt et al., 2015).

ARL3 exerts its function as a release factor only when bound to GTP during the ARL3-ARL13B interaction. Since we concluded that ARL3 mutation variant R149H disrupts this interaction, we predicted the ciliary localization of GSF cargo to be decreased. The prenylated GSF ciliary cargo includes INPP5E, GRK1, and PDE6 catalytic subunits (Fansa et al., 2016), whereas the myristoylated ciliary cargo includes NPHP3, GNAT1, and Cystin1 (Jaiswal et al., 2016).

We considered to study INPP5E ciliary localisation to represent the prenylated cargo proteins. After 48 hours of serum starvation, fibroblasts from affected individuals (II:5, II:4, II:1) and controls (I:1, I:2, II:3) were fixed and stained with antibodies directed towards INPP5E, PERICENTRIN as basal body marker, ARL13B as ciliary marker, and DAPI as a nuclear marker **Figure 5.5**. INPP5E ciliary intensity was calculated and corrected to background staining using ImageJ software **Figure 5.6**. Immunofluorescence microscopy analysis of total cilia INPP5E intensity in ARL3 mutant cilia demonstrated a significant loss of INPP5E content compared to control cilia. Yet the results were variable among each group, total cilia INPP5E in control fibroblast (II:3) cilia was higher than in heterozygous fibroblast (I:1 and II:2) cilia **Figure 5.7**.

We examined NPHP3 ciliary localisation to represent the myristoylated cargo proteins. After 48 hours of serum starvation, fibroblasts from affected individuals (II:5, II:4, II:1) and controls (I:1, I:2, II:3) were fixed and stained with antibodies

directed towards NPHP3, PERICENTRIN as basal body marker, ARL13B as ciliary marker, and DAPI as a nuclear marker **Figure 5.8**. NPHP3 ciliary intensity was calculated and corrected to background staining using ImageJ software **Figure 5.9**. Using the NPHP3 antibody we noted both ciliary and cellular (mostly nuclear) staining. The cellular staining does not seem to correspond to genotype and is likely to be non-specific. As expected, the immunofluorescence microscopy analysis of total cilia NPHP3 intensity in *ARL3* mutant cilia confirmed a significant loss of NPHP3 content compared to control cilia **Figure 5.10**.

Our data validated the role of ARL3 in the release of both prenylated and myristoylated ciliary cargo proteins. We proved that this function is disrupted by the *ARL3* Arg149His mutation and that WT ARL3 is required for normal release of these cargos into the ciliary axoneme.
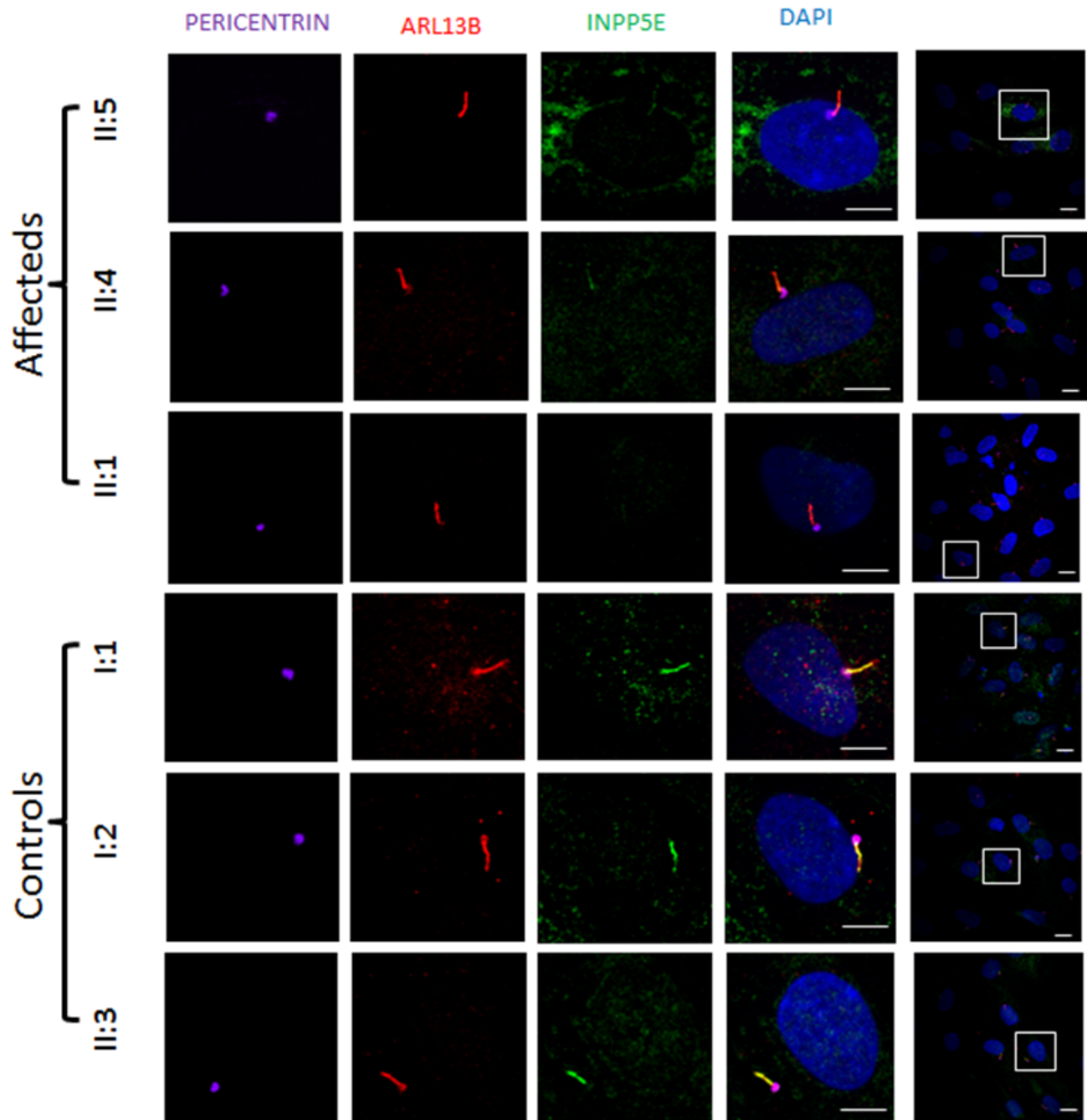
Figure 5.5 Immunofluorescence analysis of cilia INPP5E content in *ARL3* mutant and control fibroblasts.

Fibroblasts from affected individuals (II:1, II:4 and II:5) and controls (I:1, I:2, II:3) were fixed and stained with antibodies directed towards PERICENTRIN (magenta), ARL13B (red), INPP5E (green) and DAPI (blue) as a nuclear marker. Representative individual images are shown for PERICENTRIN, ARL13B and INPP5E as well as overlay images at high and low power. Scale bar = 10 μm.
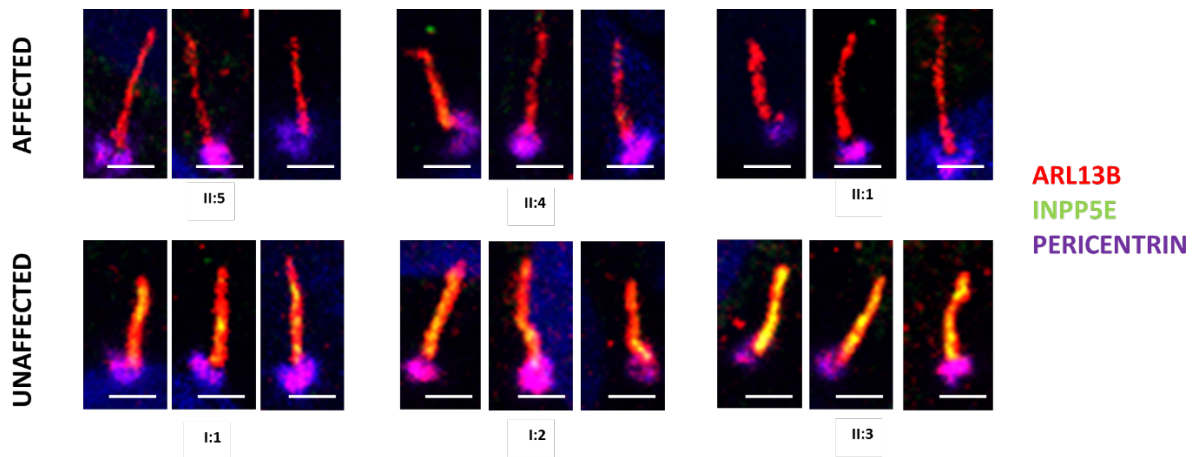
Figure 5.6 INPP5E content in fibroblast cilia

Zoomed overlay images of fibroblast primary cilia from affected individuals in family 2 (II:5, II:4, II:1) and controls (I:1, I:2, II:3) were fixed and stained with antibodies directed towards PERICENTRIN (magenta), ARL13B (red), and INPP5E (green) and DAPI (blue) as a nuclear marker.
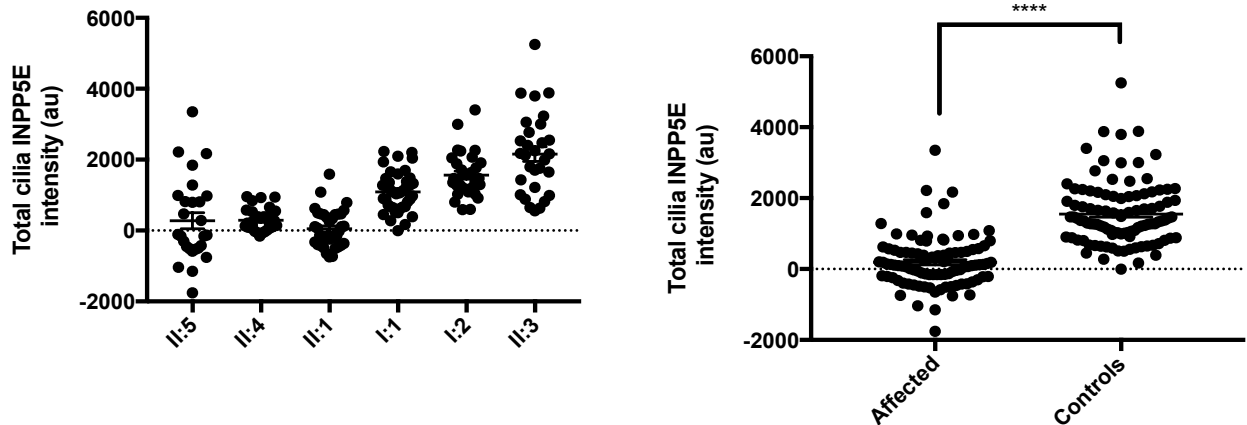
Figure 5.7 Quantification of ciliary localization of INPP5E

(A) Quantification of ciliary localization of INPP5E in each affected (II:1, II:4 and II:5) and controls (I:1, I:2, II:3).

(B) Quantification of ciliary localization of INPP5E in affected and controls groups (****$p < 0.0001$, unpaired t test, n > 150 cilia for each group).
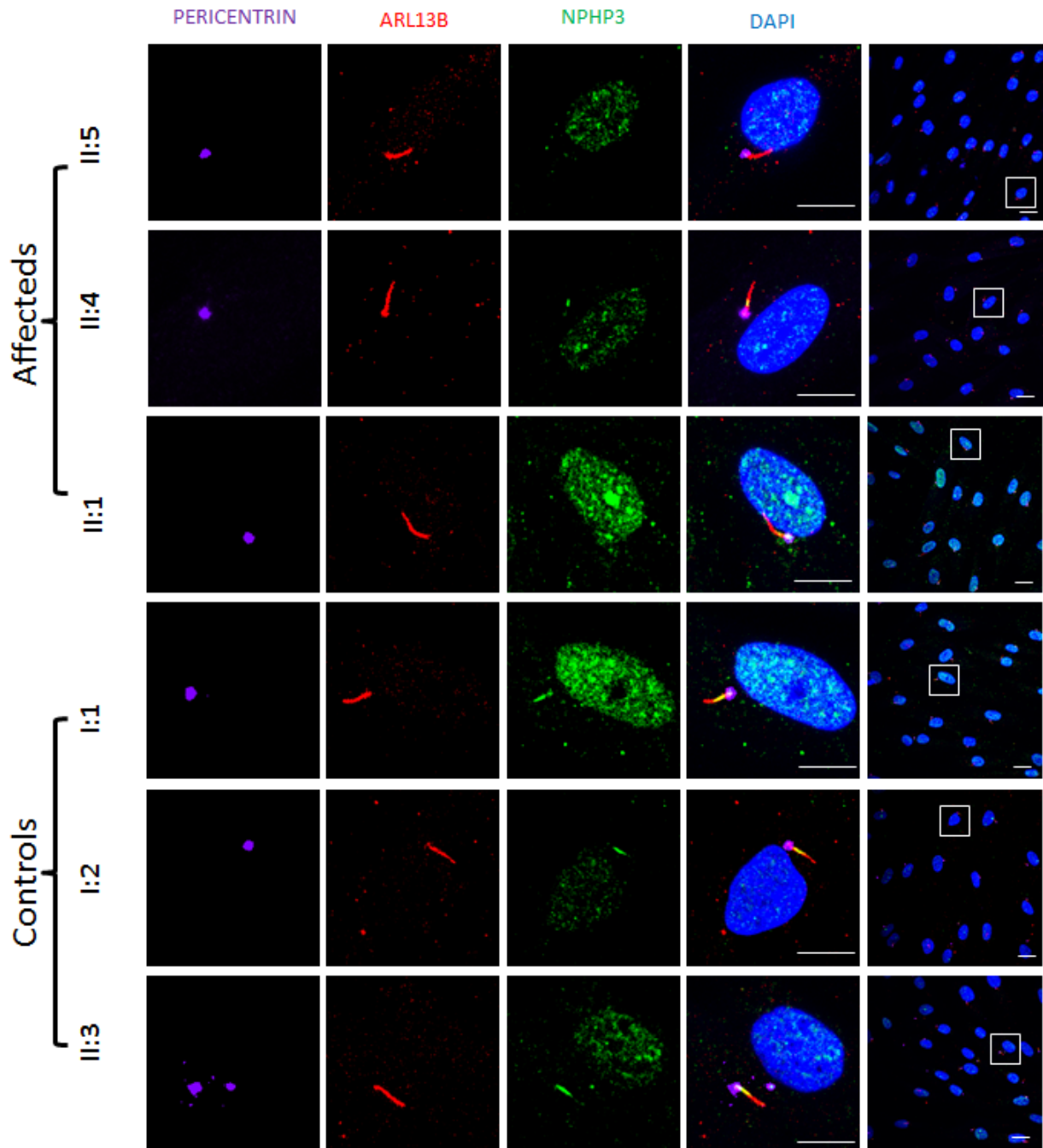
Figure 5.8 Immunofluorescence analysis of cilia NPHP3 content in *ARL3* mutant and control fibroblasts.

Fibroblasts from affected individuals (II:1, II:4 and II:5) and controls (I:1, I:2, II:3) were fixed and stained with antibodies directed towards PERICENTRIN (magenta), ARL13B (red), NPHP3 (green) and DAPI (blue) as a nuclear marker. Representative individual images are shown for PERICENTRIN, ARL13B and NPHP3 as well as overlay images at high and low power. Scale bar = 10 µm.
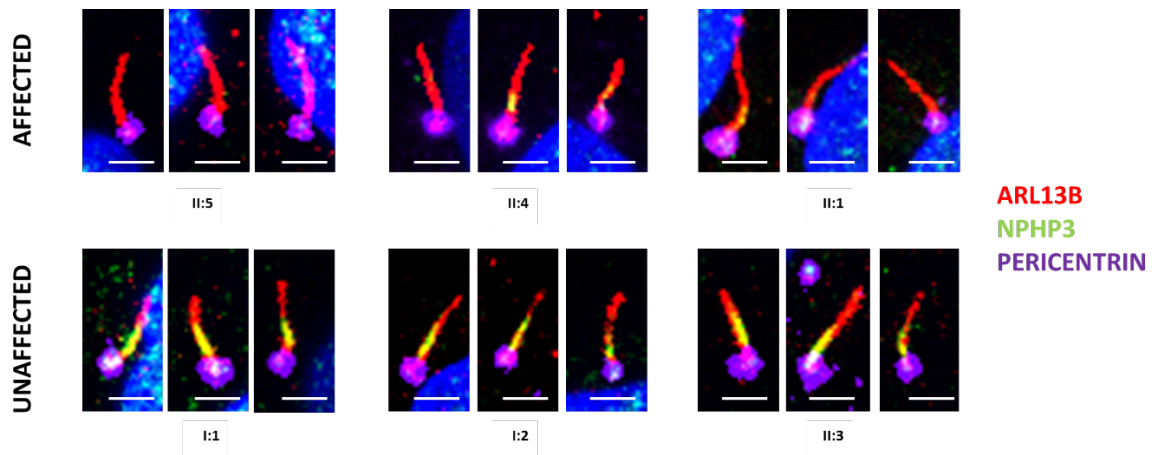
Figure 5.9 NPHP3 content in fibroblast cilia

Zoomed overlay images of fibroblast primary cilia from affected individuals in family 2 (II:5, II:4, II:1) and controls (I:1, I:2, II:3) were fixed and stained with antibodies directed towards PERICENTRIN (magenta), ARL13B (red), NPHP3 (green) and DAPI (blue) as a nuclear marker.
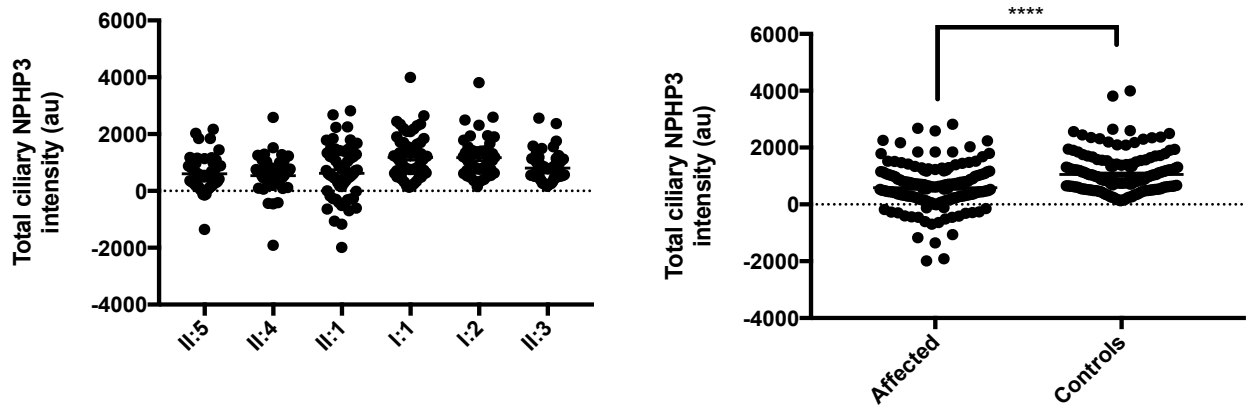
Figure 5.10 Quantification of ciliary localization of NPHP3

(A) Quantification of ciliary localization of NPHP3 in each affected (II:1, II:4 and II:5) and controls (I:1, I:2, II:3).

(B) Quantification of ciliary localization of NPHP3 in affected and controls groups ($****$p < 0.0001, unpaired t test, n > 150 cilia for each group).

To further confirm our previous finding to be specific to the loss of ARL3 function as an allosteric release factor of all GSFs members, we studied intraflagellar transport (IFT) and Sonic Hedgehog signal transduction. We examined the ciliary content of another protein, GLI3, known to be translocated independently of the GSF transport (Haycraft et al., 2005). After 24 hours of serum starvation, fibroblasts from affected individuals (II:5, II:4, II:1) and controls (I:1, I:2, II:3) were treated with Sonic Hedgehog pathway agonist (SAG). 24 hours later, cells were fixed and stained with antibodies directed towards GLI3, PERICENTRIN as basal body marker, ARL13B as ciliary marker, and DAPI as a nuclear marker. GLI3 ciliary intensity was calculated at cilia tip and along the axoneme and corrected to background staining using ImageJ software. As expected, the immunofluorescence analysis of both total cilia intensity of GLI3 and cilia tip GLI3 had no significant differences in ARL3 mutant and control fibroblasts **Figure 5.11**.

We reported no defect in GLI3 ciliary localisation confirming that *ARL3* Arg149His mutation doesn't disturb ciliary Hedgehog signalling pathway.
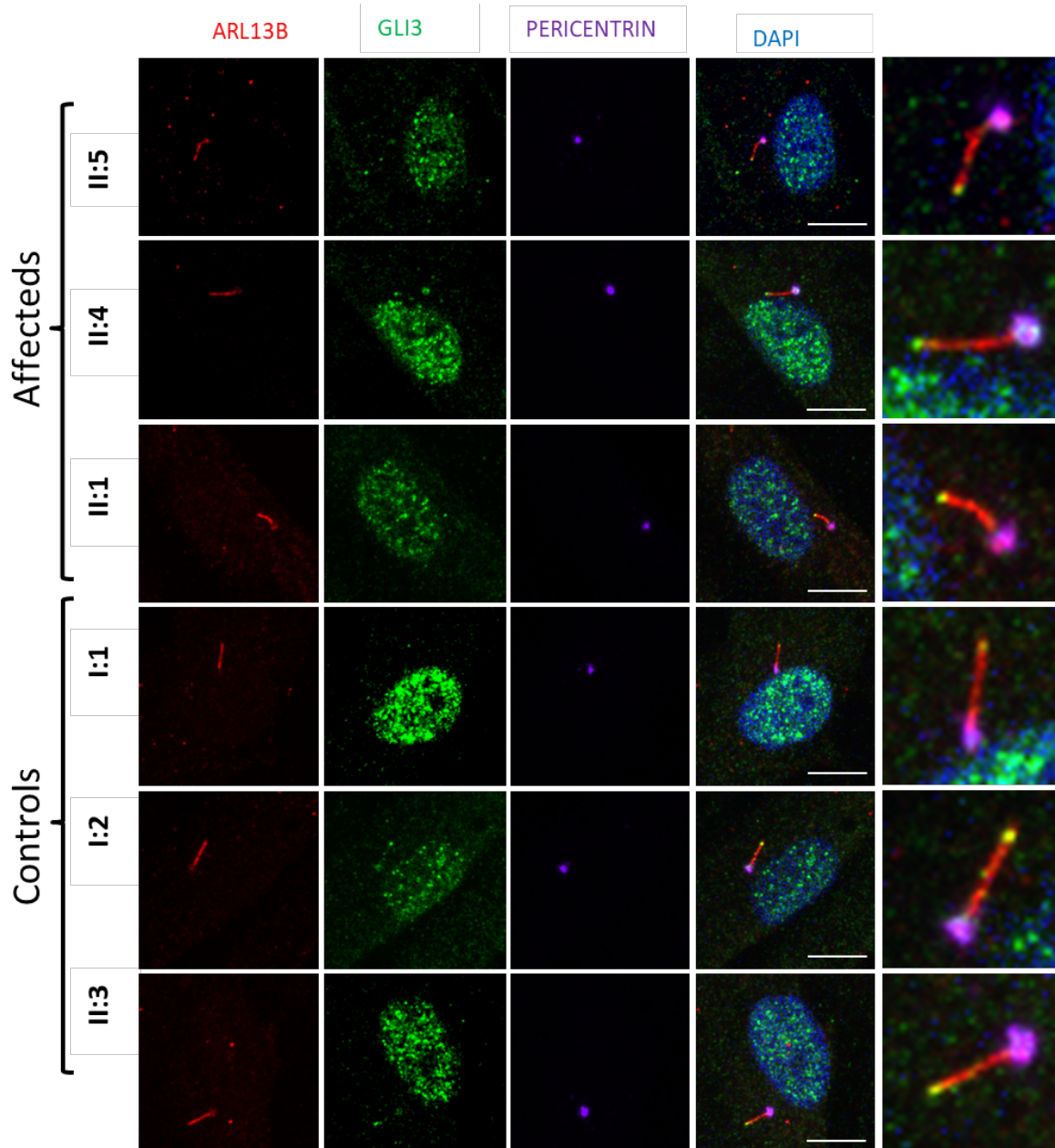
Figure 5.11 Lack of disruption of GLI3 localisation in cilia axoneme and tip in _ARL3_ mutant fibroblasts

Fibroblasts from affected individuals in family 2 (II:5, II:4, II:1) and controls (I:1, I:2, II:3) were treated with 100 nM SAG then fixed and stained with antibodies directed towards ARL13B (red), GLI3 (green), PERICENTRIN (magenta) and DAPI (blue) as a nuclear marker. Representative single channel images are shown for ARL13B, GLI3 and PERICENTRIN as well as overlay images at low power (scale bar = 10 µm) and zoomed (scale bar = 5 µm).
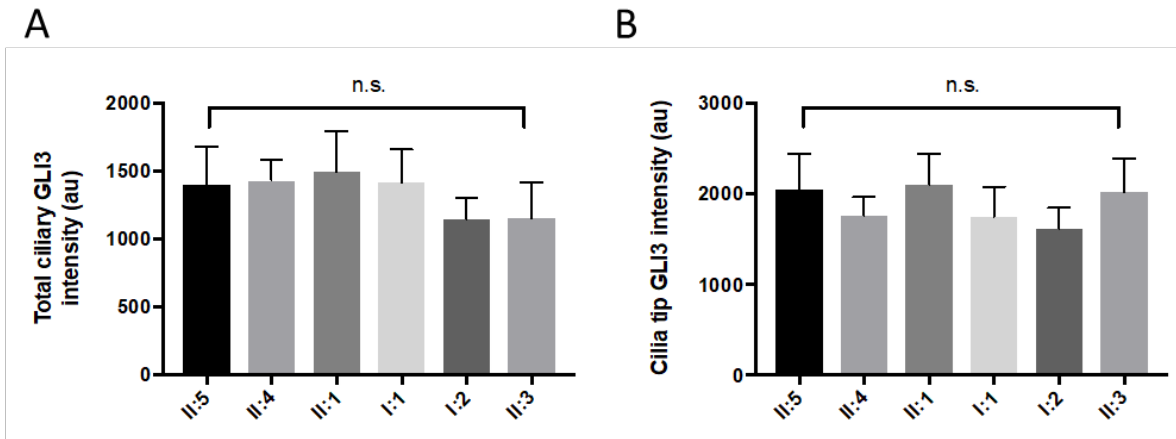
Figure 5.12 Quantification of ciliary localization of GLI3

(A) Quantification of ciliary localisation of GLI3 is shown (n >35 for each group, n.s. not significant, ANOVA).

(B) Quantification of ciliary tip localisation of GLI3 is shown (n >35 for each group, n.s. not significant, ANOVA).

5.2.5. siRNA mediated knockdown of ARL3 in WT HUREC

JBTS phenotype in family 2 involved renal manifestation in the form of multicystic kidney. To further investigate whether the role of ARL3 in ciliary cargo protein trafficking is tissue specific, we sought to study its function on kidney cells model. Human Urine derived Renal Epithelial Cell (HUREC) culture is a non-invasive way of isolating human renal tubular epithelial cells from both adults and children and serving as an excellent model to study ciliopathies (Srivastava et al., 2017, Ajzenberg et al., 2015). HUREC were cultured from age-matched donor not known to have kidney problems. Cells were obtained from 100 ml urine sample from wild-type (WT) donor and plated in 12 well cell culture plates. HUREC proliferate and form monolayer 2D culture within a period of 14 days. HUREC can be used in experiments when reaching confluency of 70-80% and lasts up to 6 passages.
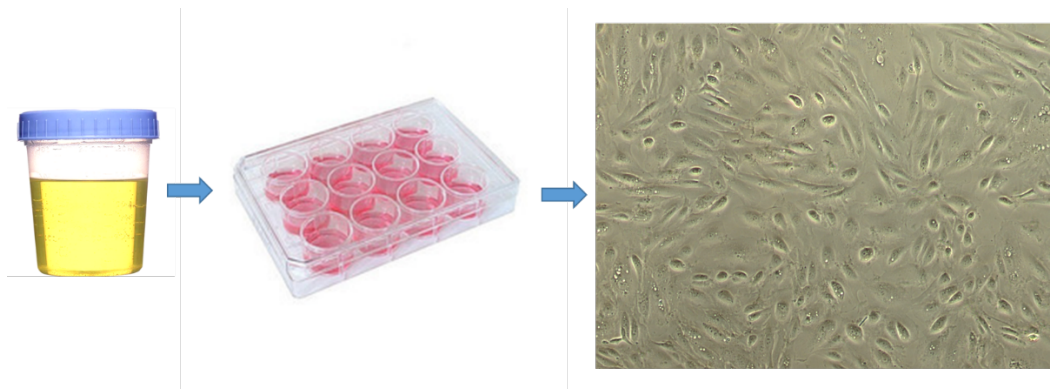
Figure 5.13 Non-invasive method of isolating HUREC from urine sample
Urine collected from patients and healthy donors was processed within 4 hours of collection. The resulting pallets of cells were plated and grown in 12 well plate. The epithelial cells begin to appear on day 5 and can be used for passaging or experiments after reaching 80- 90% confluence.

We conducted a small interfering RNA (siRNA) mediated *ARL3* knockdown experiment on WT HUREC. The knockdown was confirmed by gene expression analysis using RT PCR of HUREC obtained from siRNA mediated knockdown of ARL3 (siARL3) and siRNA mediated control (siCtrl), the experiment demonstrated loss of ARL3 mRNA. **Figure 5.14**. Once again, immunofluorescent microscopy used to study the structural and the functional of the treated HUREC. Consistent with morphologically normal cilia in *ARL3*-mutant fibroblasts, no structural defect seen siARL3 HUREC. Since primary cilia tissue specific, the cilia length of siARL3 and siCtrl HUREC were analysed, and no significant difference in cilia length reported **Figure 5.15**. Next, we determined the localisation of GSF cargo proteins (INPP5E and NPHP3) in siARL3 HUREC compared to siCtrl HUREC. In agreement with our previous results on *ARL3*-mutant fibroblasts cilia, immunofluorescent microscopy analysis revealed significant reduction in ciliary content of both INPP5E (**Figure 5.16** and **Figure 5.17**) and NPHP3 (**Figure 5.18** and **Figure 5.19**).
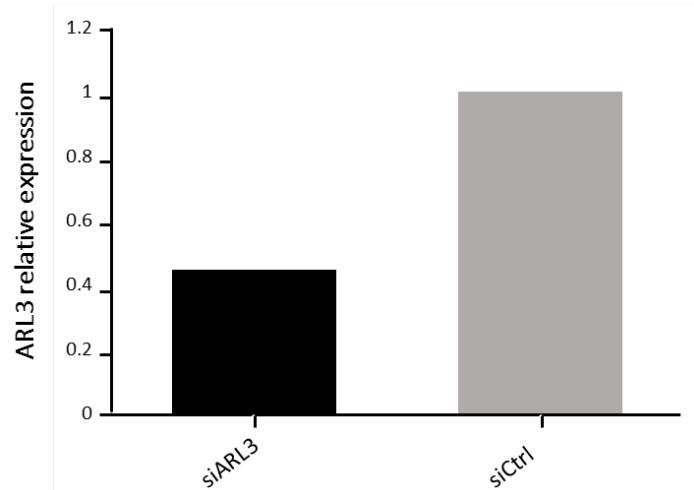
Figure 5.14 *ARL3* gene expression analysis using quantitative real time PCR to demonstrate the effect of ARL3 knockdown experiment on HURECs
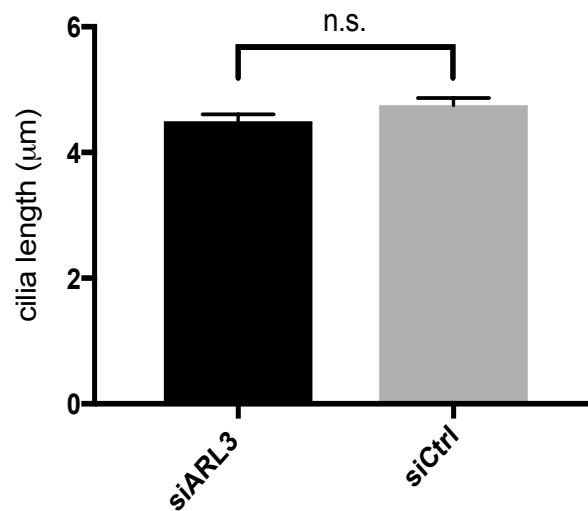
Figure 5.15 Quantification of cilia length siRNA mediated ARL3 knockdown in HUREC

Quantification of cilia length in siARL3 and siCtrl groups (n.s. not significant, unpaired t test, >90 cilia for each group).
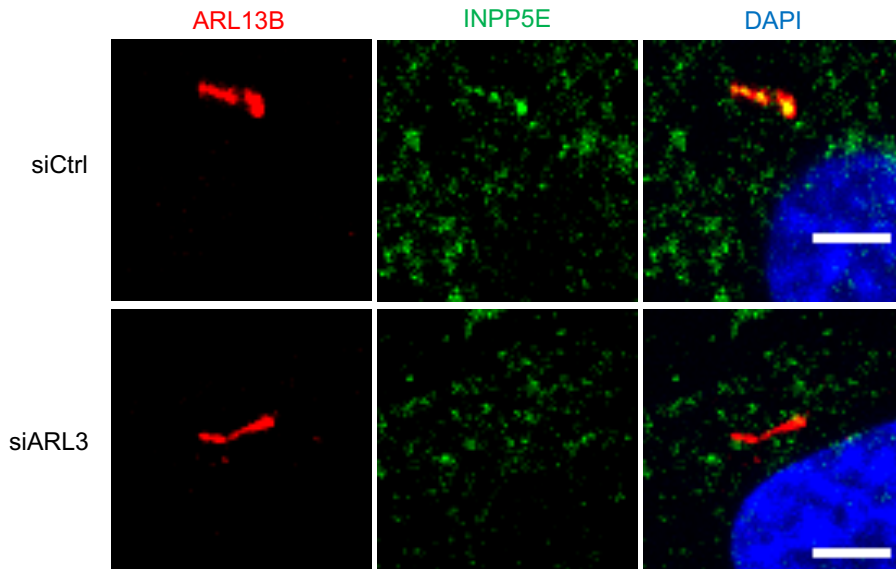
Figure 5.16 Immunofluorescence analysis WT HUREC cilia treated with *ARL3* siRNA demonstrate decrease of cilia INPP5E content

siRNA mediated knockdown of *ARL3* leads to reduction in ciliary content of INPP5E in comparison with siCtrl. HURECs were fixed and stained with antibodies directed towards ARL13B (red), INPP5E (green) and DAPI (blue) as a nuclear marker. Representative individual images are shown for ARL13B and INPP5E as well as overlay images at high power. Scale bar = 5 μm.
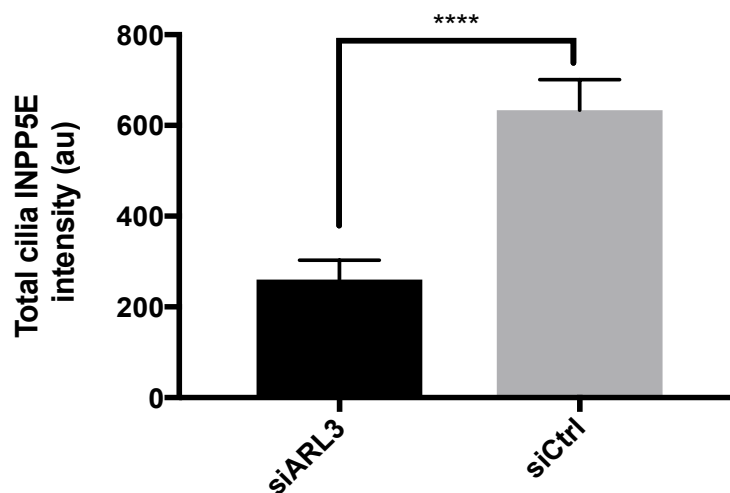
Figure 5.17 Quantification of ciliary localization of INPP5E in siRNA mediated ARL3 knockdown in HUREC

Quantification of ciliary localization of INPP5E in siARL3 and siCtrl groups (****$p < 0.0001$, unpaired t test, n > 45 cilia for each group).
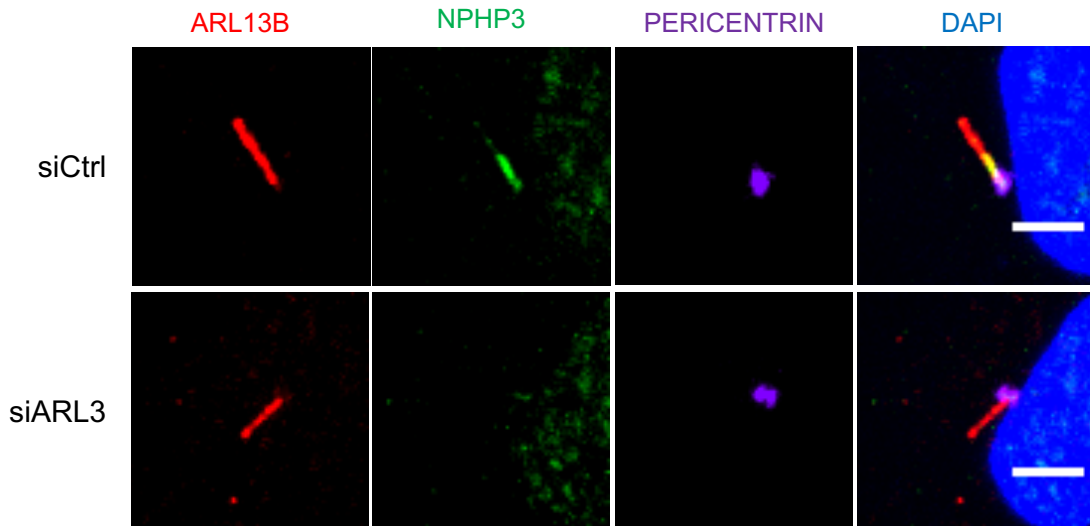
Figure 5.18 Immunofluorescence analysis WT HUREC cilia treated with *ARL3* siRNA demonstrate decrease of cilia NPHP3 content

siRNA mediated knockdown of *ARL3* leads to reduction in ciliary content of NPHP3 in comparison with siCtrl. HURECs were fixed and stained with antibodies directed towards ARL13B (red), INPP5E (green), PERICENTRIN (magenta) and DAPI (blue) as a nuclear marker. Representative individual images are shown for ARL13B, NPHP3 and PERICENTRIN as well as overlay images at high power. Scale bar = 5 μm.
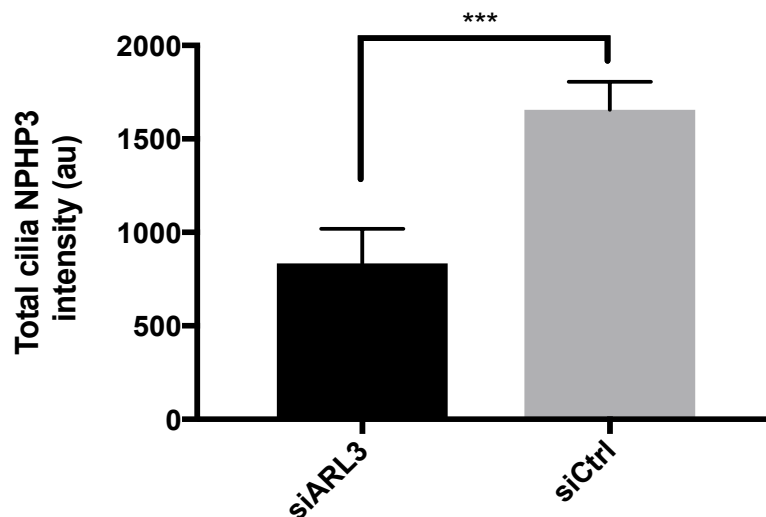
Figure 5.19 Quantification of ciliary localization of NPHP3 in siRNA mediated ARL3 knockdown in HUREC

Quantification of ciliary localization of INPP5E in siARL3 and siCtrl groups (***p = 0.0007, unpaired t test, n > 45 cilia for each group).

5.3. **Discussion**

ARL3 cycles between inactive-GDP bound and active-GTP bound forms. Activated ARL3 binds to cargo-carrier complex to induce conformational changes leading to the release of the ciliary cargo. In the cilia, ARL3 gets activated by the exclusive presence of its GEF ARL13B, while the presence of ARL3 GAP, RP2, outside the cilia creates an ARL3GTP gradient across the transition zone acting like a driving force to transport the lipidated cargo protein to the cilia (Gotthardt et al., 2015).

Our results have shown the essential implication of ARL3 Arg149 residue for the regulation of sorting and transport of ciliary cargo protein to the cilia. By employing crystallography to elucidate the structural basis for the interaction, the structure showed the evolutionarily conserved and the ARL3 Arg149 residue (R148 [Arg148] in *Cr*ARL3) is located in the loop region between the α4 and β6 domains of ARL3 that directedly interact with the ARL13B Glu88 residue located in the switch II domain of ARL13B (E86 [Glu86] in *C. reinhardtii* ARL13B [*Cr*ARL13B]) during interaction interface to form ARL13B-ARL3 complex described by Gotthardt et al. (2015). **Figure 5.20**. A marked decrease in GEF activity assay was detected during the interaction of the exact ARL3 Arg149 mutant residue with ARL13B compared to wild type, indicating disruption in the cargo release function of ARL13B-ARL3 complex.

We studied the ciliary phenotype of ARL3 Arg149His patient derived fibroblasts, as changes in cilia length or structure can reflect the ciliogenesis process. As we expected from previous reports, the detected ARL3 Arg149 mutant variant exhibit no significant change in the frequency of ciliation, cilia length or morphology when compared to healthy carriers and wildtype fibroblasts. Our immunofluorescence microscopy results were confirmed with scanning electron microscopy. However, Zhang et al. (2016) reported an excess of ARL3-GDP may affect ciliogenesis indirectly by titrating out its GEF or other protein involved in ciliogenesis, our data contradict their conclusion.

Moreover, we examined the allosteric release function of the ARL3 Arg149His on lipidated protein trafficking to the cilia on patients derived fibroblasts. Myristoylated proteins and prenylated proteins are lipid modified proteins required an interaction with carrier protein to prevent their interaction with plasma membrane and gain a

soluble transient at ciliary fate and transition zone (Hu et al., 2010). INPP5E an example of prenylated ciliary protein, involved in ciliogenesis and known to cause JBTS1 when its encoded gene is mutated, binds to its carrier PDE6D to form a solubilised ciliary cargo-carrier complex (Humbert et al., 2012). NPHP3 an example of myristoylated ciliary protein, localised to cilia and involved in signalling pathways, binds to its carrier UNC119 (Wright et al., 2011). In the wild-type cilia, ARL3 is GTP bound an active allowing the docking of ciliary cargo INPP5E/NPHP3 and the release of its carrier PDE6D/UNC119. Thereby, the lipid moiety of cargo protein will be exposed and associate with the ciliary membrane and localise to the cilia.

Based on the above mentioned model of trafficking, we speculated that the ciliary localisation of ciliary cargo protein to be reduced in ARL3 Arg149His cilia. As expected, the immunofluorescence microscopy analysis of total cilia INPP5E/NPHP3 protein content in *ARL3* mutant cilia confirmed a significant loss of INPP5E/NPHP3 content compared to control cilia. We also confirmed that the ciliary Sonic hedgehog pathway is not disturbed by ARL3 Arg149His variant.

To further explain the renal phenotype of ARL3 mutation in the second JBTS family (ARL3 Arg149Cys), we sought to determine the effect of ARL3 knockdown on wild-type HUREC. Interestingly, total loss of function mutation of ARL3 had the same effect as the missense mutation ARL3. Our data showed that siRNA mediated knockdown of ARL3 cilia replicated the phenotype of ARL3 Arg149His patient fibroblasts. No significant change found in cilia length and a marked loss of both ciliary content of cargo protein INPP5E and NPHP3.

We conclude that ARL3 mutation disturb the ciliary protein composition by disrupting ARL13B-ARL3 interaction manifesting in JBTS35. **Figure 5.21**
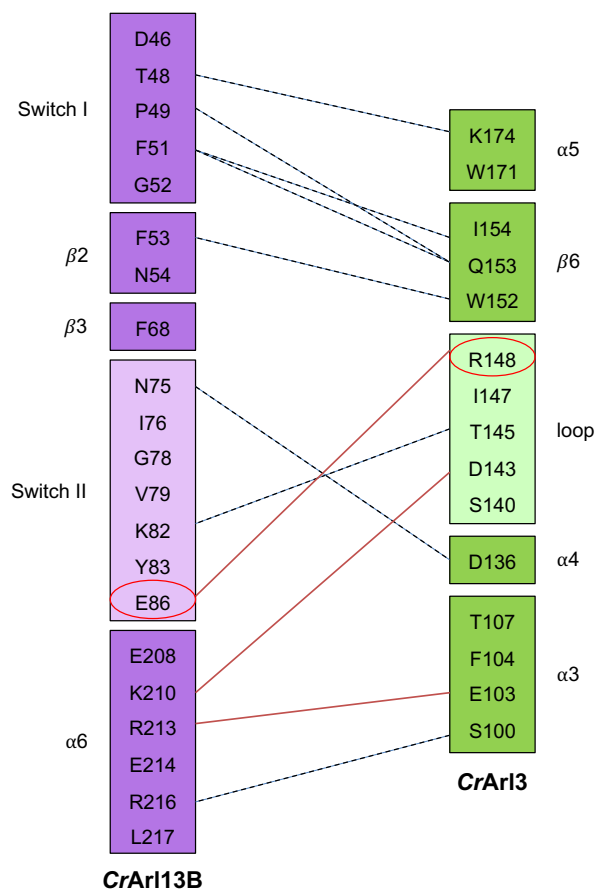
Figure 5.20 The *Cr*Arl13B-*Cr*Arl3 complex

Schematic representation of residues located in the interaction interface of the CrArl13B-CrArl3 complex. The dashed lines illustrate the hydrogen bonds between residues and red lines illustrate the salt bridges. The red circles indicate the *Cr* analogue of the detected human ARL3 Arg149 residue. Adapted from (Gotthardt et al., 2015)
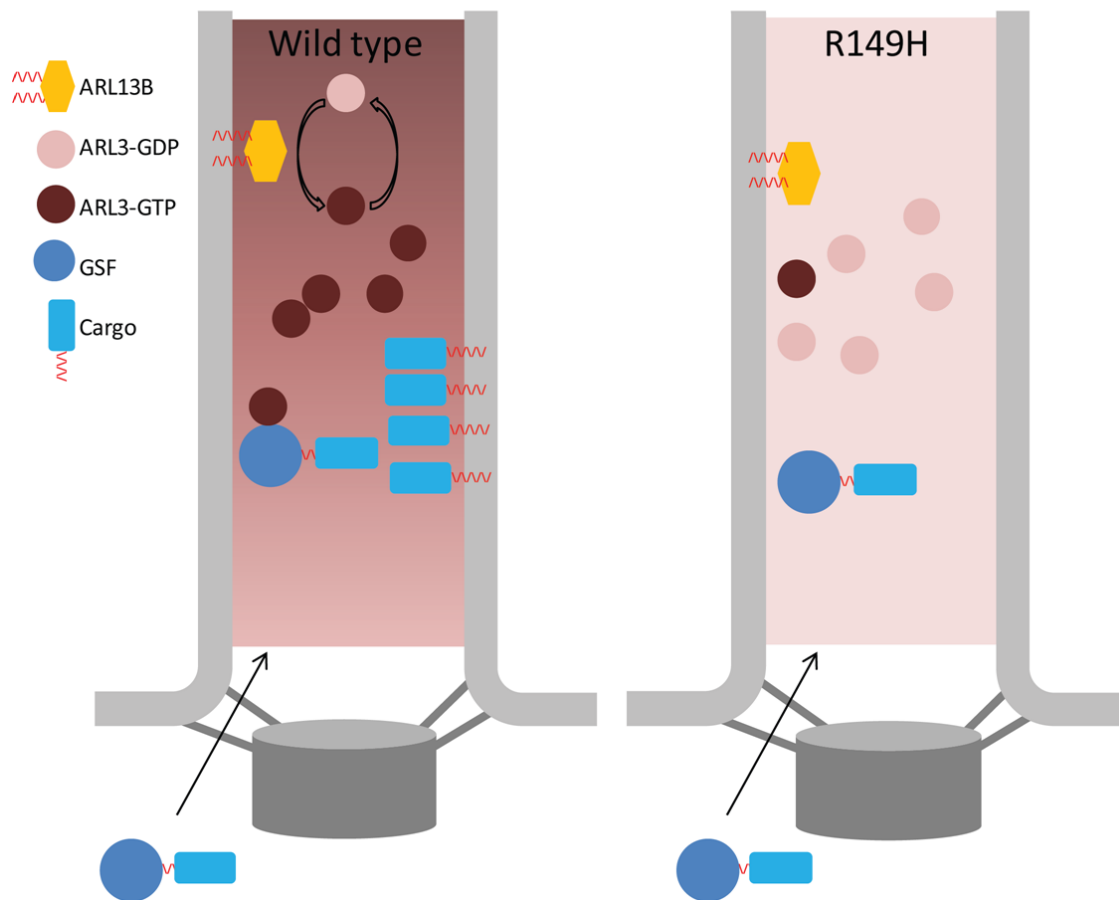
Figure 5.21 Model of GSF-cargo release in cilia with wild-type ARL3 versus R149H ARL3

ARL13B assists ARL3 in cilia to exchange its bound GDP to GTP. The specific localisation of ARL13B in the cilia creates a high concentration of ARL3-GTP. ARL3-GTP in turn can release the cargo bound to its cognate GSF and results in ciliary localisation. Mutant ARL3 (R149H) is not able to interact with ARL13B and the ARL3GTP concentration is therefore low in the cilia, which results in inefficient release of GSF cargo in the cilia.

Chapter 6 **Final discussion and concluding remarks**

6.1. **Lessons learned from the Renal-Genetic family clinic**

The constant expanding list of genotypes and phenotypes associated with inherited renal disorders make the correct identification of inherited renal syndromes and disorders quite challenging. NGS technologies have helped speed up the discoveries of novel genes in inherited renal disorders, an allow known genetic disorders to be screened rapidly, for example the successful multigene panel to screen for Alport syndrome (Artuso et al., 2012). NGS gene panels have recently been applied to patients with atypical kidney disease phenotypes for genetic diagnosis (Bullich et al., 2018).

Whole exome sequencing (WES) is a proven approach to identify novel genes causing inherited renal disorders, however it is hindered by the high numbers of variants detected when all the exons-coding sequences in human genome are analysed. Such obstacles can be overcome by limiting the analysis to smaller regions of the exome detected by means of linkage analysis or homozygosity mapping (MacArthur et al., 2014).

We found that the practice of a multidisciplinary renal genetic clinic provides added value and improved patient care though identifying the precise molecular genetic diagnosis **Figure 6.1**. Despite all the challenges, applying highly advanced NGS technologies will certainly improve diagnosis efficiency, prognosis, and genetic counselling for patients in clinical practice every day. Moreover, following a genetic diagnosis, patients are often able to receive better healthcare and the cost of additional investigation maybe reduced. The implementation of genomic medicine throughout the NHS services is the core vision of Genomics England.
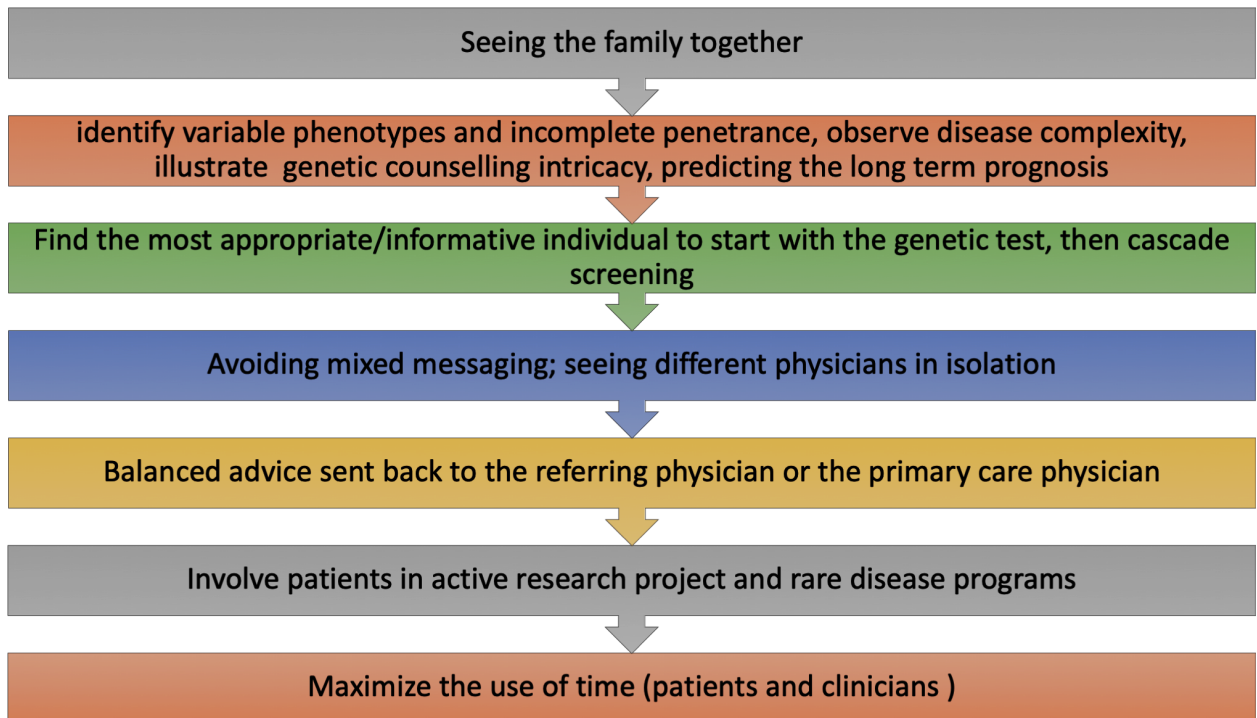
Figure 6.1 Lessons learnt from multidisciplinary renal-genetic family clinic

6.2. *ARL3* mutations cause Joubert syndrome by disrupting ciliary protein composition

ARL3 is a highly conserved gene, and its encoded soluble small G protein is found in all ciliated organisms, several human tissues and tumour cell lines (Cavenagh et al., 1994). We present *ARL3* as a ciliopathy and JBTS associate gene. *ARL3* role in ciliogenesis and axoneme formation was first noted by studying the *Leishmania* homolog of ARL3, LdARL-3A, where it is found to be crucial for flagellum formation (Cuvillier et al., 2000). A germline mutation in mice leading to knockout of *Arl3* gave rise to classic syndromic ciliopathy phenotype similar to that found in ARPKD. These Arl3$^{-/-}$ mice developed cysts formation in kidneys, liver and pancreas, pancreatic hypoplasia, ductal plate malformation, retinal dystrophy in addition to photoreceptors degeneration (Schrick et al., 2006). *Arl3*$^{-/-}$ manifestations were severe and mutant mice failed to thrive beyond postnatal week 3; the nonsense phenotype in these mice seems much more detrimental than the missense phenotype we reported in our JBTS families. We hypothesize that nonsense *ARL3* mutation in human may cause a distinct ciliopathy phenotype as severe as the murine phenotype and may be perinatally lethal, just like Meckel syndrome, perhaps in part explaining its rarity.

The previously reported *ARL3* mutation in human was not linked to a human multisystem ciliopathy disorder. A heterozygous missense variant of *ARL3* was reported by Strom et al. (2016) in a Caucasian family with non-syndromic retinitis pigmentosa. The *ARL3* missense variant (p.Tyr90Cys) was identified in three affected individuals, appeared de *novo*, and transmitted in an autosomal dominant fashion. *ARL3* Tyr90Cys was rare and found to be pathogenic by *in silico* prediction tools. A second allele within *ARL3* was not identified and no further mechanistic evaluation was carried out. On the other hand, we have identified pathogenic biallelic variants in *ARL3* in two different families with JBTS. *ARL3* mutations fully segregated with a classical JBTS phenotype, in addition to the retinal changes. We present strong evidence that biallelic *ARL3* deleterious variants are sufficient to cause JBTS.

Mutations in the genes encoding ARL3 effectors (interaction partners) ARL13B and PDE6D are also known to cause JBTS. Mutations in *ARL13B* (JBTS8) led to classic neurodevelopmental phenotype without reported renal involvement (Cantagrel et al., 2008). Thomas et al. (2015) identified another variant in ARL13B that extended the

phenotypic presentation of JBTS8 to include retinal defects and obesity. Mutation in *PDE6D* were found to cause JBTS22, in a consanguineous family of 3 affected siblings (Thomas et al., 2014). The neurodevelopmental phenotype was associated with hands and feet post axial polydactyly, coloboma, facial dysmorphism, retinal dysplasia or renal hypoplasia. Moreover, the genes *INPP5E* and *NPHP3* encoding the disrupted ciliary cargo proteins (INPP5E and NPHP3) we have identified may also be responsible for JBTs phenotypes. Mutations in *INPP5E* can cause JBTS1, in a cohort of JBTS patients that presented with neurodevelopmental phenotypes with retinopathy in a subgroup, no polydactyly or renal disease reported (Bielas et al., 2009). However, 10% of JBTS patient with *INPP5E* mutation can develop renal manifestations (Kroes et al., 2016). On the other hand, mutation in *NPHP3* were first found to cause adolescent nephronophthisis, a progressive form of renal failure , in a large Venezuelan family (Omran et al., 2000). Later *NPHP3* phenotypes expanded to include infantile nephronophthisis, lethal neonatal nephronophthisis and renal hepatic pancreatic dysplasia and Meckel syndrome (Tory et al., 2009, Simpson et al., 2009, Bergmann et al., 2008).

Interestingly, ARL3 role in releasing lipid modified protein extends beyond the cilium to the immune synapse (Stephen et al., 2018). T cells lack the presence of cilia, however, similarities between cilia and the immune synapses have been clearly recognized (de la Roche et al., 2016). Lymphocyte- specific tyrosine protein kinase (LCK) initiate the interaction at the immune synapse between T cells and antigen-presenting cells (APC). LCK undergoes post-translational myristoylation to facilitate plasma membrane localisation and require a solubilising carrier for proper trafficking to immune synapse. Stephen et al. reported that trafficking of lipid modified LCK is mediated by UNC119A to the immune synapse where its release by ARL3-GTP. Their work has also identified the endogenous localization of ARL3 GEF, ARL13B, at the T cell membrane and outside the cilia (Stephen et al., 2018).

Ciliopathies in general and JBTS in particular exhibit an overlapping phenotype as well as genotypes. Such overlap can be explained by the fact that proteins coded by ciliary genes function through an interaction networking and don't work in isolation (Humbert et al., 2012). We propose *ARL3* as a JBTS causing gene and a novel hub in a network of ciliopathy causing genes and ARL3 is now recognized as JBTS35 https://www.omim.org/phenotypicSeries/PS213300 (Alkanderi et al., 2018).

6.3. Future directions

We have identified two missense mutations of *ARL3* at the same amino acid Arg149 but resulting in two different amino acids changes and eventually leading to different phenotypic presentation in two different JBTS families. Phenotypic differences may be related to differences in the genetic background of both families. However, this phenotypic heterogeneity requires further explanation and understanding of the ciliopathy pathways involved. Future work will aim to develop mouse models to characterise the two different mutations identified in *ARL3* (Arg149His and Arg149Cys) using CRISPR/Cas9. Together with our collaborators at the Beatson Institute, University of Glasgow, we aim to compare Arl3 mutant mice with Arl13b mutant mice to further study the ARL3-ARL13b interaction and the GEF role in the release of ciliary cargo proteins.

Chapter 7 **References**

ADALAT, S., BOCKENHAUER, D., LEDERMANN, S. E., HENNEKAM, R. C. & WOOLF, A. S. 2010. Renal malformations associated with mutations of developmental genes: messages from the clinic. *Pediatric Nephrology,* 25**,** 2247-2255.

ADAM, J., BROWNING, A. C., VAIDEANU, D., HEIDET, L., GOODSHIP, J. A. & SAYER, J. A. 2013. A wide spectrum of phenotypes in a family with renal coloboma syndrome caused by a PAX2 mutation. *Clinical kidney journal,* 6**,** 410-413.

AJZENBERG, H., SLAATS, G. G., STOKMAN, M. F., ARTS, H. H., LOGISTER, I., KROES, H. Y., RENKEMA, K. Y., HAELST, M. M., TERHAL, P. A. & ROOIJ, I. A. J. C. 2015. Non-invasive sources of cells with primary cilia from pediatric and adult patients. *Cilia,* 4**,** 8.

AKIZU, N., SILHAVY, J. L., ROSTI, R. O., SCOTT, E., FENSTERMAKER, A. G., SCHROTH, J., ZAKI, M. S., SANCHEZ, H., GUPTA, N., KABRA, M., KARA, M., BEN-OMRAN, T., ROSTI, B., GUEMEZ-GAMBOA, A., SPENCER, E., PAN, R., CAI, N., ABDELLATEEF, M., GABRIEL, S., HALBRITTER, J., HILDEBRANDT, F., VAN BOKHOVEN, H., GUNEL, M. & GLEESON, J. G. 2014. Mutations in CSPP1 lead to classical Joubert syndrome. *Am J Hum Genet,* 94**,** 80-6.

ALAZAMI, A. M., ALSHAMMARI, M. J., SALIH, M. A., ALZAHRANI, F., HIJAZI, H., SEIDAHMED, M. Z., SAFIEH, L. A., ALDOSARY, M., KHAN, A. O. & ALKURAYA, F. S. J. H. M. 2012. Molecular characterization of Joubert syndrome in Saudi Arabia. *Human Mutation,* 33**,** 1423-1428.

ALEXIEV, B. A., LIN, X., SUN, C.-C. & BRENNER, D. S. 2006. Meckel-Gruber syndrome: pathologic manifestations, minimal diagnostic criteria, and differential diagnosis. *Archives of pathology & laboratory medicine,* 130**,** 1236-1238.

ALIEVA, I., GORGIDZE, L., KOMAROVA, Y. A., CHERNOBELSKAYA, O. & VOROBJEV, I. J. M. C. B. 1999. Experimental model for studying the primary cilia in tissue culture cells. *Mebbr Cell Biol,* 12**,** 895-905.

ALKANDERI, S., MOLINARI, E., SHAHEEN, R., ELMAGHLOOB, Y., STEPHEN, L. A., SAMMUT, V., RAMSBOTTOM, S. A., SRIVASTAVA, S., CAIRNS, G. & EDWARDS, N. 2018. ARL3 Mutations Cause Joubert Syndrome by Disrupting Ciliary Protein Composition. *The American Journal of Human Genetics*.

ARTS, H. H., DOHERTY, D., VAN BEERSUM, S. E., PARISI, M. A., LETTEBOER, S. J., GORDEN, N. T., PETERS, T. A., MÄRKER, T., VOESENEK, K. & KARTONO, A. J. N. G. 2007. Mutations in the gene encoding the basal body protein RPGRIP1L, a nephrocystin-4 interactor, cause Joubert syndrome. *Nature genetics,* 39**,** 882.

ARTS, H. H. & KNOERS, N. V. 2013. Current insights into renal ciliopathies: what can genetics teach us? *Pediatric nephrology,* 28**,** 863-874.

ARTUSO, R., FALLERINI, C., DOSA, L., SCIONTI, F., CLEMENTI, M., GAROSI, G., MASSELLA, L., EPISTOLATO, M. C., MANCINI, R. & MARI, F. 2012. Advances in Alport syndrome diagnosis using next-generation sequencing. *European Journal of Human Genetics,* 20**,** 50.

BAALA, L., AUDOLLENT, S., MARTINOVIC, J., OZILOU, C., BABRON, M.-C., SIVANANDAMOORTHY, S., SAUNIER, S., SALOMON, R., GONZALES, M. & RATTENBERRY, E. J. T. A. J. O. H. G. 2007a. Pleiotropic effects of CEP290 (NPHP6) mutations extend to Meckel syndrome. *The American Journal of Human Genetics,* 81**,** 170-179.

BAALA, L., ROMANO, S., KHADDOUR, R., SAUNIER, S., SMITH, U. M., AUDOLLENT, S., OZILOU, C., FAIVRE, L., LAURENT, N. & FOLIGUET, B. 2007b. The Meckel-Gruber syndrome gene, MKS3, is mutated in Joubert syndrome. *The American Journal of Human Genetics,* 80**,** 186-194.

BACHMANN-GAGESCU, R., DEMPSEY, J., PHELPS, I., O'ROAK, B., KNUTZEN, D., RUE, T., ISHAK, G., ISABELLA, C., GORDEN, N. & ADKINS, J. 2015. Joubert syndrome: a model for untangling recessive disorders with extreme genetic heterogeneity. *Journal of medical genetics***,** 103087.

BACHMANN-GAGESCU, R., PHELPS, I. G., DEMPSEY, J. C., SHARMA, V. A., ISHAK, G. E., BOYLE, E. A., WILSON, M., MARQUES LOURENÇO, C. & ARSLAN, M. 2015. KIAA0586 is mutated in Joubert syndrome. *Human mutation,* 36**,** 831-835.

BADANO, J. L., MITSUMA, N., BEALES, P. L. & KATSANIS, N. 2006. The ciliopathies: an emerging class of human genetic disorders. *Annu. Rev. Genomics Hum. Genet.,* 7**,** 125-148.

BARKER, D. F., HOSTIKKA, S. L., ZHOU, J., CHOW, L. T., OLIPHANT, A. R., GERKEN, S. C., GREGORY, M. C., SKOLNICK, M. H., ATKIN, C. L. & TRYGGVASON, K. 1990. Identification of mutations in the COL4A5 collagen gene in Alport syndrome. *Science,* 248**,** 1224-1227.

BERGMANN, C. 2012. Educational paper. *European journal of pediatrics,* 171**,** 1285-1300.

BERGMANN, C., FLIEGAUF, M., BRÜCHLE, N. O., FRANK, V., OLBRICH, H., KIRSCHNER, J., SCHERMER, B., SCHMEDDING, I., KISPERT, A. & KRÄNZLIN, B. J. T. A. J. O. H. G. 2008. Loss of nephrocystin-3 function can cause embryonic lethality, Meckel-Gruber-like syndrome, situs inversus, and renal-hepatic-pancreatic dysplasia. *American Journal of Human Genetics,* 482**,** 959-970.

BIELAS, S. L., SILHAVY, J. L., BRANCATI, F., KISSELEVA, M. V., AL-GAZALI, L., SZTRIHA, L., BAYOUMI, R. A., ZAKI, M. S., ABDEL-ALEEM, A., ROSTI, R. O., KAYSERILI, H., SWISTUN, D., SCOTT, L. C., BERTINI, E., BOLTSHAUSER, E., FAZZI, E., TRAVAGLINI, L., FIELD, S. J., GAYRAL, S., JACOBY, M., SCHURMANS, S., DALLAPICCOLA, B., MAJERUS, P. W., VALENTE, E. M. & GLEESON, J. G. 2009. Mutations in INPP5E, encoding inositol polyphosphate-5-phosphatase E, link phosphatidyl inositol signaling to the ciliopathies. *Nat Genet,* 41**,** 1032-6.

BOLAR, N. A., GOLZIO, C., ŽIVNÁ, M., HAYOT, G., VAN HEMELRIJK, C., SCHEPERS, D., VANDEWEYER, G., HOISCHEN, A., HUYGHE, J. R. & RAES, A. 2016. Heterozygous loss-of-function SEC61A1 mutations cause autosomal-dominant tubulo-interstitial and glomerulocystic kidney disease with anemia. *The American Journal of Human Genetics,* 99**,** 174-187.

BOLTSHAUSER, E., FORSTER, I., DEONNA, T. & WILLI, U. 1995. Joubert syndrome: are kidneys involved? *Neuropaediatrics,* 26**,** 320-321.

BOLTSHAUSER, E. & ISLER, W. 1977. Joubert syndrome: episodic hyperpnea, abnormal eye movements, retardation and ataxia, associated with dysplasia of the cerebellar vermis. *Neuropaediatrie,* 8**,** 57-66.

BRANCATI, F., BARRANO, G., SILHAVY, J. L., MARSH, S. E., TRAVAGLINI, L., BIELAS, S. L., AMORINI, M., ZABLOCKA, D., KAYSERILI, H. & AL-GAZALI, L. 2007. CEP290 Mutations Are Frequently Identified in the Oculo-Renal Form of Joubert Syndrome–Related Disorders. *The American Journal of Human Genetics,* 81**,** 104-113.

BRANCATI, F., DALLAPICCOLA, B. & VALENTE, E. M. 2010. Joubert Syndrome and related disorders. *Orphanet Journal of Rare Diseases,* 5**,** 20.

BRANCATI, F., IANNICELLI, M., TRAVAGLINI, L., MAZZOTTA, A., BERTINI, E., BOLTSHAUSER, E., D'ARRIGO, S., EMMA, F., FAZZI, E. & GALLIZZI, R. 2009. MKS3/TMEM67 mutations are a major cause of COACH Syndrome, a Joubert Syndrome related disorder with liver involvement. *Human mutation,* 30**,** E432-E442.

BRANCATI, F., TRAVAGLINI, L., ZABLOCKA, D., BOLTSHAUSER, E., ACCORSI, P., MONTAGNA, G., SILHAVY, J. L., BARRANO, G., BERTINI, E. & EMMA, F. 2008. RPGRIP1L mutations are mainly associated with the cerebello-renal phenotype of Joubert syndrome-related disorders. *Clinical genetics,* 74**,** 164-170.

BULLICH, G., DOMINGO-GALLEGO, A., VARGAS, I., RUIZ, P., LORENTE-GRANDOSO, L., FURLANO, M., FRAGA, G., MADRID, Á., ARICETA, G. & BORREGÁN, M. 2018. A kidney-disease gene panel allows a comprehensive genetic diagnosis of cystic and glomerular inherited kidney diseases. *Kidney international*.

BURD, C. G., STROCHLIC, T. I. & SETTY, S. R. G. 2004. Arf-like GTPases: not so Arf-like after all. *Trends in cell biology,* 14**,** 687-694.

CANTAGREL, V., SILHAVY, J. L., BIELAS, S. L., SWISTUN, D., MARSH, S. E., BERTRAND, J. Y., AUDOLLENT, S., ATTIÉ-BITACH, T., HOLDEN, K. R. & DOBYNS, W. B. 2008. Mutations in the cilia gene ARL13B lead to the classical form of Joubert syndrome. *The American Journal of Human Genetics,* 83**,** 170-179.

CAVENAGH, M. M., BREINER, M., SCHURMANN, A., ROSENWALD, A. G., TERUI, T., ZHANG, C.-J., RANDAZZO, P. A., ADAMS, M., JOOST, H. G. & KAHN, R. A. 1994. ADP-ribosylation factor (ARF)-like 3, a new member of the ARF family of GTP-binding proteins cloned from human and rat tissues. *Journal of Biological Chemistry,* 269**,** 18937-18942.

CHAKI, M., AIRIK, R., GHOSH, A. K., GILES, R. H., CHEN, R., SLAATS, G. G., WANG, H., HURD, T. W., ZHOU, W., CLUCKEY, A., GEE, H. Y., RAMASWAMI, G., HONG, C. J., HAMILTON, B. A., CERVENKA, I., GANJI, R. S., BRYJA, V., ARTS, H. H., VAN REEUWIJK, J., OUD, M. M., LETTEBOER, S. J., ROEPMAN, R., HUSSON, H., IBRAGHIMOV-BESKROVNAYA, O., YASUNAGA, T., WALZ, G., ELEY, L., SAYER, J. A., SCHERMER, B., LIEBAU, M. C., BENZING, T., LE CORRE, S., DRUMMOND, I., JANSSEN, S., ALLEN, S. J., NATARAJAN, S., O'TOOLE, J. F., ATTANASIO, M., SAUNIER, S., ANTIGNAC, C., KOENEKOOP, R. K., REN, H., LOPEZ, I., NAYIR, A., STOETZEL, C., DOLLFUS, H., MASSOUDI, R., GLEESON, J. G., ANDREOLI, S. P., DOHERTY, D. G., LINDSTRAD, A., GOLZIO, C., KATSANIS, N., PAPE, L., ABBOUD, E. B., AL-RAJHI, A. A., LEWIS, R. A., OMRAN, H., LEE, E. Y., WANG, S., SEKIGUCHI, J. M., SAUNDERS, R., JOHNSON, C. A., GARNER, E., VANSELOW, K., ANDERSEN, J. S., SHLOMAI, J., NURNBERG, G., NURNBERG, P., LEVY, S., SMOGORZEWSKA, A., OTTO, E. A. & HILDEBRANDT, F. 2012. Exome capture reveals ZNF423 and CEP164

mutations, linking renal ciliopathies to DNA damage response signaling. *Cell,* 150**,** 533-48.

CHERFILS, J. & ZEGHOUF, M. 2013. Regulation of small gtpases by gefs, gaps, and gdis. *Physiological reviews,* 93**,** 269-309.

COENE, K. L., ROEPMAN, R., DOHERTY, D., AFROZE, B., KROES, H. Y., LETTEBOER, S. J., NGU, L. H., BUDNY, B., VAN WIJK, E. & GORDEN, N. T. 2009. OFD1 is mutated in X-linked Joubert syndrome and interacts with LCA5-encoded lebercilin. *The American Journal of Human Genetics,* 85**,** 465-481.

CORAPI, K. M., CHEN, J. L., BALK, E. M. & GORDON, C. E. 2012. Bleeding complications of native kidney biopsy: a systematic review and meta-analysis. *American Journal of Kidney Diseases,* 60**,** 62-73.

CUVILLIER, A., REDON, F., ANTOINE, J.-C., CHARDIN, P., DEVOS, T. & MERLIN, G. 2000. LdARL-3A, a Leishmania promastigote-specific ADP-ribosylation factor-like protein, is essential for flagellum integrity. *J Cell Sci,* 113**,** 2065-2074.

DAFINGER, C., LIEBAU, M. C., ELSAYED, S. M., HELLENBROICH, Y., BOLTSHAUSER, E., KORENKE, G. C., FABRETTI, F., JANECKE, A. R., EBERMANN, I. & NÜRNBERG, G. 2011. Mutations in KIF7 link Joubert syndrome with Sonic Hedgehog signaling and microtubule dynamics. *The Journal of clinical investigation,* 121**,** 2662-2667.

DAVIS, E. E., ZHANG, Q., LIU, Q., DIPLAS, B. H., DAVEY, L. M., HARTLEY, J., STOETZEL, C., SZYMANSKA, K., RAMASWAMI, G. & LOGAN, C. V. 2011. TTC21B contributes both causal and modifying alleles across the ciliopathy spectrum. *Nature genetics,* 43**,** 189.

DAWE, H. R., SMITH, U. M., CULLINANE, A. R., GERRELLI, D., COX, P., BADANO, J. L., BLAIR-REID, S., SRIRAM, N., KATSANIS, N. & ATTIE-BITACH, T. 2006. The Meckel–Gruber syndrome proteins MKS1 and meckelin interact and are required for primary cilium formation. *Human molecular genetics,* 16**,** 173-186.

DE LA ROCHE, M., ASANO, Y. & GRIFFITHS, G. M. 2016. Origins of the cytolytic synapse. *Nature Reviews Immunology,* 16**,** 421.

DE MORI, R., ROMANI, M., D'ARRIGO, S., ZAKI, M. S., LOREFICE, E., TARDIVO, S., BIAGINI, T., STANLEY, V., MUSAEV, D. & FLUSS, J. 2017. Hypomorphic Recessive Variants in SUFU Impair the Sonic Hedgehog Pathway and Cause Joubert Syndrome with Cranio-facial and Skeletal Defects. *The American Journal of Human Genetics,* 101**,** 552-563.

DEKABAN, A. S. 1969. Hereditary syndrome of congenital retinal blindness (Leber), polycystic kidneys and maldevelopment of the brain. *American journal of ophthalmology,* 68**,** 1029-1037.

DELOUS, M., BAALA, L., SALOMON, R., LACLEF, C., VIERKOTTEN, J., TORY, K., GOLZIO, C., LACOSTE, T., BESSE, L. & OZILOU, C. 2007. The ciliary gene RPGRIP1L is mutated in cerebello-oculo-renal syndrome (Joubert syndrome type B) and Meckel syndrome. *Nature genetics,* 39**,** 875.

DEN HOLLANDER, A. I., KOENEKOOP, R. K., YZER, S., LOPEZ, I., ARENDS, M. L., VOESENEK, K. E., ZONNEVELD, M. N., STROM, T. M., MEITINGER, T. & BRUNNER, H. G. 2006. Mutations in the CEP290 (NPHP6) gene are a frequent cause of Leber congenital amaurosis. *The American Journal of Human Genetics,* 79**,** 556-561.

DERETIC, D. 2006. A role for rhodopsin in a signal transduction cascade that regulates membrane trafficking and photoreceptor polarity. *Vision research,* 46**,** 4427-4433.

DEVUYST, O., KNOERS, N. V., REMUZZI, G. & SCHAEFER, F. 2014. Rare inherited kidney diseases: challenges, opportunities, and perspectives. *The Lancet,* 383**,** 1844-1859.

DIXON-SALAZAR, T., SILHAVY, J. L., MARSH, S. E., LOUIE, C. M., SCOTT, L. C., GURURAJ, A., AL-GAZALI, L., AL-TAWARI, A. A., KAYSERILI, H., SZTRIHA, L. & GLEESON, J. G. 2004. Mutations in the AHI1 gene, encoding jouberin, cause Joubert syndrome with cortical polymicrogyria. *Am J Hum Genet,* 75**,** 979-87.

DOHERTY, D. Joubert syndrome: insights into brain development, cilium biology, and complex disease. Seminars in pediatric neurology, 2009. Elsevier, 143-154.

DOHERTY, D., PARISI, M. A., FINN, L. S., GUNAY-AYGUN, M., AL-MATEEN, M., BATES, D., CLERICUZIO, C., DEMIR, H., DORSCHNER, M. & VAN ESSEN, A. J. 2010. Mutations in 3 genes (MKS3, CC2D2A and RPGRIP1L) cause COACH syndrome (Joubert syndrome with congenital hepatic fibrosis). *Journal of medical genetics,* 47**,** 8-21.

DONALDSON, J. G. & JACKSON, C. L. 2011. ARF family G proteins and their regulators: roles in membrane transport, development and disease. *Nature reviews Molecular cell biology,* 12**,** 362.

DOWDLE, W. E., ROBINSON, J. F., KNEIST, A., SIREROL-PIQUER, M. S., FRINTS, S. G., CORBIT, K. C., ZAGHLOUL, N. A., VAN LIJNSCHOTEN, G., MULDERS, L.

& VERVER, D. E. 2011. Disruption of a ciliary B9 protein complex causes Meckel syndrome. *The American Journal of Human Genetics,* 89**,** 94-110.

ECKARDT, K.-U., CORESH, J., DEVUYST, O., JOHNSON, R. J., KÖTTGEN, A., LEVEY, A. S. & LEVIN, A. 2013. Evolving importance of kidney disease: from subspecialty to global health burden. *The Lancet,* 382**,** 158-169.

EDVARDSON, S., SHAAG, A., ZENVIRT, S., ERLICH, Y., HANNON, G. J., SHANSKE, A. L., GOMORI, J. M., EKSTEIN, J. & ELPELEG, O. 2010. Joubert syndrome 2 (JBTS2) in Ashkenazi Jews is associated with a TMEM216 mutation. *The American Journal of Human Genetics,* 86**,** 93-97.

FAN, Y., ESMAIL, M. A., ANSLEY, S. J., BLACQUE, O. E., BOROEVICH, K., ROSS, A. J., MOORE, S. J., BADANO, J. L., MAY-SIMERA, H. & COMPTON, D. S. 2004. Mutations in a member of the Ras superfamily of small GTP-binding proteins causes Bardet-Biedl syndrome. *Nature genetics,* 36**,** 989.

FANSA, E. K., KOSLING, S. K., ZENT, E., WITTINGHOFER, A. & ISMAIL, S. 2016. PDE6delta-mediated sorting of INPP5E into the cilium is determined by cargo-carrier affinity. *Nat Commun,* 7**,** 11366.

FIELD, M., SCHEFFER, I. E., GILL, D., WILSON, M., CHRISTIE, L., SHAW, M., GARDNER, A., GLUBB, G., HOBSON, L. & CORBETT, M. 2012. Expanding the molecular basis and phenotypic spectrum of X-linked Joubert syndrome associated with OFD1 mutations. *European Journal of Human Genetics,* 20**,** 806.

FLEMING, L. R., DOHERTY, D. A., PARISI, M. A., GLASS, I. A., BRYANT, J., FISCHER, R., TURKBEY, B., CHOYKE, P., DARYANANI, K. & VEMULAPALLI, M. 2017. Prospective evaluation of kidney disease in Joubert syndrome. *Clinical Journal of the American Society of Nephrology***,** CJN. 05660517.

GARCIA-GONZALO, F. R., CORBIT, K. C., SIREROL-PIQUER, M. S., RAMASWAMI, G., OTTO, E. A., NORIEGA, T. R., SEOL, A. D., ROBINSON, J. F., BENNETT, C. L. & JOSIFOVA, D. J. 2011. A transition zone complex regulates mammalian ciliogenesis and ciliary membrane composition. *Nature genetics,* 43**,** 776.

GARCIA-GONZALO, F. R. & REITER, J. F. 2017. Open sesame: how transition fibers and the transition zone control ciliary composition. *Cold Spring Harbor perspectives in biology,* 9**,** a028134.

GAST, C., PENGELLY, R. J., LYON, M., BUNYAN, D. J., SEABY, E. G., GRAHAM, N., VENKAT-RAMAN, G. & ENNIS, S. 2016. Collagen (COL4A) mutations are

the most frequent mutations underlying adult focal segmental glomerulosclerosis. *Nephrology Dialysis Transplantation,* 31**,** 961-970.

GILLINGHAM, A. K. & MUNRO, S. 2007. The small G proteins of the Arf family and their regulators. *Annu. Rev. Cell Dev. Biol.,* 23**,** 579-611.

GLEESON, J. G., KEELER, L. C., PARISI, M. A., MARSH, S. E., CHANCE, P. F., GLASS, I. A., GRAHAM JR, J. M., MARIA, B. L., BARKOVICH, A. J. & DOBYNS, W. B. 2004. Molar tooth sign of the midbrain–hindbrain junction: occurrence in multiple distinct syndromes. *American journal of medical genetics Part A,* 125**,** 125-134.

GOETZ, S. C. & ANDERSON, K. V. 2010. The primary cilium: a signalling centre during vertebrate development. *Nature reviews genetics,* 11**,** 331.

GORDEN, N. T., ARTS, H. H., PARISI, M. A., COENE, K. L., LETTEBOER, S. J., VAN BEERSUM, S. E., MANS, D. A., HIKIDA, A., ECKERT, M. & KNUTZEN, D. 2008. CC2D2A is mutated in Joubert syndrome and interacts with the ciliopathy-associated basal body protein CEP290. *The American Journal of Human Genetics,* 83**,** 559-571.

GOTTHARDT, K., LOKAJ, M., KOERNER, C., FALK, N., GIESS, A. & WITTINGHOFER, A. 2015. A G-protein activation cascade from Arl13B to Arl3 and implications for ciliary targeting of lipidated proteins. *Elife,* 4**,** e11859.

GRAYSON, C., BARTOLINI, F., CHAPPLE, J. P., WILLISON, K. R., BHAMIDIPATI, A., LEWIS, S. A., LUTHERT, P. J., HARDCASTLE, A. J., COWAN, N. J. & CHEETHAM, M. E. 2002. Localization in the human retina of the X-linked retinitis pigmentosa protein RP2, its homologue cofactor C and the RP2 interacting protein Arl3. *Human molecular genetics,* 11**,** 3065-3074.

HARRIS, P. C. 2009. 2008 Homer W. Smith Award: insights into the pathogenesis of polycystic kidney disease from gene discovery. *Journal of the American Society of Nephrology,* 20**,** 1188-1198.

HAYCRAFT, C. J., BANIZS, B., AYDIN-SON, Y., ZHANG, Q., MICHAUD, E. J. & YODER, B. K. 2005. Gli2 and Gli3 localize to cilia and require the intraflagellar transport protein polaris for processing and function. *PLoS Genet,* 1**,** e53.

HILDEBRANDT, F. 2010. Genetic kidney diseases. *The Lancet,* 375**,** 1287-1295.

HILDEBRANDT, F., ATTANASIO, M. & OTTO, E. 2009. Nephronophthisis: disease mechanisms of a ciliopathy. *Journal of the American Society of Nephrology,* 20**,** 23-35.

HILDEBRANDT, F., BENZING, T. & KATSANIS, N. 2011a. Ciliopathies. *N Engl J Med,* 364**,** 1533-43.

HILDEBRANDT, F., BENZING, T. & KATSANIS, N. 2011b. Ciliopathies. *New England Journal of Medicine,* 364**,** 1533-1543.

HO, P. T. & TUCKER, R. W. 1989. Centriole ciliation and cell cycle variability during G1 phase of BALB/c 3T3 cells. *Journal of cellular physiology,* 139**,** 398-406.

HSIAO, Y.-C., TONG, Z. J., WESTFALL, J. E., AULT, J. G., PAGE-MCCAW, P. S. & FERLAND, R. J. 2009. Ahi1, whose human ortholog is mutated in Joubert syndrome, is required for Rab8a localization, ciliogenesis and vesicle trafficking. *Human Molecular Genetics,* 18**,** 3926-3941.

HU, Q., MILENKOVIC, L., JIN, H., SCOTT, M. P., NACHURY, M. V., SPILIOTIS, E. T. & NELSON, W. J. 2010. A septin diffusion barrier at the base of the primary cilium maintains ciliary membrane protein distribution. *Science,* 329**,** 436-439.

HUANG, L., SZYMANSKA, K., JENSEN, V. L., JANECKE, A. R., INNES, A. M., DAVIS, E. E., FROSK, P., LI, C., WILLER, J. R. & CHODIRKER, B. N. 2011. TMEM237 is mutated in individuals with a Joubert syndrome related disorder and expands the role of the TMEM family at the ciliary transition zone. *The American Journal of Human Genetics,* 89**,** 713-730.

HUGHES, J., WARD, C. J., PERAL, B., ASPINWALL, R., CLARK, K., SAN MILLÁN, J. L., GAMBLE, V. & HARRIS, P. C. 1995. The polycystic kidney disease 1 (PKD1) gene encodes a novel protein with multiple cell recognition domains. *Nature genetics,* 10**,** 151.

HUMBERT, M. C., WEIHBRECHT, K., SEARBY, C. C., LI, Y., POPE, R. M., SHEFFIELD, V. C. & SEO, S. 2012. ARL13B, PDE6D, and CEP164 form a functional network for INPP5E ciliary targeting. *Proceedings of the National Academy of Sciences of the United States of America,* 109**,** 19691-6.

HUPPKE, P., WEGENER, E., BÖHRER-RABEL, H., BOLZ, H. J., ZOLL, B., GÄRTNER, J. & BERGMANN, C. 2015. Tectonic gene mutations in patients with Joubert syndrome. *European Journal of Human Genetics,* 23**,** 616.

ISHIKAWA, H. & MARSHALL, W. F. 2011. Ciliogenesis: building the cell's antenna. *Nature reviews Molecular cell biology,* 12**,** 222.

ISMAIL, S. A., CHEN, Y.-X., RUSINOVA, A., CHANDRA, A., BIERBAUM, M., GREMER, L., TRIOLA, G., WALDMANN, H., BASTIAENS, P. I. &

WITTINGHOFER, A. 2011. Arl2-GTP and Arl3-GTP regulate a GDI-like transport system for farnesylated cargo. *Nature chemical biology,* 7**,** 942-949.

ISMAIL, S. A., CHEN, Y. X., MIERTZSCHKE, M., VETTER, I. R., KOERNER, C. & WITTINGHOFER, A. 2012. Structural basis for Arl3-specific release of myristoylated ciliary cargo from UNC119. *EMBO J,* 31**,** 4085-94.

JACOB, H. J., ABRAMS, K., BICK, D. P., BRODIE, K., DIMMOCK, D. P., FARRELL, M., GEURTS, J., HARRIS, J., HELBLING, D. & JOERS, B. J. 2013. Genomics in clinical practice: lessons from the front lines. *Science translational medicine,* 5**,** 194cm5-194cm5.

JAISWAL, M., FANSA, E. K., KOSLING, S. K., MEJUCH, T., WALDMANN, H. & WITTINGHOFER, A. 2016. Novel Biochemical and Structural Insights into the Interaction of Myristoylated Cargo with Unc119 Protein and Their Release by Arl2/3. *J Biol Chem,* 291**,** 20766-78.

JOLY, D., BÉROUD, C. & GRÜNFELD, J.-P. 2015. Rare inherited disorders with renal involvement—approach to the patient. *Kidney international,* 87**,** 901-908.

JOUBERT, M., EISENRING, J., ROBB, J. P. & ANDERMANN, F. 1969. Familial agenesis of the cerebellar vermis. *Neurology,* 19**,** 813-825.

JULIE GILG, R. P., DAMIAN FOGARTY 2015. UK Renal Registry 17th Annual Report: Chapter 1UK Renal Replacement Therapy Incidence in 2013: National and Centre-specific Analyses. *Nephron*

KAHN, R. A., VOLPICELLI-DALEY, L., BOWZARD, B., SHRIVASTAVA-RANJAN, P., LI, Y., ZHOU, C. & CUNNINGHAM, L. 2005. Arf family GTPases: roles in membrane traffic and microtubule dynamics. *Biochemical Society Transactions***,** 1269-1272.

KARGER, S. & PARIS, B. F. 2013. UK Renal Registry 2013. *Nephron,* 125**,** 1-364.

KEE, H. L., DISHINGER, J. F., BLASIUS, T. L., LIU, C.-J., MARGOLIS, B. & VERHEY, K. J. 2012. A size-exclusion permeability barrier and nucleoporins characterize a ciliary pore complex that regulates transport into cilia. *Nature cell biology,* 14**,** 431.

KEELER, L. C., MARSH, S. E., LEEFLANG, E. P., WOODS, C. G., SZTRIHA, L., AL-GAZALI, L., GURURAJ, A. & GLEESON, J. G. 2003. Linkage analysis in families with Joubert syndrome plus oculo-renal involvement identifies the CORS2 locus on chromosome 11p12-q13. 3. *The American Journal of Human Genetics,* 73**,** 656-662.

KILMARTIN, J., WRIGHT, B. & MILSTEIN, C. 1982. Rat monoclonal antitubulin antibodies derived by using a new nonsecreting rat cell line. *The Journal of Cell Biology,* 93**,** 576-582.

KROES, H. Y., MONROE, G. R., VAN DER ZWAAG, B., DURAN, K. J., DE KOVEL, C. G., VAN ROOSMALEN, M. J., HARAKALOVA, M., NIJMAN, I. J., KLOOSTERMAN, W. P. & GILES, R. H. 2016. Joubert syndrome: genotyping a Northern European patient cohort. *European Journal of Human Genetics,* 24**,** 214.

KYTTÄLÄ, M., TALLILA, J., SALONEN, R., KOPRA, O., KOHLSCHMIDT, N., PAAVOLA-SAKKI, P., PELTONEN, L. & KESTILÄ, M. 2006. MKS1, encoding a component of the flagellar apparatus basal body proteome, is mutated in Meckel syndrome. *Nature genetics,* 38**,** 155.

LAMBACHER, N. J., BRUEL, A.-L., VAN DAM, T. J., SZYMAŃSKA, K., SLAATS, G. G., KUHNS, S., MCMANUS, G. J., KENNEDY, J. E., GAFF, K. & WU, K. M. 2016. TMEM107 recruits ciliopathy proteins to subdomains of the ciliary transition zone and causes Joubert syndrome. *Nature cell biology,* 18**,** 122.

LAMBERT, S. R., KRISS, A., GRESTY, M., BENTON, S. & TAYLOR, D. 1989. Joubert syndrome. *Archives of Ophthalmology,* 107**,** 709-713.

LARKINS, C. E., AVILES, G. D. G., EAST, M. P., KAHN, R. A. & CASPARY, T. 2011. Arl13b regulates ciliogenesis and the dynamic localization of Shh signaling proteins. *Molecular biology of the cell,* 22**,** 4694-4703.

LEE, J. E., SILHAVY, J. L., ZAKI, M. S., SCHROTH, J., BIELAS, S. L., MARSH, S. E., OLVERA, J., BRANCATI, F., IANNICELLI, M. & IKEGAMI, K. 2012a. CEP41 is mutated in Joubert syndrome and is required for tubulin glutamylation at the cilium. *Nature genetics,* 44**,** 193.

LEE, J. H., SILHAVY, J. L., LEE, J. E., AL-GAZALI, L., THOMAS, S., DAVIS, E. E., BIELAS, S. L., HILL, K. J., IANNICELLI, M. & BRANCATI, F. 2012b. Evolutionarily assembled cis-regulatory module at a human ciliopathy locus. *Science***,** 1213506.

LEITCH, C. C., ZAGHLOUL, N. A., DAVIS, E. E., STOETZEL, C., DIAZ-FONT, A., RIX, S., ALFADHEL, M., LEWIS, R. A., EYAID, W. & BANIN, E. 2008. Hypomorphic mutations in syndromic encephalocele genes are associated with Bardet-Biedl syndrome. *Nature genetics,* 40**,** 443.

LI, Y., WEI, Q., ZHANG, Y., LING, K. & HU, J. 2010. The small GTPases ARL-13 and ARL-3 coordinate intraflagellar transport and ciliogenesis. *The Journal of cell biology***,** jcb. 200912001.

MACARTHUR, D. G., MANOLIO, T. A., DIMMOCK, D. P., REHM, H. L., SHENDURE, J., ABECASIS, G. R., ADAMS, D. R., ALTMAN, R. B., ANTONARAKIS, S. E. & ASHLEY, E. A. 2014. Guidelines for investigating causality of sequence variants in human disease. *Nature,* 508**,** 469.

MADHIVANAN, K. & AGUILAR, R. C. 2014. Ciliopathies: the trafficking connection. *Traffic,* 15**,** 1031-1056.

MALAKI, M., NEMATI, M. & SHOARAN, M. 2012. Joubert syndrome presenting as unilateral dysplastic kidney, hypotonia, and respiratory problem. *Saudi Journal of Kidney Diseases and Transplantation,* 23**,** 325.

MALICKI, J. & AVIDOR-REISS, T. 2014. From the cytoplasm into the cilium: bon voyage. *Organogenesis,* 10**,** 138-157.

MALLETT, A., FOWLES, L. F., MCGAUGHRAN, J., HEALY, H. & PATEL, C. 2016. A multidisciplinary renal genetics clinic improves patient diagnosis. *The Medical journal of Australia,* 204**,** 58-59.

MANOLIO, T. A., CHISHOLM, R. L., OZENBERGER, B., RODEN, D. M., WILLIAMS, M. S., WILSON, R., BICK, D., BOTTINGER, E. P., BRILLIANT, M. H. & ENG, C. 2013. Implementing genomic medicine in the clinic: the future is here. *Genetics in Medicine,* 15**,** 258.

MARIA, B. L., HOANG, K. B., TUSA, R. J., MANCUSO, A. A., HAMED, L. M., QUISLING, R. G., HOVE, M. T., FENNELL, E. B., BOOTH-JONES, M. & RINGDAHL, D. M. 1997. " Joubert syndrome" revisited: key ocular motor signs with magnetic resonance imaging correlation. *Journal of child neurology,* 12**,** 423-430.

MCCLOSKEY, S., YATES, L. & SAYER, J. 2016. The importance of taking a family history in the nephrology clinic. *Br J Renal Med,* 21**,** 38-42.

MERRILL, A. E., MERRIMAN, B., FARRINGTON-ROCK, C., CAMACHO, N., SEBALD, E. T., FUNARI, V. A., SCHIBLER, M. J., FIRESTEIN, M. H., COHN, Z. A. & PRIORE, M. A. 2009. Ciliary abnormalities due to defects in the retrograde transport protein DYNC2H1 in short-rib polydactyly syndrome. *The American Journal of Human Genetics,* 84**,** 542-549.

MOCHIZUKI, T., WU, G., HAYASHI, T., XENOPHONTOS, S. L., VELDHUISEN, B., SARIS, J. J., REYNOLDS, D. M., CAI, Y., GABOW, P. A. & PIERIDES, A. 1996. PKD2, a gene for polycystic kidney disease that encodes an integral membrane protein. *Science,* 272**,** 1339-1342.

NACHURY, M. V., SEELEY, E. S. & JIN, H. 2010. Trafficking to the ciliary membrane: how to get across the periciliary diffusion barrier? *Annual review of cell and developmental biology,* 26**,** 59-87.

NOOR, A., WINDPASSINGER, C., PATEL, M., STACHOWIAK, B., MIKHAILOV, A., AZAM, M., IRFAN, M., SIDDIQUI, Z. K., NAEEM, F. & PATERSON, A. D. 2008. CC2D2A, encoding a coiled-coil and C2 domain protein, causes autosomal-recessive mental retardation with retinitis pigmentosa. *The American Journal of Human Genetics,* 82**,** 1011-1018.

NOVARINO, G., AKIZU, N. & GLEESON, J. G. 2011. Modeling human disease in humans: the ciliopathies. *Cell,* 147**,** 70-79.

OMRAN, H., FERNANDEZ, C., JUNG, M., HÄFFNER, K., FARGIER, B., VILLAQUIRAN, A., WALDHERR, R., GRETZ, N., BRANDIS, M. & RÜSCHENDORF, F. 2000. Identification of a new gene locus for adolescent nephronophthisis, on chromosome 3q22 in a large Venezuelan pedigree. *The American Journal of Human Genetics,* 66**,** 118-127.

OTTO, E. A., HURD, T. W., AIRIK, R., CHAKI, M., ZHOU, W., STOETZEL, C., PATIL, S. B., LEVY, S., GHOSH, A. K. & MURGA-ZAMALLOA, C. A. 2010. Candidate exome capture identifies mutation of SDCCAG8 as the cause of a retinal-renal ciliopathy. *Nature genetics,* 42**,** 840.

OTTO, E. A., RAMASWAMI, G., JANSSEN, S., CHAKI, M., ALLEN, S. J., ZHOU, W., AIRIK, R., HURD, T. W., GHOSH, A. K. & WOLF, M. T. 2011. Mutation analysis of 18 nephronophthisis associated ciliopathy disease genes using a DNA pooling and next generation sequencing strategy. *Journal of medical genetics,* 48**,** 105-116.

OTTO, E. A., TORY, K., ATTANASIO, M., ZHOU, W., CHAKI, M., PARUCHURI, Y., WISE, E. L., WOLF, M. T., UTSCH, B. & BECKER, C. 2009. Hypomorphic mutations in meckelin (MKS3/TMEM67) cause nephronophthisis with liver fibrosis (NPHP11). *Journal of medical genetics,* 46**,** 663-670.

PARISI, M. A., BENNETT, C. L., ECKERT, M. L., DOBYNS, W. B., GLEESON, J. G., SHAW, D. W., MCDONALD, R., EDDY, A., CHANCE, P. F. & GLASS, I. A. 2004. The NPHP1 gene deletion associated with juvenile nephronophthisis is present in a subset of individuals with Joubert syndrome. *The American Journal of Human Genetics,* 75**,** 82-91.

PARISI, M. A., DOHERTY, D., CHANCE, P. F. & GLASS, I. A. J. E. J. O. H. G. 2007. Joubert syndrome (and related disorders)(OMIM 213300). 15**,** 511.

PAZOUR, G. J., DICKERT, B. L., VUCICA, Y., SEELEY, E. S., ROSENBAUM, J. L., WITMAN, G. B. & COLE, D. G. 2000. Chlamydomonas IFT88 and its mouse homologue, polycystic kidney disease gene tg737, are required for assembly of cilia and flagella. *The Journal of cell biology,* 151**,** 709-718.

PELLEGRINO, J. E., LENSCH, M. W., MUENKE, M. & CHANCE, P. F. 1997. Clinical and molecular analysis in Joubert syndrome. *American journal of medical genetics* 72**,** 59-62.

PORATH, B., GAINULLIN, V. G., CORNEC-LE GALL, E., DILLINGER, E. K., HEYER, C. M., HOPP, K., EDWARDS, M. E., MADSEN, C. D., MAURITZ, S. R. & BANKS, C. J. 2016. Mutations in GANAB, encoding the glucosidase IIα subunit, cause autosomal-dominant polycystic kidney and liver disease. *The American Journal of Human Genetics,* 98**,** 1193-1207.

PORETTI, A., BOLTSHAUSER, E. & VALENTE, E. M. 2014a. The molar tooth sign is pathognomonic for Joubert syndrome! *Pediatric neurology,* 50**,** e15-e16.

PORETTI, A., BOLTSHAUSER, E. & VALENTE, E. M. 2014b. The molar tooth sign is pathognomonic for Joubert syndrome! *Pediatric neurology,* 50**,** e15.

PORETTI, A., BREHMER, U., SCHEER, I., BERNET, V. & BOLTSHAUSER, E. 2008. Prenatal and neonatal MR imaging findings in oral-facial-digital syndrome type VI. *American Journal of Neuroradiology,* 29**,** 1090-1091.

PUTOUX, A., THOMAS, S., COENE, K. L., DAVIS, E. E., ALANAY, Y., OGUR, G., UZ, E., BUZAS, D., GOMES, C. & PATRIER, S. 2011. KIF7 mutations cause fetal hydrolethalus and acrocallosal syndromes. *Nature genetics,* 43**,** 601.

REEDERS, S., BREUNING, M., DAVIES, K., NICHOLLS, R., JARMAN, A., HIGGS, D., PEARSON, P. & WEATHERALL, D. 1985. A highly polymorphic DNA marker linked to adult polycystic kidney disease on chromosome 16. *Nature,* 317**,** 542.

REITER, J. F. & SKARNES, W. 2006. Tectonic, a novel regulator of the Hedgehog pathway required for both activation and inhibition. *Genes development,* 20**,** 22-27.

RIEDER, C. L., RUPP, G. & BOWSER, S. S. 1985. Electron microscopy of semithick sections: Advantages for biomedical research. *Journal of electron microscopy technique,* 2**,** 11-28.

ROMANI, M., MICALIZZI, A., KRAOUA, I., DOTTI, M. T., CAVALLIN, M., SZTRIHA, L., RUTA, R., MANCINI, F., MAZZA, T., CASTELLANA, S., HANENE, B., CARLUCCIO, M. A., DARRA, F., MATE, A., ZIMMERMANN, A., GOUIDER-KHOUJA, N. & VALENTE, E. M. 2014. Mutations in B9D1 and MKS1 cause

mild Joubert syndrome: expanding the genetic overlap with the lethal ciliopathy Meckel syndrome. *Orphanet J Rare Dis,* 9**,** 72.

ROMANI, M., MICALIZZI, A. & VALENTE, E. M. 2013. Joubert syndrome: congenital cerebellar ataxia with the molar tooth. *The Lancet Neurology,* 12**,** 894-905.

ROOSING, S., HOFREE, M., KIM, S., SCOTT, E., COPELAND, B., ROMANI, M., SILHAVY, J. L., ROSTI, R. O., SCHROTH, J. & MAZZA, T. 2015. Functional genome-wide siRNA screen identifies KIAA0586 as mutated in Joubert syndrome. *Elife,* 4**,** e06602.

ROOSING, S., ROMANI, M., ISRIE, M., ROSTI, R. O., MICALIZZI, A., MUSAEV, D., MAZZA, T., AL-GAZALI, L., ALTUNOGLU, U., BOLTSHAUSER, E., D'ARRIGO, S., DE KEERSMAECKER, B., KAYSERILI, H., BRANDENBERGER, S., KRAOUA, I., MARK, P. R., MCKANNA, T., VAN KEIRSBILCK, J., MOERMAN, P., PORETTI, A., PURI, R., VAN ESCH, H., GLEESON, J. G. & VALENTE, E. M. 2016a. Mutations in CEP120 cause Joubert syndrome as well as complex ciliopathy phenotypes. *J Med Genet,* 53**,** 608-15.

ROOSING, S., ROSTI, R. O., ROSTI, B., DE VRIEZE, E., SILHAVY, J. L., VAN WIJK, E., WAKELING, E. & GLEESON, J. G. 2016b. Identification of a homozygous nonsense mutation in KIAA0556 in a consanguineous family displaying Joubert syndrome. *Human genetics,* 135**,** 919-921.

ROSSETTI, S. & HARRIS, P. C. 2007. Genotype–phenotype correlations in autosomal dominant and autosomal recessive polycystic kidney disease. *Journal of the American Society of Nephrology,* 18**,** 1374-1380.

SALOMON, R., SAUNIER, S. & NIAUDET, P. 2009. Nephronophthisis. *Pediatric nephrology,* 24**,** 2333-2344.

SANDERS, A. A., DE VRIEZE, E., ALAZAMI, A. M., ALZAHRANI, F., MALARKEY, E. B., SORUSCH, N., TEBBE, L., KUHNS, S., VAN DAM, T. J. & ALHASHEM, A. 2015. KIAA0556 is a novel ciliary basal body component mutated in Joubert syndrome. *Genome biology,* 16**,** 293.

SANG, L., MILLER, J. J., CORBIT, K. C., GILES, R. H., BRAUER, M. J., OTTO, E. A., BAYE, L. M., WEN, X., SCALES, S. J., KWONG, M., HUNTZICKER, E. G., SFAKIANOS, M. K., SANDOVAL, W., BAZAN, J. F., KULKARNI, P., GARCIA-GONZALO, F. R., SEOL, A. D., O'TOOLE, J. F., HELD, S., REUTTER, H. M., LANE, W. S., RAFIQ, M. A., NOOR, A., ANSAR, M., DEVI, A. R., SHEFFIELD, V. C., SLUSARSKI, D. C., VINCENT, J. B., DOHERTY, D. A., HILDEBRANDT, F., REITER, J. F. & JACKSON, P. K. 2011. Mapping the NPHP-JBTS-MKS

protein network reveals ciliopathy disease genes and pathways. *Cell,* 145**,** 513-28.

SARAIVA, J. M. & BARAITSER, M. J. A. J. O. M. G. 1992. Joubert syndrome: a review. 43**,** 726-731.

SATIR, P., PEDERSEN, L. B. & CHRISTENSEN, S. T. 2010. The primary cilium at a glance. *J Cell Sci,* 123**,** 499-503.

SATRAN, D., PIERPONT, M. E. M. & DOBYNS, W. B. 1999. Cerebello–oculo–renal syndromes including Arima, Senior-Löken and COACH syndromes: More than just variants of Joubert syndrome. *American journal of medical genetics,* 86**,** 459-469.

SAYER, J. A., OTTO, E. A., O'TOOLE, J. F., NURNBERG, G., KENNEDY, M. A., BECKER, C., HENNIES, H. C., HELOU, J., ATTANASIO, M. & FAUSETT, B. V. 2006. The centrosomal protein nephrocystin-6 is mutated in Joubert syndrome and activates transcription factor ATF4. *Nature genetics,* 38**,** 674.

SCHIEPPATI, A., HENTER, J.-I., DAINA, E. & APERIA, A. 2008. Why rare diseases are an important medical and social issue. *The Lancet,* 371**,** 2039-2041.

SCHRICK, J. J., VOGEL, P., ABUIN, A., HAMPTON, B. & RICE, D. S. 2006. ADP-ribosylation factor-like 3 is involved in kidney and photoreceptor development. *The American journal of pathology,* 168**,** 1288-1298.

SHAHEEN, R., ALMOISHEER, A., FAQEIH, E., BABAY, Z., MONIES, D., TASSAN, N., ABOUELHODA, M., KURDI, W., AL MARDAWI, E. & KHALIL, M. M. 2015. Identification of a novel MKS locus defined by TMEM107 mutation. *Human molecular genetics,* 24**,** 5211-5218.

SHAHEEN, R., SHAMSELDIN, H. E., LOUCKS, C. M., SEIDAHMED, M. Z., ANSARI, S., KHALIL, M. I., AL-YACOUB, N., DAVIS, E. E., MOLA, N. A. & SZYMANSKA, K. 2014. Mutations in CSPP1, encoding a core centrosomal protein, cause a range of ciliopathy phenotypes in humans. *The American Journal of Human Genetics,* 94**,** 73-79.

SHASHI, V., MCCONKIE-ROSELL, A., ROSELL, B., SCHOCH, K., VELLORE, K., MCDONALD, M., JIANG, Y.-H., XIE, P., NEED, A. & GOLDSTEIN, D. B. 2014. The utility of the traditional medical genetics diagnostic evaluation in the context of next-generation sequencing for undiagnosed genetic disorders. *Genetics in Medicine,* 16**,** 176.

SIMMS, R. J., ELEY, L. & SAYER, J. A. 2009. Nephronophthisis. *European Journal of Human Genetics,* 17**,** 406.

SIMPSON, M. A., CROSS, H. E., CROSS, L., HELMUTH, M. & CROSBY, A. H. 2009. Lethal cystic kidney disease in Amish neonates associated with homozygous nonsense mutation of NPHP3. *American Journal of Kidney Diseases,* 53**,** 790-795.

SMITH, J., CHRISTIE, K. & FRAME, J. 1969. Desmosomes, cilia and acanthosomes associated with keratocytes. *Journal of Anatomy,* 105**,** 383.

SMITH, J. M., STABLEIN, D. M., MUNOZ, R., HEBERT, D. & MCDONALD, R. A. 2007. Contributions of the transplant registry: the 2006 annual report of the North American Pediatric Renal Trials and Collaborative Studies (NAPRTCS). *Pediatric transplantation,* 11**,** 366-373.

SMITH, U. M., CONSUGAR, M., TEE, L. J., MCKEE, B. M., MAINA, E. N., WHELAN, S., MORGAN, N. V., GORANSON, E., GISSEN, P. & LILLIQUIST, S. 2006. The transmembrane protein meckelin (MKS3) is mutated in Meckel-Gruber syndrome and the wpk rat. *Nature genetics,* 38**,** 191.

SOLIMAN, N. A. 2012. Orphan kidney diseases. *Nephron Clinical Practice,* 120**,** c194-c199.

SRIVASTAVA, S., MOLINARI, E., RAMAN, S. & SAYER, J. A. 2018. Many Genes—One Disease? Genetics of Nephronophthisis (NPHP) and NPHP-Associated Disorders. *Frontiers in pediatrics,* 5**,** 287.

SRIVASTAVA, S., RAMSBOTTOM, S. A., MOLINARI, E., ALKANDERI, S., FILBY, A., WHITE, K., HENRY, C., SAUNIER, S., MILES, C. G. & SAYER, J. A. 2017. A human patient-derived cellular model of Joubert syndrome reveals ciliary defects which can be rescued with targeted therapies. *Hum Mol Genet,* 26**,** 4657-4667.

SROUR, M., HAMDAN, F. F., MCKNIGHT, D., DAVIS, E., MANDEL, H., SCHWARTZENTRUBER, J., MARTIN, B., PATRY, L., NASSIF, C. & DIONNE-LAPORTE, A. 2015. Joubert syndrome in French Canadians and identification of mutations in CEP104. *The American Journal of Human Genetics,* 97**,** 744-753.

SROUR, M., HAMDAN, F. F., SCHWARTZENTRUBER, J. A., PATRY, L., OSPINA, L. H., SHEVELL, M. I., DÉSILETS, V., DOBRZENIECKA, S., MATHONNET, G. & LEMYRE, E. 2012a. Mutations in TMEM231 cause Joubert syndrome in French Canadians. *Journal of medical genetics***,** 101132.

SROUR, M., SCHWARTZENTRUBER, J., HAMDAN, F. F., OSPINA, L. H., PATRY, L., LABUDA, D., MASSICOTTE, C., DOBRZENIECKA, S., CAPO-CHICHI, J.-M. & PAPILLON-CAVANAGH, S. 2012b. Mutations in C5ORF42 cause Joubert

syndrome in the French Canadian population. *The American Journal of Human Genetics,* 90**,** 693-700.

STEPHEN, L. A., ELMAGHLOOB, Y., MCILWRAITH, M. J., YELLAND, T., SANCHEZ, P. C., RODA-NAVARRO, P. & ISMAIL, S. J. D. C. 2018. The Ciliary Machinery Is Repurposed for T Cell Immune Synapse Trafficking of LCK. 47**,** 122-132. e4.

STROM, S. P., CLARK, M. J., MARTINEZ, A., GARCIA, S., ABELAZEEM, A. A., MATYNIA, A., PARIKH, S., SULLIVAN, L. S., BOWNE, S. J. & DAIGER, S. P. 2016. De Novo Occurrence of a Variant in ARL3 and Apparent Autosomal Dominant Transmission of Retinitis Pigmentosa. *PloS one,* 11**,** e0150944.

TAMMANA, T. V. S., TAMMANA, D., DIENER, D. R. & ROSENBAUM, J. 2013. Centrosomal protein CEP104/Chlamydomonas FAP256 moves to the ciliary tip during cilia assembly. *J Cell Sci***,** 133439.

THIEL, C., KESSLER, K., GIESSL, A., DIMMLER, A., SHALEV, S. A., VON DER HAAR, S., ZENKER, M., ZAHNLEITER, D., STÖSS, H. & BEINDER, E. 2011. NEK1 mutations cause short-rib polydactyly syndrome type majewski. *The American Journal of Human Genetics,* 88**,** 106-114.

THOMAS, R., SANNA-CHERCHI, S., WARADY, B. A., FURTH, S. L., KASKEL, F. J. & GHARAVI, A. G. 2011. HNF1B and PAX2 mutations are a common cause of renal hypodysplasia in the CKiD cohort. *Pediatric Nephrology,* 26**,** 897-903.

THOMAS, S., CANTAGREL, V., MARIANI, L., SERRE, V., LEE, J.-E., ELKHARTOUFI, N., DE LONLAY, P., DESGUERRE, I., MUNNICH, A. & BODDAERT, N. 2015. Identification of a novel ARL13B variant in a Joubert syndrome-affected patient with retinal impairment and obesity. *European Journal of Human Genetics,* 23**,** 621.

THOMAS, S., LEGENDRE, M., SAUNIER, S., BESSIÈRES, B., ALBY, C., BONNIÈRE, M., TOUTAIN, A., LOEUILLET, L., SZYMANSKA, K. & JOSSIC, F. J. T. A. J. O. H. G. 2012. TCTN3 mutations cause Mohr-Majewski syndrome. 91**,** 372-378.

THOMAS, S., WRIGHT, K. J., LE CORRE, S., MICALIZZI, A., ROMANI, M., ABHYANKAR, A., SAADA, J., PERRAULT, I., AMIEL, J., LITZLER, J., FILHOL, E., ELKHARTOUFI, N., KWONG, M., CASANOVA, J. L., BODDAERT, N., BAEHR, W., LYONNET, S., MUNNICH, A., BURGLEN, L., CHASSAING, N., ENCHA-RAVAZI, F., VEKEMANS, M., GLEESON, J. G., VALENTE, E. M., JACKSON, P. K., DRUMMOND, I. A., SAUNIER, S. & ATTIE-BITACH, T. 2014. A homozygous PDE6D mutation in Joubert syndrome impairs targeting

of farnesylated INPP5E protein to the primary cilium. *Hum Mutat,* 35**,** 137-46.

TORY, K., ROUSSET-ROUVIERE, C., GUBLER, M.-C., MORINIERE, V., PAWTOWSKI, A., BECKER, C., GUYOT, C., GIÉ, S., FRISHBERG, Y. & NIVET, H. J. K. I. 2009. Mutations of NPHP2 and NPHP3 in infantile nephronophthisis. 75**,** 839-847.

TRAN, P. V., TALBOTT, G. C., TURBE-DOAN, A., JACOBS, D. T., SCHONFELD, M. P., SILVA, L. M., CHATTERJEE, A., PRYSAK, M., ALLARD, B. A. & BEIER, D. R. 2014. Downregulating hedgehog signaling reduces renal cystogenic potential of mouse models. *Journal of the American Society of Nephrology,* 25**,** 2201-2212.

TUZ, K., BACHMANN-GAGESCU, R., O'DAY, D. R., HUA, K., ISABELLA, C. R., PHELPS, I. G., STOLARSKI, A. E., O'ROAK, B. J., DEMPSEY, J. C. & LOURENCO, C. 2014. Mutations in CSPP1 cause primary cilia abnormalities and Joubert syndrome with or without Jeune asphyxiating thoracic dystrophy. *The American Journal of Human Genetics,* 94**,** 62-72.

UTSCH, B., SAYER, J. A., ATTANASIO, M., PEREIRA, R. R., ECCLES, M., HENNIES, H.-C., OTTO, E. A. & HILDEBRANDT, F. 2006. Identification of the first AHI1 gene mutations in nephronophthisis-associated Joubert syndrome. *Pediatric nephrology,* 21**,** 32-35.

VALENTE, E. M., BRANCATI, F., BOLTSHAUSER, E. & DALLAPICCOLA, B. 2013a. Clinical utility gene card for: Joubert Syndrome-update 2013. *European Journal of Human Genetics,* 21.

VALENTE, E. M., BRANCATI, F., BOLTSHAUSER, E. & DALLAPICCOLA, B. 2013b. Clinical utility gene card for: Joubert Syndrome-update 2013. *European journal of human genetics: EJHG,* 21.

VALENTE, E. M., BRANCATI, F., SILHAVY, J. L., CASTORI, M., MARSH, S. E., BARRANO, G., BERTINI, E., BOLTSHAUSER, E., ZAKI, M. S. & ABDEL-ALEEM, A. 2006a. AHI1 gene mutations cause specific forms of Joubert syndrome–related disorders. *Annals of neurology,* 59**,** 527-534.

VALENTE, E. M., LOGAN, C. V., MOUGOU-ZERELLI, S., LEE, J. H., SILHAVY, J. L., BRANCATI, F., IANNICELLI, M., TRAVAGLINI, L., ROMANI, S. & ILLI, B. 2010. Mutations in TMEM216 perturb ciliogenesis and cause Joubert, Meckel and related syndromes. *Nature genetics,* 42**,** 619.

VALENTE, E. M., SILHAVY, J. L., BRANCATI, F., BARRANO, G., KRISHNASWAMI, S. R., CASTORI, M., LANCASTER, M. A., BOLTSHAUSER, E., BOCCONE, L. & AL-GAZALI, L. 2006b. Mutations in CEP290, which encodes a centrosomal

protein, cause pleiotropic forms of Joubert syndrome. *Nature genetics,* 38**,** 623.

VAN DE WEGHE, J. C., RUSTERHOLZ, T. D. S., LATOUR, B., GROUT, M. E., ALDINGER, K. A., SHAHEEN, R., DEMPSEY, J. C., MADDIREVULA, S., CHENG, Y. H., PHELPS, I. G., GESEMANN, M., GOEL, H., BIRK, O. S., ALANZI, T., RAWASHDEH, R., KHAN, A. O., BAMSHAD, M. J., NICKERSON, D. A., NEUHAUSS, S. C. F., DOBYNS, W. B., ALKURAYA, F. S., ROEPMAN, R., BACHMANN-GAGESCU, R. & DOHERTY, D. 2017. Mutations in ARMC9, which Encodes a Basal Body Protein, Cause Joubert Syndrome in Humans and Ciliopathy Phenotypes in Zebrafish. *Am J Hum Genet,* 101**,** 23-36.

VELTEL, S., GASPER, R., EISENACHER, E. & WITTINGHOFER, A. 2008. The retinitis pigmentosa 2 gene product is a GTPase-activating protein for Arf-like 3. *Nat Struct Mol Biol,* 15**,** 373-80.

VILBOUX, T., DOHERTY, D. A., GLASS, I. A., PARISI, M. A., PHELPS, I. G., CULLINANE, A. R., ZEIN, W., BROOKS, B. P., HELLER, T. & SOLDATOS, A. 2017. Molecular genetic findings and clinical correlations in 100 patients with Joubert syndrome and related disorders prospectively evaluated at a single center. *Genetics in Medicine,* 19**,** 875.

WARD, C. J., YUAN, D., MASYUK, T. V., WANG, X., PUNYASHTHITI, R., WHELAN, S., BACALLAO, R., TORRA, R., LARUSSO, N. F. & TORRES, V. E. 2003. Cellular and subcellular localization of the ARPKD protein; fibrocystin is expressed on primary cilia. *Human molecular genetics,* 12**,** 2703-2710.

WATERS, A. M. & BEALES, P. L. 2011. Ciliopathies: an expanding disease spectrum. *Pediatric Nephrology,* 26**,** 1039-1056.

WHEATLEY, D. N. 1995. Primary cilia in normal and pathological tissues. *Pathobiology,* 63**,** 222-238.

WHEWAY, G., SCHMIDTS, M., MANS, D. A., SZYMANSKA, K., NGUYEN, T.-M. T., RACHER, H., PHELPS, I. G., TOEDT, G., KENNEDY, J. & WUNDERLICH, K. A. 2015. An siRNA-based functional genomics screen for the identification of regulators of ciliogenesis and ciliopathy genes. *Nature cell biology,* 17**,** 1074.

WILLIAMS, C. L., LI, C., KIDA, K., INGLIS, P. N., MOHAN, S., SEMENEC, L., BIALAS, N. J., STUPAY, R. M., CHEN, N. & BLACQUE, O. E. 2011. MKS and NPHP modules cooperate to establish basal body/transition zone membrane associations and ciliary gate function during ciliogenesis. *The Journal of cell biology,* 192**,** 1023-1041.

WILSON, R. & MCWHORTER, C. 1963. Isolated flagella in human skin. Election microscopic observations. *Laboratory investigation: a journal of technical methods pathology,* 12**,** 242-249.

WRIGHT, K. J., BAYE, L. M., OLIVIER-MASON, A., MUKHOPADHYAY, S., SANG, L., KWONG, M., WANG, W., PRETORIUS, P. R., SHEFFIELD, V. C. & SENGUPTA, P. 2011. An ARL3–UNC119–RP2 GTPase cycle targets myristoylated NPHP3 to the primary cilium. *Genes & development,* 25**,** 2347-2360.

YODER, B. K., HOU, X. & GUAY-WOODFORD, L. M. 2002. The polycystic kidney disease proteins, polycystin-1, polycystin-2, polaris, and cystin, are co-localized in renal cilia. *Journal of the American Society of Nephrology,* 13**,** 2508-2516.

ZHANG, H., LIU, X.-H., ZHANG, K., CHEN, C.-K., FREDERICK, J. M., PRESTWICH, G. D. & BAEHR, W. 2004. Photoreceptor cGMP phosphodiesterase δ subunit (PDEδ) functions as a prenyl-binding protein. *Journal of Biological Chemistry,* 279**,** 407-413.

ZHANG, Q., HU, J. & LING, K. 2013. Molecular views of Arf-like small GTPases in cilia and ciliopathies. *Experimental cell research,* 319**,** 2316-2322.

ZHANG, Q., LI, Y., ZHANG, Y., TORRES, V. E., HARRIS, P. C., LING, K. & HU, J. 2016. GTP-binding of ARL-3 is activated by ARL-13 as a GEF and stabilized by UNC-119. *Scientific reports,* 6.

ZHOU, C., CUNNINGHAM, L., MARCUS, A. I., LI, Y. & KAHN, R. A. 2006. Arl2 and Arl3 regulate different microtubule-dependent processes. *Molecular biology of the cell,* 17**,** 2476-2487.